Russian Original Vol. 44, No. 4, April, 1978

October, 1978

SATEAZ 44(4) 343-456 (1978)

SOVIET ATOMIC ENERGY

АТОМНАЯ ЭНЕРГИЯ
(ATOMNAYA ÉNERGIYA)

TRANSLATED FROM RUSSIAN

CONSULTANTS BUREAU, NEW YORK

SOVIET ATOMIC ENERGY

Soviet Atomic Energy is a cover-to-cover translation of *Atomnaya Énergiya*, a publication of the Academy of Sciences of the USSR.

An agreement with the Copyright Agency of the USSR (VAAP) makes available both advance copies of the Russian journal and original glossy photographs and artwork. This serves to decrease the necessary time lag between publication of the original and publication of the translation and helps to improve the quality of the latter. The translation began with the first issue of the Russian journal.

Consultants Bureau journals appear about six months after the publication of the original Russian issue. For bibliographic accuracy, the English issue published by Consultants Bureau carries the same number and date as the original Russian from which it was translated. For example, a Russian issue published in December will appear in a Consultants Bureau English translation about the following June, but the translation issue will carry the December date. When ordering any volume or particular issue of a Consultants Bureau journal, please specify the date and, where applicable, the volume and issue numbers of the original Russian. The material you will receive will be a translation of that Russian volume or issue.

Subscription
$130 per volume (6 Issues)
2 volumes per year
Prices somewhat higher outside the United States.

Single Issue: $50
Single Article: $7.50

CONSULTANTS BUREAU, NEW YORK AND LONDON

c/b
227 West 17th Street
New York, New York 10011

Published monthly. Second-class postage paid at Jamaica, New York 11431.

Soviet Atomic Energy is abstracted or indexed in *Applied Mechanics Reviews, Chemical Abstracts, Engineering Index, INSPEC—Physics Abstracts and Electrical and Electronics Abstracts, Current Contents,* and *Nuclear Science Abstracts.*

SOVIET ATOMIC ENERGY

A translation of *Atomnaya Énergiya*
October, 1978

Volume 44, Number 4 April, 1978

CONTENTS

CONTENTS

(continued)

CONTENTS

(continued)

The Russian press date (podpisano k pechati) of this issue was 3/23/1978. Publication therefore did not occur prior to this date, but must be assumed to have taken place reasonably soon thereafter.

ARTICLES

INTRODUCTION OF ATOMIC POWER STATIONS WITH THE VVÉR-440 REACTOR

V. A. Voznesenskii

UDC 621.039.566

At present, a number of the atomic power stations (APS) operational in COMECON member-countries include units based on VVÉR (water-cooled–water-moderated) reactors of thermal power 1375 MW that yield a power of 440 MW(electrical) at the design pressure (0.035 kgf/cm^2) in the turbine condensers. These are the third and fourth units of the Kolsk APS, the first and second units of the Kolsk APS, the Nord APS in the German Democratic Republic, and the Kozlodui APS in Bulgaria.

In the late 1970s and early 1980s further APS with the VVÉR-440 reactor are to be built, bringing the total number of units to more than twenty.

GENERAL INFORMATION ON ATOMIC POWER STATIONS WITH THE VVÉR-440 REACTOR

The main design parameters of APS with the VVÉR-440 reactor, the parameters of the reactor and the active region (AR), are given below [1-3].

Thermal power of reactor, MW	1375
Electrical power of unit (gross) with 0.035 kgf/cm^2 pressure in turbine condensers, MW	440
Electrical-energy consumption for internal requirements of APS for two-unit operation, %	7.15
Number of turbogenerators per block	2
Pressure in first loop at reactor outlet, kgf/cm^2	125
Coolant flow rate in first loop, m^3/h	39,000
Coolant temperature, °C:	
at reactor inlet	270
at reactor outlet	301
Pressure drop in first loop, kgf/cm^2	5.5
Steam flow rate in steam generators, tons/h	2710
Steam pressure, kgf/cm^2:	
in steam generators	47
in steam collector	45
before turbines	44
Internal diameter of reactor body, mm	3560
Number of working modules and control and safety rods (CSR) modules in AR	349
Number of CSR modules	73; 37
Distance between centers of modules, mm	147
Module size (outer measurement), mm	143-144
Module wall thickness, mm	1.5; 2.1
Module wall material	Alloy (Zr + 2.5% Nb)
Number of fuel elements in module	120, 126
Fuel-element diameter, mm	9.1
Thickness of fuel-element cladding, mm	0.65
Material of fuel-element cladding	Zr + 1% Nb
AR loading (in terms of metallic uranium), tons	41-42
Effective AR diameter and height, cm	312; 245
Mean bulk power of AR, kW/liter	86
Mean energy yield, kW/kg U	33.0-33.5
Fraction of fuel discharged on reloading	1/3
Design burnup depth in steady reloading conditions with 3.5% enrichment of fresh fuel, MW-day/ton U	28,600

Translated from Atomnaya Énergiya, Vol. 44, No. 4, pp. 299-305, April, 1978. Original article submitted February 28, 1977.

0038-531X/78/4404-0343 $07.50

The APS presently in operation are designed to work in baseload conditions and use two types of VVÉR-440 differing in the basic number of control and safety rods (CSR) modules containing boron–steel absorber in the upper part and nuclear fuel (UO_2) in the lower part. The difference arose when in the course of preparing the reactor bodies for the third and fourth units of the Novovoronezh APS it was decided to use boron regulation, which allowed the number of CSR modules to be reduced in all subsequent units from 73 to 37, without changing the interval between fuel reloadings (1 year).

Atomic power stations with the VVÉR-440 reactor characteristically have a two-unit structure in which the turbine and reactor chambers are common to the two units, as are the systems for circulational and technical water, chemical water preparation, pure condensate, etc. The first APS loop, containing six circulational subloops, consists of a hermetic chamber, designed for an excess pressure of 1 kgf/cm^2, with automatic release of steam from the chamber to the atmosphere when the excess pressure reaches 0.8 kgf/cm^2. In each subloop there are two main stop valves (MSV), a sealed glandless main circulation pump (MCP), and a horizontal steam generator. Access to the MSV and MCP chambers is possible in the course of reactor operation, which permits maintenance of the equipment without reactor shutdown and ensures efficient use of the units. In the reactor body (its size allows it to be transported as desired), an active region of 349 hexagonal working modules and CSR modules is built. In operation at power, practically all the CSR modules are placed in an extreme upper position, which ensures uniform filling of the active region by fuel and prevents additional distortion of the energy-liberation field due to the presence of solid adsorbent or aqueous cavities. At the inlet to the modules an additional hydraulic drag is provided (by disks for the working modules and by sets of holes in the damper tubes for the CSR modules); this decreases the discrepancy in flow rate over the modules and provides the required interval before heat-transfer crisis in emergency situations with loss of flow rate. The module walls and the cladding of the cylindrical fuel cells are of zirconium–niobium alloy; the reactor body and the volume compensator are of high-strength thermostable steel without a noncorrosive surface. To prevent corrosion of the reactor body and the volume compensator for the first loop of the APS, a special ammonium–potassium water system has been developed. The supply to the MCP is provided from several independent sources: internal-supply generators (ISG) and the main generators on the same axis as the turbines.

The reactor-power regulator maintains a constant pressure in the steam collector (45 kgf/cm^2), while a special regulator ensures discharge of the turbine when the pressure in the steam collector decreases to 44 kgf/cm^2.

Atomic Power Station Characteristics in Startup and Running-in Period and in Use

Thermal and Electrical Power of Units. The thermal power of the reactor is determined on the basis of the heat balance in the first and second loops of the APS. Only using the correct prescribed instruments may five independent balances be formulated. The appropriate tests are preceded by careful checking of the measuring equipment. The discrepancy between the thermal-power values in different balances achieved in practice is not more than ± 2%. (The margin for inaccuracy of the thermal-power value in the design calculations is 4%.) To obtain a measured value of the thermal power for the reactor, the data of the different balances are averaged and the maximum value is taken for the most accurate measurements of the feedwater balance in the steam generators. Special measurement programs are prescribed for the determination of the turbine and electrical parameters in the course of testing. The deviation of the test conditions from the design conditions is taken into account by the appropriate correction in the calculations.

As a result of measurements in different units soon after startup [4] it was established that when K-220-44 turbines with nozzle regulation of the power are used the electrical power of the unit (gross) corresponding to a thermal power of 1375 MW is about 445 MW. The margin in the transmission of the turbogenerators is 10% but its realization requires a corresponding increase in reactor power. The measured energy consumption to meet the internal requirements of units with the VVÉR-440 reactor (except at the Novovoronezh APS) was found to be 6.0-6.4%, which is significantly below the design value.

Hydraulic Characteristics of Reactor and First Loop. In the course of startup and use the hydraulic characteristics of the first loop and reactor are determined and on the basis of the correspondence between these results and the design values it is possible to evaluate the prospects for reactor operation at the nominal thermal power and the safety of the unit. Relevant parameters are the coolant flow rate and pressure drop in the first loop and the individual subloops; the coolant flow rate and pressure drop in the working modules and the CSR modules; the coolant flow bypassing the AR modules. Direct measurement in use is possible only

for the pressure drops in the reactor (ΔP reactor) and the MCP. The flow rate in the subloops of the first loop is determined using the pressure characteristics (the dependence of the pressure drop at the pump on the flow rate through the pump) obtained for each specific MCP on a factory test bed. The flow rate through the reactor (G reactor) is determined initially as the sum of the flow rates over the subloops. Measurements of the pressure drop in the reactor for different numbers of working subloops are used to construct the dependence $\Delta P_p = f(G_p)$, which is then used to determine the flow rate. The pressure drop in the individual elements of the reactor (the active region, the working modules) is measured in one of the stages of the running-in period, by leading out additional pressure-sampling tubes through the reactor roof. The hydraulic characteristics of the VVÉR-440 reactor of the third unit at the Novovoronezh APS and others are given below.

Flow rate through reactor, m^3/h	48,000, 43,500-46,000
Pressure drop, kgf/cm^2	
in first loop	4.1, 4.5-4.8
in reactor	2.2, 3.1-3.4
in AR	1.4, 2.3-2.6
in working module	0.9, 0.8-0.85

These differences are due to the individual properties of the equipment used, in particular, the pumps. For all the units, the coolant flow rate significantly exceeds the design value; this is because the value of the resistance of the first loop assumed in the design calculations was too high. As a result, there are good prospects for an increase in the thermal power of the VVÉR-440 but at the same time additional investigations are necessary to determine the performance of the equipment in the first loop, including the reactor and the active region, in conditions of enhanced flow rate.

At reactor startup great care is taken to establish the correct value of the flow rate through the CSR modules. If this flow rate is not to limit the thermal power of the reactor, it must be close to the flow rate through the working modules. At the same time, increase in the flow rate through the CSR module (> 140 m^3/h) is not permitted by the design, since it may lead to floating of the fuel component on separation of the pump and, as shown by testbed trials, to increased vibration of the structural elements of the module. Measurements on different units, using special attachments recording the weight loss of the CSR module under the action of the flow, show that the real flow rate does not always correspond with sufficient accuracy to the desired value. As a result, in some units additional correction of the flow rate through the CSR module is required. Steps are being taken to refine the calculations and to establish narrower tolerances in the preparation of structural components affecting the hydraulic drag at the inlet to the CSR module.

The coolant flow bypassing the AR modules (calculated value 5%) is determined from the balance equation between the thermal power of the reactor found from the flow rate and heating of the coolant in the reactor and the total thermal power of the working modules and the CSR modules (determined by a special method based on temperature measurements at the outlet from the working modules) and is 4%.

Physical and Thermophysical Characteristics of the Active Region. The main requirements in developing the active region of the VVÉR-440 reactor include the following:

an operating period of 6000-7000 eff. h between reloadings; residence of fuel modules in reactor 3-4 years;

negative or near-zero temperature coefficient and reactivity and negative total power coefficient of reactivity;

nonuniformity of energy liberation no more than 1.35 over the AR modules, and no more than 1.5 between fuel elements;

sufficient CSR-module efficiency to compensate for rapidly appearing reactivity effects (power effects and some temperature effects).

Table 1 gives the calculated physical characteristics of the primary AR of reactors at different APS developed to meet these requirements; for comparison, the results of experimental measurements are also given. As follows from Table 1, the primary AR at present in operation are of five different types, differing in the mean initial enrichment and the use of consumable adsorbents. To a certain extent, this diversity reflects the gradual refinement of design concepts. Following measurements of the reactivity and the nonuniformity of energy liberation, the use of consumable absorbent in the active regions of VVÉR-440 has been completely discontinued. It has been established that a working period of 7000 eff. h between reloadings is achieved with 2.3% mean enrichment of the first charge and 3.3% enrichment of the feed fuel (instead of the

TABLE 1. Basic Physical AR Characteristics of VVÉR-440 at Beginning of Service

Parameter	Novovoronezh		Kolsk and Nord	Kolsk	Nord, second unit; Kolodui, first and second units
	third unit	fourth unit	first unit	second unit	
Composition of primary AR (enrichment and number of modules with fuel)	1%; 49 1,5%; 66 2,0%; 114 3,3%; 120	1,6%; 138 2,4%; 127 3,6%; 84	1,6%; 114 2,4%; 133 3,6%; 102	1,6%; 162 2,4%; 103 3,6%; 84	1,6%; 114 2,4%; 133 3,6%; 102
Presence of consumable absorbent	108 modules with 3.3% enrichment each contain 6 BCA*	—	108 modules with 2.4% enrichment and 102 with 3.6% enrichment contain 0.07% natural boron in walls	—	—
Mean enrichment, %	2,2	2,37	2,5	2,3	2,5
Total margin of reactivity, $\Delta k/k$	0,147	0,177	0,168	0,173	0,188
Total eff. of CSR module at t = 20°C, $\Delta k/k$	0,18	0,15	0,095	0,088	0,088
Temp. coeff. of reactivity at 260°C and zero power, $\Delta k/k/°C$	$\frac{-1,4\cdot10^{-4}\dagger}{-1,8\cdot10^{-4}}$	$\frac{-4\cdot10^{-5}}{+3\cdot10^{-5}}$	$\frac{-2\cdot10^{-5}}{-1,5\cdot10^{-5}}$	$\frac{-5\cdot10^{-5}}{-3\cdot10^{-5}}$	$\frac{-2,5\cdot10^{-5}}{+1,4\cdot10^{-5}}$
Power coeff. of reactivity in working state, $\Delta k/k/\%$	$-2,2\cdot10^{-4}$	$-1,9\cdot10^{-4}$	$-1,8\cdot10^{-4}$	$-2\cdot10^{-4}$	$-1,85\cdot10^{-4}$
Critical concn. of boric acid at 100°C for completely raised CSR modules, g H_3BO_3/kg H_2O	5,2/4,8	7,6/6,9	7,8/6,4	6,8/6,2	8,8/8,0

*BCA – Blocked consumable absorbent.

†The numerator gives the calculated value and the denominator the experimental value.

design values of 2.5 and 3.5%, respectively). The disagreement between the calculated and experimental values of the physical characteristics (burnout depth, the efficiency of boric acid, etc.) indicates the need for improvement in the methods of calculation currently in use.

Atomic Power Station Operation in the Case of Accident and Transient Conditions. The operating program for the running in of VVÉR-440 power reactors involves complex checking of the APS performance in the event of accident or transient conditions. Special tests are carried out to establish the conformity of the operation of the regulation, blocking, and safety systems with the design requirements, and to investigate the dynamics of APS-parameter variation under different perturbations and at different power levels. The most important of these include tests of total APS shutdown and the investigation of module response to variation and reduction in the electrical load and to MCP failure.

Complete APS shutdown (for safety reasons the tests are carried out with the reactor at 17-20% thermal power) involves the combined operation of equipment and systems ensuring safe stoppage and adequate cooling of the APS (even with sodium leakage in the first loop) in the event of disconnection from the energy system and switching off (stop-valve closure) of the APS turbogenerators. The tests check APS shutdown by the emergency-protection systems; the duration of MCP operation on the "rundown" energy of the main generators and the ISG; continuous supply of the most important electrical-energy requirements (initially from accumulator batteries and then from diesel generators); connection to the diesel generators (after their startup) in turn (in order of importance) of those electrical units that can tolerate a brief (up to 3 min) interruption of supply; and the establishment of natural circulation in the first loop and shutdown cooling.

At startup, as a rule, one test is sufficient to demonstrate the satisfactory conformity of APS performance in emergency conditions with the design specifications. It is found that the MCP operates for not less than 180 sec (design time – 100 sec) on the rundown energy of the ISG and the main generator; the diesel startup time is 70-90 sec; the length of connection of electrical units to the diesels is about 70 sec: the deviation of the potential in the electrical supply system of the APS is not more than 10%. In the startup of APS with the VVÉR-440 reactor, successful completion of the tests on total shutdown is a necessary preliminary to increase in the reactor power (> 17-20%).

Tests of the response to reduction and variation in the electrical load are carried out at APS startup to adjust the turbine control system and the main regulators of the unit and to determine their static and dynamic

characteristics, to confirm the possibility of successful (while maintaining the APS at the power level appropriate to its internal requirements) reduction in electrical load, to investigate the dynamics of parameter variation in the operation of the APS control systems, and to confirm the guaranteed indices with respect to the rate of change of the load of the units.

Experience shows that after the necessary adjustment for any load reduction, up to a complete reduction from 100% to the level of internal requirements, the fluctuation of the APS parameters does not trigger the emergency protection systems of the turbine and reactor, or lead to the opening of the steam-generator safety valves. For example, on complete reduction in load the maximum speed does not exceed 3200-3240 rpm and after 20-30 sec the turbine rotation stabilizes. Rise in pressure in the steam collector for 5-8 sec triggers the reduction valves, which release steam from the turbine condensers, and the maximum pressure does not exceed 52 kgf/cm^2. The brief increase in the first loop is 1.5-2.0 kgf/cm^2. Trial loadings of the turbogenerators at the guaranteed rates (2 and 5 MW/min from the cold and hot states, respectively) show that these rates do not lead to any deviations from the required indices of the turbine heating.

The design allows for the disconnection of up to two MCPS (e.g., on short-circuiting in the supply section) without the operation of the reactor emergency systems. In these circumstances the reactor power regulator reduces the neutron flux in the active region by 50%. At the same time, the reduction in pressure in the steam collector is accompanied by automatic reduction in turbine load. If, after stabilization of the parameters, the thermal power of the reactor does not correspond to the number of MCP remaining in operation, the operator makes an additional correction to the reactor power level. Tests of APS startup with one or two MCP disconnected have been carried out at 3-4 different power levels, including the nominal power. The control systems of the units successfully deal with transient processes when MCP are disconnected. The deviation of the APS parameters does not trigger the emergency and blocking systems. Stabilization of the conditions at the new power level takes $\approx$300 sec.

Radiation Equipment

The state of the radiation equipment is determined continuously using specified measurement and monitoring systems. In addition, special programs of measurement must be carried out at APS startup and periodically in the course of APS operation for the detailed verification of the conformity of the APS radiation equipment with the design data. It is necessary to monitor the neutron and γ-ray dose rate; the gas and aerosol activity in the APS structure; the release of radioactive gases, aerosols, iodine, and strontium to the atmosphere; the activity of water in the first loop, the steam generator, the reloading tanks and the spent-fuel stores, the tanks of the active-water retreatment system, etc.; the activity of the steam arriving at the turbine; the gas and aerosol activity of the air; the radioactivity of water and soil in the area around the APS; and the sealing of the heat-liberating modules on reloading.

Measurements on different units show that the dose rates from external fluxes of ionizing radiation in APS structures established by the operating norms (1.4, 2.8, and 28 mrem/h for attended, semiattended, and unattended chambers, respectively) are not exceeded on the average. Isolated deviations (by a factor of 5-10) noted in semiattended chambers (at points of penetration through the walls and at the overlapping of the biological protection) must be easily localized, and additional measures are taken to this end.

The release of radioactivity to the atmosphere in normal operation is 5-100 (radioactive gases); 10^{-2}-10^{-4} (aerosols); 10^{-3}-10^{-4} (^{131}I); 10^{-4}-10^{-6} Ci/day (^{89}Sr + ^{90}Sr) with norms of 3500, 0.5, 0.1, and 10^{-3} Ci/day, respectively.

The activity of the coolant in the first loop is determined both using continuous-monitoring equipment and by periodic analysis of samples. Under normal conditions, the analysis of the specific activity of dry residues and iodine isotopes is carried out once a day and once every 2 days, respectively; for the total isotope state the rate is once a month.

The reactor operation is regarded as satisfactory up to a total specific activity of the first-loop coolant of 0.1 Ci/liter at the moment of sampling for 100% thermal power of the reactor (the specific activity of nongaseous fission products 2 h after sampling is 10^{-2} Ci/liter). The actual activity in operating units is considerably below these limits. For example, in the first half of 1976 the figure for nongaseous fission products (mainly iodine isotopes) was 10^{-4}-$2 \cdot 10^{-3}$ Ci/liter and for most units this corresponds to the end of the operating period. The corrosion products of the first-loop materials make an insignificant contribution (10^{-8}-10^{-7} Ci/liter) to the total specific activity of the coolant.

Analysis of the specific activity of the fission products by a special method allows the state of sealing of the fuel elements to be evaluated. The specific modules with unsealed fuel elements are determined at the time of reloading. To monitor the sealing of fuel-element shells on reloading, individual modules are placed in a sealed can with subsequent holding in air (the method used at the Voronezh APS) or water and analysis of samples.

On Sept. 1, 1976, 12 planned reloadings were carried out at reactors (three each in the third and fourth units of the Novovoronezh APS, two in the first unit of the Kolsk APS, and one each in the other units). Practically at each reloading the sealing of the modules remaining in the reactor for the next term of operation was checked ($\approx 2/3$ of the total number of modules with fuel). Between each reloading there are improvements in the methods of detecting unsealed modules and developments in the quality standards.

According to the results of six reloadings in various units with a VVÉR-440 reactor in the summer and autumn of 1968, one module on the average was removed from the reactor ahead of schedule.

No relation has been found between conditions of reactor use and the number of unsealed modules.

Work in Startup and Running-In Period

This work is carried out at the APS after the installation is complete and includes the following main stages:

1) introduction into use of the electrical supply for the internal requirements of the unit and the chemical water treatment;
2) washing and functional testing of the auxiliary APS systems;
3) hydraulic testing and circulational washing of first loop;
4) first inspection of first-loop equipment;
5) cold and hot running in of first-loop equipment;
6) second inspection of first-loop equipment;
7) loading of active region and physical startup of reactor;
8) operation of unit at 1-5% power as a preliminary to the introduction of the turbogenerators in circuit;
9) raising the unit to the design power, with successive operation at 17-20, 30-35, 75-80, 90, and 100% power followed by 72-h continuous operation at the nominal power.

The mechanical purpose of the work at the stage of hydraulic testing and circulational washing is the demonstration that the first loop is watertight and also washing of the loop after installation. Depending on the conditions at each specific APS the sealing of the reactor at this stage is either by a temporary roof or by the prescribed upper unit. The CSR drive is not fitted. The hydraulic drag of the missing active region is simulated by a temporary throttling device. In the circulational washing the heat of the operating MCP raises the coolant to 220-230°C, which facilitates the washing of the first-loop surface; the operation of the MCP and the auxiliary systems of the reactor is checked, the specified technological operations are completed; and the vibration and degree of expansion of the equipment and the turbine ducts are checked.

After the circulational washing the first loop is cooled, the reactor roof is removed, and the in-reactor equipment is dismantled. The first inspection of the APS equipment and systems is then conducted; defects observed in the hydraulic testing and circulational washing are eliminated; the state of the metal in the basic equipment is monitored; the equipment and systems are prepared for hot and cold running in; and the specified reactor pile is fitted with the CSR drive and the subcritical region. At the startup of the first units the region was partially loaded with modules containing fuel for the hot running in. In conditions of imperfect adjustment of the equipment, this led to difficulties in ensuring nuclear safety and the possibility of mechanical damage of the regular modules.

The present practice at the time of running in is to load the region with stimulation modules that do not contain fuel. One set of such modules is used successively in the startup of several different units. At the stage of cold and hot running in, the electrical circuitry of the CSR system is adjusted and the CSR drive is run in; the hydraulic characteristics of the reactor and the first loop are investigated; the stress–strain dynamics of in-reactor instruments (for the principal units) is studied; and the blocking and safety systems of the reactor are tested.

The second inspection, following the cold and hot running in, must ensure that the equipment and systems of the power stations are in full readiness for the loading of the specified active region, physical startup, and the buildup to full power. The main equipment is examined again and the state of the metal is monitored by various methods. All defects appearing in the course of running in and the subsequent inspection are eliminated. The second inspection is concluded by the loading of the specified active region and the sealing of the reactor. At stages 3-6, in parallel with the work on the first loop, the sealing of the hermetic chambers of the reactor installations is checked and the ventilation and dosimetry systems are adjusted.

The beginning of physical startup concludes the multiple testing of the second-loop equipment, together with the checking of the vibrational state of the turbogenerators and, if necessary, balancing and electrical testing of the ISG and the main generators with a set of loads up to 20 MW. The source of the steam for this work is either an energy train of temporarily installed steam boilers for the first units of an APS; for the subsequent units, the units already operational are used.

The final check on the combined operation of all the systems in steady, transient, and emergency conditions is made at physical startup and in the course of buildup to full power. The lengths of the main stages of this work are as follows, days: hydraulic testing and circulational washing, 8-30; first inspection, 29-62; cold and hot running in, 15-22; second inspection of equipment, 15-60; loading of active region and physical startup, 15-34; total duration of buildup to design power (from the end of physical startup to the completion of 72-h testing at 100% power), 75-211, including 6-85 for planned inspection.

Discrepancies in the length of the stages of this work for different APS may be due to a number of factors. For example, significantly more time was required for startup of the first units of each APS than for the subsequent units, as a result of the broader test program, the larger number of defects discovered in the equipment, the installation, and the design, and the lack of experience of the personnel involved. Some redistribution of the work between the individual stages has been observed; different levels of APS reliability have been noted by maintenance personnel; and different forms of operational organization of the work have been developed.

LITERATURE CITED

1. V. P. Denisov et al., Paper at the Soviet–French Seminar on Steam Generators, Structural Materials, and Production Technology of First-Loop Components of Water–Water Reactors [in Russian], Saclay (Sept. 17-23, 1975).
2. V. P. Denisov et al., Fourth Geneva Conference, USSR Paper No. 639 [in Russian] (1971).
3. K. Gorski and M. Ivanov, Kernenergie, 7, 200 (1974).
4. G. M. Konovalov et al., Teploenergetika, No. 9, 52 (1975).

EVALUATION OF PLANT-LOCATION STRATEGIES FOR THE NUCLEAR-POWER FUEL CYCLE

B. B. Baturov and V. M. Urezchenko

UDC 621.039.003

The development of nuclear power (NP) necessitates considerable increase in capacity of the components of the fuel cycle. A wide range of predictive studies of different aspects of this problem have been undertaken, with a view to evolving the optimal NP development strategy [1-5]. A question of considerable interest concerns the options for the location and development of plants for fuel-element preparation and for the chemical reprocessing of spent fuel.

Various strategies are possible for the location of fuel-reprocessing plants. The first of these envisages the construction of small plants close to a single atomic power station (APS) or a number of adjacent APS (Fig. 1a). In the second, the development of the fuel-reprocessing industry occurs through the construction of centralized large-capacity plants that serve many APS; these plants always have an unused, reserve capacity in relation to demand (Fig. 1b). The third strategy again involves centralized reprocessing plants but in this case their capacity is calculated on the basis of the demand, without providing any unused reserve capacity (Fig. 1c).

An analysis using economic estimates is necessary if the optimal strategy is to be chosen for the location of the components of the fuel cycle (FC). The three plant-location strategies differ in their capital and current expenditures. The third strategy involves storage of the fuel, since the fuel is to be used in the future and awaits subsequent use or subsequent reprocessing. This storage leads to the freezing of considerable capital.

In [6] an economic functional was proposed for the analysis of the different NP development strategies, taking into account the possible factors; the functional was constructed on the reduced-expenditure principle but also taking into account the long-term working capital

$$F = \frac{K + T + D_f + D_{st}}{\sum_{t=1}^{T_{pr}} N_t \theta \varphi_t (1+\sigma)^{1-t}}, \quad (1)$$

where K is the total capital expenditure; T is the total current expenditure; D_f and D_{st} are the long-term working capital due to the prolonged residence of fuel in the cycle and the steplike growth in the FC capacity, respectively; N_t is the estimated APS power introduced in year t; θ is the number of hours of operation per year; φ_t is the use factor of the established power; T_{pr} is the time depth of the prediction; σ is the norm in taking into account the different time scales of the expenditures.

K and T are determined as the total values at all the FC plants over the whole period of prediction, taking into account the different time scales of the expenditures. The long-term working capital is formed as a result of the annual deduction of frozen capital and represents the sum over all the FC plants throughout the whole period of prediction of these deductions, taking into account the different time scales; the deduction is only taken from the moment of capital introduction until its recovery.

The various distribution strategies for the FC plants differ in the level of capacity of the plants introduced. The values of the capital expenditure and costs of reprocessing at the plants depends on their capacities.

Analysis of the available data for the existing and projected FC plants shows that, for capital expenditure in the range of capacity from 0.1 to a few tons per day, the following relation may be used [6]

$$K = K_0 (G/G_0)^{\alpha}, \quad (2)$$

where K and K_0 are the total capital expenditures in building plants of capacity G and G_0, respectively; $\alpha < 1$ is the index corresponding to the different FC plants.

Translated from Atomnaya Énergiya, Vol. 44, No. 4, pp. 306-310, April, 1978. Original article submitted October 4, 1976; revision submitted December 14, 1977.

0038-531X/78/4404-0350 $07.50

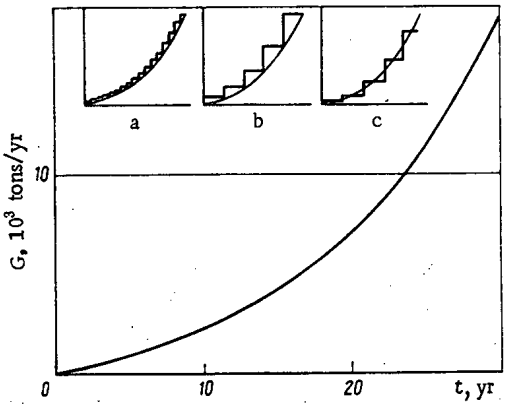

Fig. 1. Demand for fuel and strategies for demand satisfaction for different approaches to increasing the total capacity of fuel-reprocessing plants.

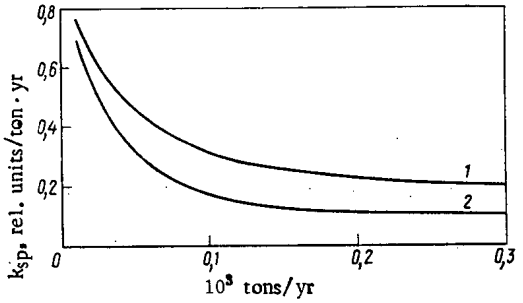

Fig. 2

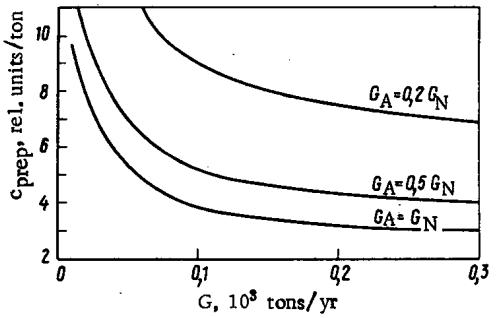

Fig. 3

Fig. 2. Dependence of specific capital expenditure on the capacity of plants for the chemical reprocessing (1) and preparation (2) of fuel elements.

Fig. 3. Dependence of fuel-preparation costs at plants for fuel-element production on the nominal (design) capacity G_N and the actual capacity G_A with $\alpha = 0.4$; $\delta_{const} = 0.33$.

In Fig. 2 the dependence of the specific capital expenditure on the capacity of plants for the preparation and chemical reprocessing of fast-reactor fuel elements based on oxide fuels is shown.

The total expenditure (E) in reprocessing for a plant of capacity G may be written as the sum of constant (E^{const}) and variable (E^{var}) components

$$E = E^{const} + E^{var}. \tag{3}$$

The constant component, determined mainly by the capital expenditure, also satisfies Eq. (2)

$$E^{const} = E_0^{const} (G/G_0)^{\alpha}. \tag{4}$$

The variable component is determined by the expenditure of energy and materials, i.e., is directly proportional to the actual plant capacity

$$E^{var} = E_0^{var} \frac{G}{G_0}. \tag{5}$$

The values of E_0^{const} and E^{var} may be written as fractions of the total expenditure (E_0)

$$\left.\begin{aligned} E_0^{const} &= E_0 \delta \quad ; \\ E_0^{var} &= E_0 \delta_{var}, \end{aligned}\right\} \tag{6}$$

where δ_{const} and δ_{var} are the relative fractions of the constant and variable components of the total expenditure.

Substituting Eqs. (4)-(6) in Eq. (3) and writing the total expenditure as the product of the reprocessing costs and the plant capacity, an expression that takes into account the dependence of the reprocessing costs on the plant capacity for operation with the total load is obtained,

$$c = c_0 \left[\delta_{const} \left(\frac{G}{G_0} \right)^{\alpha} + \delta_{var} (G/G_0) \right] \frac{G_0}{G}, \quad (7)$$

where c and c_0 are the reprocessing costs* at plants of capacity G and G_0, respectively.

In the operation of plants with an incomplete load, the constant expenditure corresponds to smaller production and the specific reprocessing costs rise. Suppose that a plant of nominal capacity G operates at a capacity $g < G$. The reprocessing costs for operation at the nominal capacity G are written as the sum of constant and variable components

$$c^{nom} = c^{nom}_{const} + c^{nom}_{var} = c^{nom} \delta_{const} + c^{nom} \delta_{var}. \quad (8)$$

With reduction in output, the constant component of the total reprocessing expenditure remains unchanged, since it does not depend on the amount of reprocessed production. Writing the expenditure as the product of the reprocessing costs and the capacity gives an expression for the constant component of the reprocessing costs

$$c_{const} = c^{nom}_{const} \frac{G}{g} = c^{nom} \frac{\delta_{const}}{g/G}. \quad (9)$$

The variable component of the reprocessing costs does not depend on the plant capacity; that is

$$c_{var} = c^{nom}_{var} = c^{nom} \delta_{var}. \quad (10)$$

Writing the reprocessing costs as the sum of the constant – Eq. (9) – and variable – Eq. (10) – components gives an expression that takes into account the dependence of the reprocessing costs on the level of capacity in operation with an incomplete load

$$c = c^{nom} \left(\frac{\delta_{const}}{g/G} + \delta_{var} \right). \quad (11)$$

The curves in Figs. 3 and 4 show the dependence of the costs of preparation and chemical reprocessing of fast-reactor fuel elements based on oxide fuel on the output of these plants when operating at the nominal capacity and with less than total load.

To understand the basic relations of the capital expenditures and costs of reprocessing with different location strategies for the FC plant (Fig. 5), consider an example. Suppose that in the fifth year it is required to have a capacity G_C. This requirement may be satisfied by the annual introduction of a capacity of G_D (distributed location) or at once by constructing a plant of capacity G_C (centralized location). In considering these cases, no account will be taken of the distribution of the expenditures over time, and it will be assumed that $\alpha = 0.6$ and $\delta_{const} : \delta_{pr} = 1/2 : 1/2$.

The ratio of the total capital expenditures will be

$$\frac{K_C}{K_D} = \frac{k^{sp}_D (G_C/G_D)^{\alpha}}{(G_C/G_D) k^{sp}_D} = \frac{k^{sp}_D 5^{0.6}}{5 k^{sp}_D} = 0.52, \quad (12)$$

where K_C and K_D are, respectively, the total expenditures after 5 years for centralized and distributed FC-plant location; k^{sp}_D is the capital expenditure at a plant of capacity G_D.

The ratio of the reprocessing costs under the condition that in both cases the plants operate at total capacity is

$$\frac{c^{nom}_C}{c_D} = \left[\frac{1}{2} (5)^{0.6} + \frac{1}{2} (5) \right] \frac{1}{5} = 0.76. \quad (13)$$

For centralized location the nominal plant capacity must be high, so as to satisfy the requirements over the course of several years, i.e., in this case a larger capacity is introduced in anticipation of the requirements and operates at less than total load in the initial period. Therefore, the actual reprocessing costs for this plant-location strategy are high. The ratio of the actual costs to the costs for operation at the nominal capacity for the different levels (in each of the 5 years) may be calculated from Eq. (11); the result is 3 for the first year; 1.75 for the second, 1.33 for the third, and 1.125 for the fourth.

The mean ratio of the actual costs after 5 years for the centralized plant-location strategy to the costs for operation at the nominal capacity is determined as a weighted mean, the weighting factor being the ratio between the fuel reprocessed in each year and the total fuel reprocessed over the 5 years. Then

$$c_C / c^{nom}_C = 1.17. \quad (14)$$

*The term reprocessing costs should be understood to mean the specific expenditure for the reprocessing of unit mass of fuel.

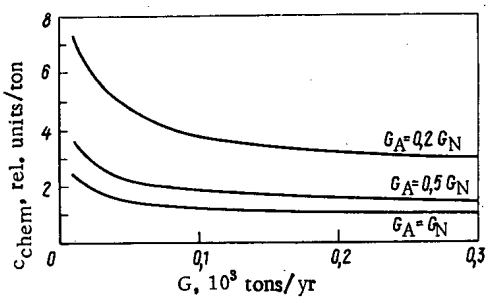

Fig. 4

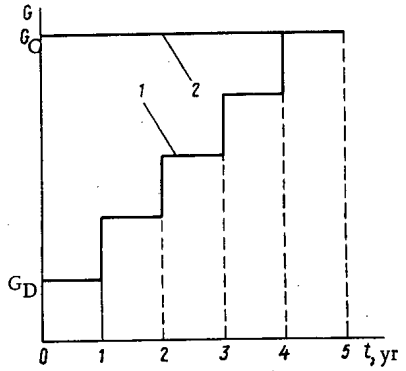

Fig. 5

Fig. 4. Dependence of chemical-reprocessing costs on nominal (design) capacity G_N and actual capacity G_A of plant with $\alpha = 0.6$; $\delta_{const} = 0.5$.

Fig. 5. Development of FC-plant capacity in the case of distributed (1) and centralized (2) location.

TABLE 1. Ratio of Capital Expenditures and Costs of Reprocessing for Centralized and Distributed Plant Location Strategies

α	$\alpha = 0{,}6$		$\alpha = 0{,}4$	
T_{step}	5 yr	10 yr	5 yr	10 yr
$\delta_{const}/\delta_{pr}$	1/0 0,5/0,5 0/1	1/0 0,5/0,5 0/1	1/0 0,5/0,5 0/1	1/0 0,5/0,5 0/1
c_C^{nom}/c_D	0,52 0,76 1	0,4 0,7 1	0,4 0,7 1	0,25 0,62 1
c_C/c_C^{nom}	1,67 1,17 1	1,82 1,41 1	1,67 1,17 1	1,82 1,41 1
c_C/c_D	0,87 0,89 1	0,73 0,99 1	0,67 0,82 1	0,45 0,88 1
K_C/K_D	0,52	0,4	0,38	0,25

The ratio of the reprocessing costs for centralized FC-plant location to those for distributed location is

$$c_C/c_D = (c_C^{nom}/c_D)\,(c_C/c_C^{nom}) = 0.76 \cdot 1.17 = 0.89. \qquad (15)$$

Table 1 gives the ratios of the capital expenditures and costs of reprocessing at FC plants for the centralized and distributed location strategies with various values of α, various periods of analysis, and various limiting values of the ratio between the fractions of constant and variable expenditures.

It follows from Table 1 that, if no account is taken of the distribution of the expenditures over time and it is assumed that the rise in capacity is uniform in all cases of the distributed plant-location strategy, centralized location of plants with reserve capacity is found to be the best. Taking into account the distribution of the expenditures over time should lead to a deterioration in the indices for the centralized plant-location strategy, since in this case the higher capital expenditures and the higher reprocessing costs correspond to the early stages. Thus, to obtain more accurate dependences detailed consideration of the time factor and the actual increase in FC capacity is necessary.

The capital expenditure and cost of centralized location of fuel-reprocessing plants without reserve capacity must also be less than for distributed location. However, the holdup of fuel in the cycle arising in this case leads to the appearance of additional expenditures due to the freezing of capital in the fuel awaiting subsequent reprocessing or use. In addition, in this case the requirement for uranium from the external part of the FC is significantly increased, which also leads to additional expenditure. Thus, in this case opposing factors operate and, if correct conclusions are to be reached as to which particular strategy for the location of fuel-reprocessing plants is the most preferable, the influence of the various factors must be carefully analyzed and taken into account.

Such analyses were carried out using the mathematical model described in [7] and using the functional in Eq. (1) for the developing system of APS with fast reactors. In considering the developing system of APS and fuel-processing plants in the given model, as in [5], the presence of stores in the FC and the holdup of fuel in the cycle are taken into account; the analysis rests on the balance equations. However, in contrast to [5], the present model is imitative and allows various possible strategies of NP-system development to be studied. The main features of the model are as follows: discrete (stepwise) increase in FC capacity is possi-

ble; the change in isotopic composition of the fuel between reloadings is taken into account for each of the reactors in the system; and a functional that takes into account the long-term working capital is used as the economic criterion.

The choice of cost factors and their long-term variation presents great difficulties in the investigation. Nuclear power is at present entering on a phase of broad development and as a result there are either no large-scale FC plants or at best isolated specimens; hence reliable estimates of the cost factors have not yet been possible. In addition, APS with fast reactors of large power are only now being constructed and to date there is no information on the costs of producing and reprocessing fuel for such reactors on a large scale. In view of all this, it is necessary to consider a fairly wide range of initial values of the cost factors.

Therefore, in the calculations the development of an APS system was considered for fast reactors with sodium and gas coolant based on oxide and carbide fuel; for different hypotheses of APS power development [established power at the end of the 30-yr period 400, 600, and 800 million kW(electrical); the rate of power development falls discretely; the load factor remains at 0.8 or falls to 0.6; the duration of the external FC is 0.66-2 years]; and for intervals of 3-6 years between the discrete increments in FC power; in taking into account the different time scales of the expenditures not only the normative value $\sigma = 0.08$ but also the value $\sigma = 1$ were considered. The values of the cost factors were chosen in the expected range: variation by a factor of 2 in the total specific capital expenditures and by a factor of 3 in the reprocessing costs; a ratio of 0.8-4 between the costs of natural uranium and the costs of separation in comparable units; and a ratio of 0.8-6 between the costs of preparation and the costs of chemical reprocessing.

For these values of the capital expenditure in the development of the fuel base, taking into account the dependence on the scale of their output, the following illustrative structure of specific capital expenditures at mining and fuel-reprocessing plants is obtained, as calculated per unit of electric power, %

Mining	25-30	Separation	45-60
Preparation	5-10	Chemical reprocessing	10-15

For the given assumptions, the mean ratio of fuel-processing at external-FC plants in comparable units is, %

Mining	45-55	Separation	30-40
Preparation	10-15	Chemical reprocessing	5-10

As a result of the calculations, the following conclusions may be obtained: the centralized strategy is the best for the location of fuel-processing and regeneration plants; these plants must have considerable capacity for the individual functions.

Both the need to reduce the requirement for natural fuel and economic considerations indicate the expendiencyof having reserve capacity in the various practically possible values and the ratios of the capital and current FC expenditures (even at a mean level of use of the design capacity of less than 50%).

These conclusions are independent of the technical solutions of reprocessing, fuel transportation and storage, and also possible changes in the value of plutonium.

LITERATURE CITED

1. V. V. Orlov, M. F. Troyanov, and V. B. Lytkin, At. Energ., 30, No. 2, 170 (1971).
2. A. A. Makarov et al., At. Energ., 32, No. 3, 187 (1972).
3. V. N. Bobolovich et al., At. Energ., 36, No. 4, 251 (1974).
4. V. M. Chakhovskii and V. V. Mattskov, At. Energ., 38, No. 5, 287 (1975).
5. A. D. Virtser et al., At. Energ., 37, No. 2, 113 (1974).
6. B. B. Baturov and V. M. Urezchenko, in: Nuclear-Reactor Physics [in Russian], No. 5 (edited by L. N. Yurova), Atomizdat, Moscow (1976), p. 68.
7. B. B. Baturov and V. M. Urezchenko, in: Nuclear-Reactor Physics [in Russian], No. 4 (edited by L. N. Yurova), Atomizdat, Moscow (1975), p. 94.

OPTIMIZATION OF ENERGY DISTRIBUTION IN ACTIVE REGION OF LARGE FUNCTIONAL POWER REACTOR

I. Ya. Emel'yanov, V. G. Nazaryan, and V. V. Postnikov

UDC 621.039.5.56

One of the recent trends in the design and use of power reactors is a growing interest in a different kind of optimization problem. The problem of optimal regulation of the energy distribution in a reactor in steady conditions was considered in [1, 2]. The investigation at the Halden reactor in Norway [1] is a representative example, and the basic concepts employed, with minor variations, are also characteristic of most of the other works. The basic idea in these studies is to shift the real energy distribution toward some specified distribution in conditions of "trailing" regulation with constant improvement and refinement of the calculated constants on the basis of continuous experiment.

Very briefly, the mathematical formulation of the problem considered in [1] is as follows: the regulation process over time is described by the differential equation

$$\dot{\Phi}(t) = \hat{A}(t)\,\varphi(t) + \hat{B}(t)\,\delta U(t) + \rho(t), \tag{1}$$

where φ describes the current neutron distribution in the regions of the reactor; δU gives the regulating effect; ρ is determined by random perturbations; the matrices $\hat{A}(t)$ and $\hat{B}(t)$ describe the state of the active region and the efficiency of the regulating effect. The process is considered as a set of discrete states with stepwise regulation, the parameters of which are determined from the condition for a minimum of the quadratic functional

$$I = [\varphi_d(t) - \varphi(t)]^{\mathrm{T}}\,\hat{P}\,[\varphi_d(t) - \varphi(t)] + \delta U^{\mathrm{T}}(t)\,\hat{U}\,\delta U(t), \tag{2}$$

where the matrix $\hat{P}$ determines the weighting factors of the neutron flux; $\hat{U}$ is the matrix of constraints on the regulating effect; the superscript T denotes transportation; $\varphi_d(t)$ characterizes the specified energy distribution.

What form should the specified energy distribution take in such optimization problems? It is readily established that it should be some energy distribution that is determined by a set of physical, thermotechnical, and other constraints on the energy intensity of the heat-liberating piles (HLP) and also the errors of monitoring and regulation.

In the general case, the specified energy distribution may take very different forms; as an example, consider a constant energy distribution over the whole active region or a constant plateau over the region with a decrease according to some law at the periphery.

The energy distribution with minimum mean square deviation from the specified distribution is higher than the specified energy distribution over approximately half the active region. A proportional reduction in the energy distribution eliminates this shortcoming. However, there then arises the question of whether there is any other energy distribution that might have better regulation quality when the permissible power is not exceeded; by regulation quality is meant the nonuniformity coefficient of the radial energy distribution K_r or the minimum safety margin K_m to the permissible HLP power (under conditions of constant total reactor power). For relative consistency of the given energy distribution, minimization of K_r (or, in the more general case, maximization of the minimum K_m) ensures high reliability of reactor operation or the possibility of increasing its power while retaining the previous reliability. The problem of accurately determining the optimum energy distribution (on the example of the high-boiling reactor) forms the subject of the present work.

Formulation of the Problem

The method rests on the following assumptions:

Translated from Atomnaya Énergiya, Vol. 44, No. 4, pp. 310-315, April, 1978. Original article submitted February 15, 1977.

0038-531X/78/4404-0355 $07.50

1) that the relative change of the power of each HLP is a linear function of the reactivity increment due to the change in position of an individual control rod (CR);

2) that the relative change in power of each HLP is an additive quantity, i.e., when a group of rods is moved, it is equal to the sum of the corresponding changes due to each rod.

The first assumption may be mathematically expressed as follows

$$\frac{\omega_i-\omega_i^{(0)}}{\omega_i^{(0)}}=\alpha_{ij}(\rho_j-\rho_j^{(0)}),$$
$$i=1, 2, \ldots, m; \quad j=1, 2, \ldots, n, \tag{3}$$

where $\omega_i^{(0)}$ and ω_i are the power of the i-th HLP before and after the j-th CR is moved from a position characterized, in reactivity units, by the quantity $\rho_j^{(0)}$ to a position characterized by ρ_j. For a CR that has been completely removed $\rho_j=0$, while for a fully inserted CR $\rho_j=1$; m is the number of HLP in the reactor; n – number of CR; α_{ij} is the influence function of the j-th CR on the i-th HLP, defined as follows

$$\alpha_{ij}=\frac{\xi_{ij}-1}{1+(\xi_{ij}-1)\rho_j^{(0)}}, \tag{4}$$

where $\xi_{ij}=\omega_i(\rho_j=1)/\omega_i(\rho_j=0)$ is a function describing the relative deformation in the power of the i-th HLP produced when the j-th CR is moved from complete removal to full insertion. The function ξ is normalized for each CR using the condition that reactor power is the same before and after the maximum change in CR position.

The mathematical expression of the second assumption takes the form

$$\omega_i=\omega_i^{(0)}\left[1+\sum_{j+1}^{n}\alpha_{ij}(\rho_j-\rho_j^{(0)})\right], \tag{5}$$

where ω_i is the power of the i-th HLP after all the CR are moved from the position characterized by the set of relative rod efficiencies $\rho_j^{(0)}$ to the position with the set ρ_j (j=1, 2, . . ., n).

Special experiments and calculations were carried out to confirm that these assumptions are valid in practice for high-boiling reactors.

The results showed: 1) that the dependence of the deformation of the HLP of this reactor on the CR position has a clearly expressed linear form over most of its course, with slight deviations from linearity close to the extreme upper and lower positions; 2) that the functions ξ of the CR may be divided into two groups, the first of which includes all the CR of the extreme peripheral ring and the second, all the CR of the plateau region; 3) the function ξ of the second group has a small azimuthal anisotropy, i.e., the difference in the power deformations of HLP equidistant from the given CR is less than 3% (for CR of the extreme peripheral ring this difference reaches 12%); 4) that the function ξ of each plateau-region CR depends only weakly on the position of the other rods.

Note that the results 2) and 3) above allow the function ξ for plateau-region CR to be represented as a function of the displacement, i.e., as a function of the HLP–rod distance. To simplify the calculations the same procedure may, at the cost of greater error, be applied to the function for the peripheral CR, on the basis of the following considerations; since the overall aim is to equalize energy distributions or distributions of the safety margin, and the "hotter" HLP are practically always in the plateau region, the main role in determining the optimum must obviously be that of the rods of that region. Moreover, in most cases the peripheral CR are removed from the reactor in operating in power modes of the high-boiling reactor.

In accordance with results 2) above, it is possible to simplify the calculations considerably and to get rid of the cumbersome (m × n) matrix describing the relation between the positions of all the CR and the power of all the HLP.

Proceeding to the mathematical formulation of the problem, the first step is to make a simplification which involves passing to the problem of zonal regulation. This simplification is of purely practical significance, and is a result of the tendency to remove large demands on computer time and also to reduce the volume of computer store required.

The active region of the reactor is divided into MQ square cells (zones) of 4 × 4 HLP; then, using Eq. (5), the mean power Q_l of the l-th zone is

$$Q_l=\frac{1}{T_l}\sum_{k=1}^{T_l}\omega_k=\frac{1}{T_l}\sum_{k=1}^{T_l}\omega_k^{(0)}+\frac{1}{T_l}\sum_{k=1}^{T_l}\sum_{j=1}^{n}\omega_k^{(0)}\alpha_{kj}(\rho_j-\rho_j^{(0)})=Q_l^{(0)}+\sum_{j=1}^{n}\beta_{ej}(\rho_j-\rho_j^{(0)}), \tag{6}$$

where T_l is the number of HLP in the l-th zone; k is the HLP index of the l-th zone; $\beta_{lj}=\frac{1}{T_l}\sum_{k=1}^{T_l}\omega_k^{(0)}\alpha_{kj}$; $Q_l^{(0)}=\frac{1}{T_l}\sum_{k=1}^{T_l}\omega_k^{(0)}$ is the mean power of the l-th zone in the initial state.

Let $K_{ml}^{\min}=\min_k\{\omega_k^{reg}\ \omega_k^{(0)}\}$ be the minimum value of the safety margin (i.e., the relative distance of the energy distribution from the specified distribution) within the limits of the l-th zone. For each zone, define

$$Q_l^{cr}=Q_l^{(0)}K_l^{\min},\quad l=1,2,\ldots,M_Q. \tag{7}$$

Then for all the regulation zones the following conditions may be imposed

$$Q_l\leqslant Q_l^{cr},\quad l=1,2,\ldots,M_Q. \tag{8}$$

There is also a natural constraint for the CR

$$0\leqslant\rho_j\leqslant 1;\quad j=1,2,\ldots,n. \tag{9}$$

Finally, for all the energy distributions considered a final condition is imposed: the balance of the total reactivity must remain within a given limit

$$\left|\sum_{j=1}^{n}(\rho_j-\rho_j^{(0)})\right|\leqslant\delta\rho. \tag{10}$$

Of all the possible energy distributions, i.e., those satisfying Eqs. (8)-(10), other conditions being equal, the best (in terms of reactor reliability or the possibility of increasing its power while retaining reliability) is that for which the maximum of Q_l/Q_l^{cr} over the active region h has the smallest value. The fundamental relation of the optimization problem may be formulated as follows

$$\max_l\{Q_l/Q_l^{cr}\}=\min. \tag{11}$$

Substituting into Eq. (8) the expression for Q_l and using Eqs. (6) and (7)

$$\frac{1}{K_{ml}^{\min}}+\sum_{j=1}^{n}\gamma_{ej}(\rho_j-\rho_j^{(0)})\leqslant 1,\quad l=1,2,\ldots,M_Q, \tag{12}$$

where $\gamma_{ej}=(1/Q_l{}^{(0)}K_{ml}^{\min})\beta_{lj}$.

Equations (9), (10), and (12) constitute the total system of constraints in the problem and its aim is given by the requirement

$$\max_l\left\{\frac{1}{K_{ml}^{\min}}+\sum_{j=1}^{n}\gamma_{ej}(\rho_j-\rho_j^{(0)})\right\}=\min. \tag{13}$$

Algorithm for the Solution of the Problem

In the given formulation, the problem is a typical minimax problem. However, the use of the methods of minimax theory is attended by a number of difficulties – primarily the tabular and not analytical description of the optimizing functions, the great dimensionality of the blocks, etc. Therefore methods of linear-programming theory were considered and used.

The specific features of the problem require its brief formulation in terms of linear-programming theory [3]. $2M_Q+2$ additional variables $Y_1, Y_2, \ldots, Y_{2M_Q+2}$ are introduced as follows.

The first M_Q variables convert Eq. (12) from an inequality to the equation

$$\frac{1}{K_{ml}^{\min}}+\sum_{j=1}^{n}\gamma_{ej}(\rho_j-\rho_j^{(0)})+Y_l=1. \tag{14}$$

The variables Y_{2M_Q+1} and Y_{2M_Q+2} are introduced from the condition

$$Y_{2M_Q+1}\geqslant\frac{1}{K_{ml}^{\min}}+\sum_{j=1}^{n}\gamma_{ej}(\rho_j-\rho_j^{(0)}), \tag{15}$$

$$l=1,2,\ldots,M_Q;$$

$$Y_{2M_Q+2} = \sum_{j=1}^{n} (\rho_j - \rho_j^{(0)}). \tag{16}$$

The variables Y_{M_Q+1}, Y_{MQ+2}, . . ., Y_{2M_Q} convert Eq. (15) from an inequality to the equation

$$Y_{2M_Q+1} = \frac{1}{K_{ml}^{\min}} + \sum_{j=1}^{n} \gamma_{ej} (\rho_j - \rho_j^{(0)}) + Y_{M_Q+l}. \tag{17}$$

It is evident that all the additional variables are obtained by the following inequalities

$$\begin{gathered} 0 \leqslant Y_l \leqslant 1, \quad l = 1, 2, \ldots, M_Q; \\ 0 \leqslant Y_{M_Q+l} \leqslant \infty, \quad l = 1, 2, \ldots, M_Q; \\ Q_l/Q_l^{cr} \leqslant Y_{2M_Q+1} \leqslant \infty; \\ -\delta\rho \leqslant Y_{2M_Q+2} \leqslant \delta\rho. \end{gathered} \tag{18}$$

The variable Y_{2M_Q+1} requires minimization

$$Y_{2M_Q+1} = \frac{1}{K_{ml}^{\min}} + \sum_{j=1}^{n} \gamma_{lj} (\rho_j - \rho_j^{(0)}) + Y_{M_Q+l} = \min. \tag{19}$$

Equation (19), together with Eqs. (9), (14), and (16)-(18), is the canonical formula of the linear-programing problem with two sets of bounds on the variables, and Eqs. (13) and (19) are then equivalent.

What conditions must the solution of this problem satisfy? Suppose that some vector $\rho^{opt} = (\rho_1^{opt}, \rho_2^{opt}, \ldots, \rho_n^{opt})$ minimizing the linear form in Eq. (19) under the conditions in Eqs. (9), (14), and (16)-(18) is found. The corresponding set of energy distributions over the cells Q_l^{opt} evidently has the following properties:

1) Q_l does not exceed Q_l^{cr} in any of the M_Q zones;

2) the maximum of the mean regulation-zone power is less than the maxima of other possible energy distributions determined by other vectors $[\rho = (\rho_1, \rho_2, \ldots, \rho_n)]$;

3) on passing from the initial energy distribution characterized by $\rho^{(0)} = (\rho_1^{(0)}, \rho_2^{(0)}, \ldots, \rho_n^{(0)})$ to the optimal distribution (with ρ^{out}) the reactivity balance is not disturbed.

Thus, within the limits of the assumptions adopted, the energy distribution having the minimum value of K_r (in the set of all possible energy distributions with fixed reactor power) is obtained.

Results of Calculations

To implement the above algorithm in ALGOL on a BÉSM-6 computer, the optimal-rod-control program OPUS was developed. It solves the optomization problem by the simplex method [3]; the minimum permissible size of a regulation zone is 3 × 3 HLP. Calculations with zones of 4 × 4 HLP and 89 CR require about 30 min, including the time for sufficiently thorough methodological calculations, mainly for the treatment of the initial energy distribution and those obtained by optimization and also for the formation of the initial simplex matrix. The "pure" time for the operation of the optimization subprogram of the simplex method is about 20 min. Hence, a successful programing solution of this problem, with the maximum possible elimination of superfluous calculations of "long-lived" constants, allows the total time for the determination of the optimum energy distribution on a BÉSM-6 computer to be reduced to 20 min.

It is of interest to consider the results of calculations with the above algorithm. The calculations also involved, as a control, the QUAM program for neutron-physics calculations of the high-boiling reactor [4], by means of which, on the basis of actual data on the state of the high-boiling reactor at any moment of its use, the energy distribution in the active zone was calculated. This energy distribution was then introduced, together with the corresponding data on CR positions, into the OPUS program. The optimum rod positions obtained were then introduced as initial data into the QUAM program, which was used to calculate a new energy distribution. The energy distributions according to the OPUS and QUAM (the second calculation with the optimum rod positions) programs were compared. The nonuniformity coefficients of the radial HLP power distribution (K_r) and the regulation zone K_Q were compared. This whole set of calculations will be referred to below as a step. The calculations were carried out for different states of the reactor.

The state of the high-boiling reactor of the second unit of the Leningrad APS on Oct. 30, 1975, was taken as an example. It should be noted that the energy distribution in the reactor differed somewhat from the calculated distribution. For example, the real value of K_r was smaller. The results are shown in Table 1, where

TABLE 1. Change in Some Characteristics of the Energy Distribution during Optimization

Characteristic	Step No.			
	0	1	2	3
$K_{r(i)}^{QUAM}$	1,529	1,398	1,379	1,378
$K_{Q(i)}^{QUAM}$	1,406	1,238	1,229	1,229
$K_{r(i)}^{OPUS}$	—	1,373	1,368	1,364
$K_{Q(i)}^{OPUS}$	—	1,228	1,220	1,220
$\sigma_{OPUS-QUAM}^{(i)}$, %	—	2,20	1,78	1,78

the following notation has been adopted: $K_{r(0)}^{QUAM}$ and $K_{Q(0)}^{QUAM}$ are the initial values of K_r and K_Q obtained by the QUAM program; $K_{r(i)}^{QUAM}$, $K_{Q(i)}^{QUAM}$, $K_{r(i)}^{OPUS}$, and $K_{Q(i)}^{OPUS}$ are the values of K_r and K_Q obtained in the QUAM and OPUS programs as a result of the i-th step of the calculation; $\sigma_{OPUS-QUAM}^{(i)}$ is the mean square deviation between the energy distribution obtained by the two programs as a result of the i-th step of the calculations. It is evident from Table 1 that the optimum energy distribution is formed practically at the second step of the calculations. Similar results were obtained for other reactor states.

The permissible reactivity imbalance $\delta\rho$ in the calculations using the OPUS program was taken to be unity, i.e., the reactivity before and after optimization may differ by no more than the mean efficiency of a single CR. Although this condition was not violated, it should nevertheless be noted that, for an actual reactivity margin smaller or larger than the optimum, this difference always had a limiting value: +1 and −1, respectively. The reactivity imbalance caused a change of within 0.05% in the effective multiplication factor Keff; this figure corresponds exactly to the main efficiency of a single CR. As calculations by the OPUS program show, the optimum reactivity margin for the high-boiling reactor (ensuring the minimum K_r) is 35-40 CR.

In analyzing the results it must first be remembered that in the QUAM program, in contrast to the OPUS program, the CR position is described in discrete steps of 0.5 m. Therefore, the accurate values of the optimum rod position obtained from the OPUS program are rounded to the nearest 0.25 m when they are introduced in the QUAM program. This may, of course, effect the results, though it would be difficult to say to what extent.

The results seem to confirm that the two assumptions on which the optimization algorithm rests are valid (at least for the high-boiling reactor). The analysis of the results indicates that the convergence of the calculation process is rapid and, for practical purposes, one step is evidently sufficient for the refinement of the influence function of the rods.

The method outlined seems to offer two possible directions of development. First, calculations once or twice a day may provide the basis for determining the operational settings and may give useful guidance to the operator of the reactor. After APS have been equipped with computers considerably faster than existing models, an optimization program based on the above algorithm may be included in a set of programs for the operational regulation of the energy distribution. The optimum energy distribution may then be realized by a simultaneous linear change in ρ from $\rho^{(0)}$ to ρ^{out} producing a linear transition from $Q_l^{(0)}$ to Q_l^{opt}. Finally, this method may serve as the control for various kinds of approximate method, which, as may be expected, ensure more rapid operation, and also may be used in different kinds of problem on the optimization of reactor use.

LITERATURE CITED

1. R. Grumbach, in: Proceedings of an IAEA Symposium on the Development and Application of Advanced Concepts for Nuclear Plant and Core Control, Prague (1973), p. 303.
2. I. Ya. Emel'yanov et al., At. Energ., 42, No. 4, 263 (1977).
3. D. B. Yudin and E. G. Gol'shtein, Linear Programming [in Russian], Fizmatgiz, Moscow (1963).
4. S. S. Gorodkov, Institute of Atomic Energy Preprint IAÉ-2294, Moscow (1973).

COMPREHENSIVE USE OF TRANSPLUTONIUM ELEMENTS – BY-PRODUCTS OF THE NUCLEAR POWER INDUSTRY

V. N. Kosyakov and I. K. Shvetsov

UDC 546.799:621.039.004.1

With the development of the nuclear power industry, in the near future transplutonium elements (TPE) will begin to build up in the fuel elements of atomic power plants in quantities running into tons. From the point of view of toxicity and half-lives, TPE pose a much greater danger than ordinary fission products do. The large quantity in which they occur can greatly complicate the problem of burial of radioactive waste and this reflects upon the cost of the energy obtained from atomic power plants.

The first step toward the solution of this problem may be made by the development of new methods for the maximum extraction of TPE in the stage of chemical processing of the nuclear fuel. It was shown in [1] that the danger in handling radioactive waste from processing of spent fuel elements containing plutonium and TPE is reduced to the danger from ordinary fission products if 99.99% of the plutonium isotopes and 99.9% of the TPE isotopes are extracted. Apparently, this is feasible in principle, although it does require some improvement in the technology for processing spent nuclear fuel. A second problem arises: what should be done with the extracted TPE? The authors of several recent papers [2, 3] considered the possibility of completely "burning" TPE to fission products in the same power reactors or special-purpose reactors. These ideas are based on the fact that roughly half the TPE isotopes, through which the nuclear transformation chain passes, are fissionable (have high values of σ_f and $\bar{\nu}$). With such an approach, however, no account is taken of the possibility of using TPE isotopes which have unique nuclear properties (Table 1). Since accumulation of considerable amounts of TPE is not expected before the end of the century, it may be assumed that by that time new possibilities will appear for the use of TPE in various branches of science and engineering.

The latest data on the accumulation of TPE isotopes in VVÉR water-moderated–water-cooled power reactors [3-5] (Table 2) can be used to estimate the annual accumulation of TPE isotopes in the reactors of an atomic power plant with a total power of, e.g., 100 GW. It follows from Table 2 that the yield of TPE isotopes depends strongly on whether or not the plutonium is used as a nuclear fuel.

For nuclear power generation with the indicated power for thermal reactors operating on uranium fuel the annual accumulation of plutonium is ~25 tons. It may be assumed that this plutonium will be burned in uranium–plutonium reactors (fast breeder reactors are not considered here for the moment). The present paper considers the annual accumulation of plutonium and TPE isotopes in the system of atomic power plant with a total power of 100 GW(electrical), consisting of reactors operating on uranium fuel (80%) and uranium–plutonium fuel (20%) and possible ways of using the plutonium and TPE isotopes obtained.

If all the plutonium separated during the chemical processing of fuel elements (it will contain 7.5 tons of ^{241}Pu in all) is held for a year, the ~380 kg of isotopically pure ^{241}Am will build up in it and this isotope can be isolated by chemical processing before the plutonium is charged into a reactor. Chemical reprocessing of irradiated fuel can separate more than two tons of a mixture of the isotopes ^{241}Am and ^{243}Am as well 225 kg of ^{244}Cm.

If the americium and curium isotopes are completely extracted during each chemical processing, the accumulation of isotopes of other TPE (e.g., berkelium and californium) can be neglected since their yields are 5-6 orders of magnitude below that of ^{244}Cm. Plutonium fuel, which in actual fact is a mixture of isotopes including ^{239}Pu and ^{241}Pu, is fissionable, can be used repeatedly, and with complete burn-up is transformed into long-lived ^{242}Pu with a yield of ~10% of the initial plutonium, i.e., 2.5 tons/yr.

Let us consider the feasibility of the practical use of the isotopes obtained. As an α-emitter ^{241}Am can be employed to remove electrostatic charge, to produce neutron sources, etc. Besides α rays, this isotope also emits monoenergetic x rays (~35%) with an energy of 59.6 keV which can be used for a number of analytical purposes, especially in x-ray fluorescence elementary analysis, as well as for continuous measuring of density, thickness, defects, etc. Only an insignificant quantity of the isotope obtained is required for this. Its

Translated from Atomnaya Énergiya, Vol. 44, No. 4, pp. 315-319, April, 1978. Original article submitted December 26, 1976; revision submitted August 1, 1977.

0038-531X/78/4404-0360$07.50

TABLE 1. Nuclear Properties of Some TPE Isotopes (according to 1975 data [9])

Isotope	Character of decay	Half-life	Specific energy release, W/g	σ_{2200}		I	
				c	f	c	f
^{238}Pu	α	87.75 yr	0,567	559	17,3	164	25
^{240}Pu	α	6537 yr	$7{,}1\cdot10^{-3}$	289,5	0,030	8013	—
^{241}Pu	β	14,8 yr	$4{,}0\cdot10^{-3}$	362	1015	162	570
^{242}Pu	α	$3{,}87\cdot10^{5}$ yr	$1{,}18\cdot10^{-4}$	18,5	0	1275	4,7
^{241}Am	α	433 yr	0,107	in G 748 in I 83,8	3,4	in G 1330 I 208	21
^{242G}Am	83% β; 17% EC*	16,02h	1000	—	2100	—	$\leqslant 300$
^{242I}Am	IR absorption	152 yr	$2{,}8\cdot10^{-3}$	—	7600	—	1570
^{243}Am	α	7400 yr	$6{,}0\cdot10^{-3}$	77	0	1927	3,34
^{242}Cm	α	163 days	122	20	$\leqslant 5$	150	~ 0
^{243}Cm	α	30 yr	1,57	—	690	0	1860
^{244}Cm	α	18,1 yr	2,91	10,6	1,1	585	17,9
^{245}Cm	α	8532 yr	$6{,}4\cdot10^{-3}$	383	2161	104	766

*EC – electron capture.

TABLE 2. Amount of Principal TPE Isotopes Formed in VVÉR Reactors of 1 GW (electrical)

Isotope	Yield, kg/yr		Isotope	Yield, kg/yr	
	U fuel	U – Pu fuel		U fuel	U – Pu fuel
^{240}Pu	56	500	^{241}Am	4,3	32
^{241}Pu	23	290	^{243}Am	2,7	43
^{242}Pu	10	200	^{244}Cm	0,66	8,7

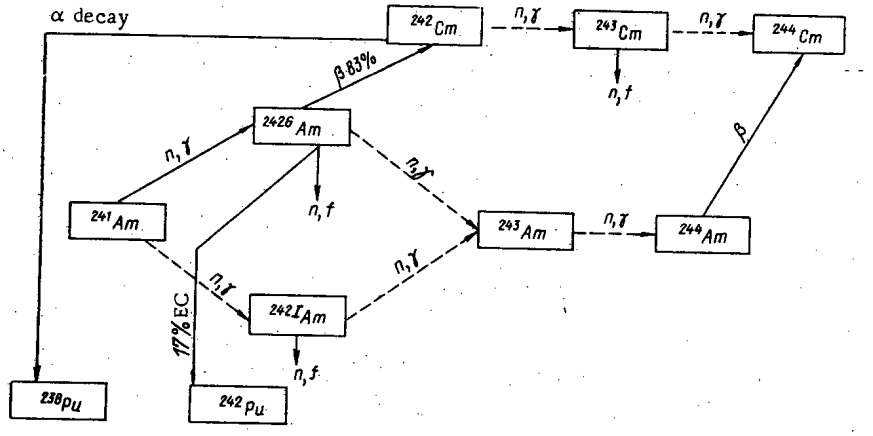

Fig. 1. Diagram illustrating production of ^{242}Cm under irradiation of americium by thermal neutrons. EC – electron capture.

main use could be as a starting material to obtain ^{242}Cm (Fig. 1). The yield of ^{242}Cm and other impurity isotopes will depend on the irradiation conditions [6]. Thus, irradiation of 1 kg ^{241}Am with a fluence of $1.2\cdot10^{21}$ neutrons/cm^2 at a flux density of $1.8\cdot10^{14}$ neutrons/cm$^2\cdot$ sec yields 350 g ^{242}Cm, 350 g ^{241}Am, 170 g of a mixture of isotopes of plutonium isotopes (mainly ^{238}Pu and ^{242}Pu with an admixture of ^{239}Pu), 30 g ^{243}Am, and 100 g fission products [7]. Hence, when chemically processed 380 kg irradiated ^{241}Am can yield ~200 kg almost isotopically pure ^{242}Cm with an extremely high specific energy release (120 W/g), which in total is equivalent to a thermal source with a power of ~25 MW. Sources based on ^{242}Cm enable high temperatures to be attained (> 1000°C). Thus, when thermally stable compounds (Cm_2O_3) of density 10 g/cm^3 are used ^{242}Cm will ensure a heat release of 1.2 kW/cm^3. Individual sources based on ^{242}Cm have limited application because of their short operating life ($T_{1/2}$ = 163 days). However, assemblies of many sources continuously replenished with fresh sources can, in our opinion, be used successfully in stationary high-temperature facilities, especially for pyrolysis of water to obtain hydrogen. Completely exhausted sources can be sent for chemical processing to separate the daughter product, isotopically pure ^{238}Pu suitable for medical applications (^{238}Pu obtained from

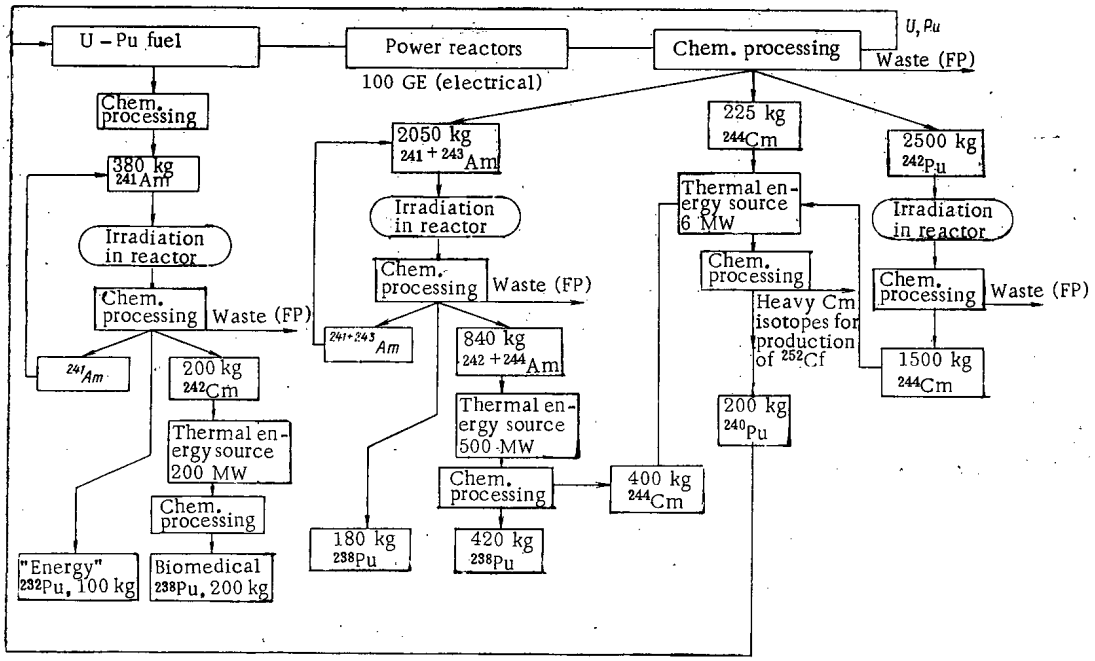

Fig. 2. Diagram of comprehensive use of TPE.

irradiation of ^{237}Np contains ^{236}Pu and is not suitable for these purposes). At the same time ~100 kg of "energy" ^{238}Pu is formed (with an admixture of ^{239}Pu and ^{242}Pu), suitable for isotopic generators; when the sources are processed, the ^{234}U formed in the decay of ^{238}Pu can be returned to the reactor cycle.

In the irradiation of a mixture of ^{241}Am and ^{243}Am, commensurate quantities of ^{244}Cm, whose content depends on the irradiation conditions, will be obtained in addition to ^{242}Cm and ^{238}Pu, containing ^{242}Pu and ^{239}Pu. Irradiation of short duration in a neutron flux of moderate density gives the best results from the point of view of ^{242}Cm yield. For example, irradiation of a mixture of ^{241}Am and ^{243}Am (60+40%) for series of short periods (of 3 months) at a flux density of $5 \cdot 10^{13}$ neutrons/cm^2 · sec until complete burnup of the americium isotopes occurs produces a mixture of ^{242}Cm and ^{244}Cm with a roughly 20% yield of each isotope [8].

Thus, if ~2 tons of a mixture of americium isotopes is irradiated under optimal conditions, after chemical processing we get ~820 kg of a mixture of ^{242}Cm and ^{244}Cm (50 MW) as well as 180 kg (90 kW) of "energy" ^{238}Pu (containing ^{242}Pu and ^{239}Pu). The mixture of curium, as well as pure ^{242}Cm, can be used in high-temperature energy installations since its specific energy release will be ~62 W/g. By processing spent sources (from the point of view of ^{242}Cm) it is possible to obtain ^{238}Pu with a low content of ^{240}Pu (~2.5%). In respect of its radiation properties, this plutonium differs little from biomedical ^{238}Pu. Its total quantity is ~420 kg (or 210 kW). In addition to plutonium there will also be 400 kg ^{244}Cm which can be combined with the ^{244}Cm obtained when spent fuel elements are processed.

Some 225 kg of ^{244}Cm can be extracted each year by processing spent fuel elements from atomic power plants. Processing of sources based on a mixture of ^{242}Cm and ^{244}Cm will leave 400 kg of ^{244}Cm. Moreover, by special irradiation of 2.5 tons ^{242}Pu it is possible to get no less than 1.5 tons of ^{244}Cm, i.e., the total ^{244}Cm yield can come to ~2 tons/yr, which is equivalent to 6 MW (thermal). The isotope ^{244}Cm is an α emitter with a half-life of 18.1 years and an energy release of 2.9 W/g and is highly suited for the construction of generators of thermal and electrical energy. The stable operating life of an isotopic generator based on ^{244}Cm (~2 years) is much higher than that of a ^{242}Cm generator. These generators have the following advantages over ^{238}Pu generators.

1. The higher energy release ensures greater compactness (29 W/cm^3) which permits higher temperatures to be attained and enables thermionic converters with a higher conversion coefficient to be used.

2. The fact that the critical mass of ^{244}Cm is higher than that of ^{238}Pu (55.8 kg for ^{244}Cm and 28.5 kg for ^{238}Pu [10]) makes it possible to construct a source with a maximum power roughly 10 times that attainable with ^{238}Pu.

A disadvantage of ^{244}Cm in comparison with ^{238}Pu is its much higher yield of spontaneous fission neutrons and highly energetic γ rays which necessitates additional biological shielding.

Upon completion of their service life ^{244}Cm sources can be subjected to chemical processing which can extract the ^{240}Pu formed and some quantities of heavy isotopes of curium. The ^{240}Pu can be returned to the plutonium fuel for burning up and the heavy curium isotopes can be irradiated in a high-flux reactor to obtain ^{252}Cf in the required quantities. The isotope ^{242}Pu is of no practical importance as yet but it can serve as a convenient starting meterial for obtaining ^{244}Cm and other heavy isotopes of curium, as well as berkelium and californium. Thus, under irradiation in a high-flux reactor it can be almost completely transmuted into ^{244}Cm, whose application has already been considered.

As is seen from the estimates made above, the total quantity of curium isotopes extracted in a year is equivalent to a thermal power of 80 MW. Such a power, besides the well-known use for low-power autonomous generators of heat and electricity, can be used in any stationary high-temperature facility, e.g., for obtaining hydrogen. Calculation shows that by using a heat source containing 10 kg ^{244}Cm (volume ~1 liter) or 250 g ^{242}Cm it is theoretically possible to obtain a flow of helium at a temperature of ~1000°C and a volume flow rate of ~30 liters/sec.

To reduce energy losses during storage and transportation of powerful thermal generators (especially when ^{242}Cm is used) it is apparently desirable to combine such a unit for the technical use of high-temperature heat into one technological complex with units for producing isotopic generators and for chemical processing as well as with a reactor making it possible to carry out irradiation under the necessary conditions. Such a unified technological complex can give maximum economic effect and appreciably reduce the potential risk from uncontrolled handling of isotopic sources ^{238}Pu and provide small users with low-power sources of radiation and energy sources based on ^{238}Pu, ^{241}Am, ^{242}Cm, ^{244}Cm, ^{252}Cf.

The comprehensive use of plutonium and TPE isotopes (Fig. 2) in the final analysis gives a large yield of high-temperature heat, ^{238}Pu (800 kg) for isotopic generators, and some quantities of ordinary fission products which are present in any case during the processing of irradiated nuclear fuel.

LITERATURE CITED

1. H. Clairborne, ORNL-TM-4724 (1975).
2. L. Koch, G. Cotton, and A. Cricchio, in: Proceedings of the Fourth International Symposium on Transplutonium Elements, North-Holland, Amsterdam (1976), p. 459.
3. S. Raman, in: Proceedings of the Advisory Group Meeting on Transactinium Isotope Nuclear Data, Karlsruhe, Nov. 3-7 (1975), Vol. 1, p. 39.
4. T. Pigford, Ann. Rev. Nucl. Sci., 24, 515 (1974).
5. H. Kunsters and M. Lalovic, in: Proceedings of the Advisory Group Meeting on Transactinium Isotope Nuclear Data, Karlsruhe, No. 3-7 (1975), Vol. 1, p. 139.
6. D. Stewart, R. Anderson, and J. Milsted, USAEC-Rep., ANL-6933 (1965).
7. E. Lamb, "Large-scale production of radioisotopes by neutron irradiation and preparation of radioisotope power sources," in: Proceedings of the ANL Conference on Large-Scale Production and Application of Radioisotopes, U. S. A., Mar. 21-23, 1966, Vol. 2.
8. L. Lang, "Application of power reactor fuel americium for optimization of alpha-isotope production," in: Proceedings of the Conference on Large-Scale Production and Application of Radioisotopes, U. S. A., Mar. 21-23, 1966, Vol. 2.
9. R. Benjamin, in: Proceedings of the Advisory Group Meeting on Transactinium Isotope Nuclear Data, Karlsruhe, Nov. 3-7 (1975), Vol. 2, p. 1.
10. E. Clayton and S. Bierman, Actinide Rev., 1, 409 (1971).

THE CONSTRUCTION OF COORDINATE FUNCTIONS IN THE METHOD OF IMBEDDED ELEMENTS FOR BOUNDARY-VALUE PROBLEMS OF REACTOR THEORY

V. V. Kuz'minov, I. S. Slesarev, and A. A. Dudnikov

UDC 539.125.52:621.039.51.12

The transition to more realistic models in computational investigations of reactors is linked with the search for the possibility of a suitable description of the model and the development of an effective algorithm for the solution of the transport equation under conditions of a complex (arbitrary in the general case) shape of the zones. The expectations determined in this way are related to the use of the method of imbedded elements (MIE) [1, 2]. Coordinate functions satisfying the principal conditions are used in the known MIE schemes. New MIE schemes are proposed in this paper. The effectiveness of the method is shown in a problem in which a part of the external boundary conditions belongs to the class of natural ones, but fulfillment of these conditions is not required of the coordinate functions. Methods are discussed of constructing coordinate functions satisfying the natural conditions, which permits one to expect an increase in the convergence rate to the exact solution.

Several methods have been suggested in [3] for constructing coordinate functions for problems having complex geometry. The regionally structured method is of special interest in problems having piecewise-constant properties of the medium. The proposed construction schemes are applicable to the special cases of heterogeneous composition of the system and are distinguished by the rather complicated structure of the coordinate functions.

The MIE has been calculated for a model representing a reactor in the form of a region consisting of arbitrarily arranged zones of complex geometrical shape with constant neutron-physical properties. The basis of MIE consists of the approximation of the solution Φ of the diffusion equation by a set of polynomials P_i which differ from zero in separate parts (elements) Ω_i of the calculated system, vanish at the boundaries of the corresponding elements, and satisfy the conditions $P_i \neq 0$ in Ω_i and $P_i \equiv 0$ outside Ω_i. The coefficients of the polynomials are the unknowns, and the system of equations which determine the coefficients is obtained from the variational principle. The construction of coordinate functions for regions of complex shape is significantly simplified within the framework of MIE (in comparison with the data of [3]), and the possibility appears of constructing an approximate solution with known coupling conditions in cases of a more complex composition of the system.

Typical boundary conditions for the neutron flux density on the external boundary Γ are represented in the form

$$\Phi(r)|_\Gamma = a, \tag{1}$$

(here a is a specified function) and

$$\left[\frac{\partial\Phi(r)}{\partial\nu} + \gamma(r)\Phi(r)\right]\Big|_\Gamma = 0, \tag{2}$$

where ν is the normal to the boundary.

On the inner boundaries of zones with the normal ν continuity conditions of the product $D(r)[\partial\Phi(r)/\partial\nu]$ are valid, where D(r), the diffusion coefficient, is a piecewise-constant function of the coordinates. Taking account of the fact that the continuity condition of $D(r)[\partial\Phi(r)/\partial\nu]$ is a natural one for the differential operator of the diffusion equation, which in operator form is

$$L\Phi(r) = \frac{1}{k} M\Phi(r), \tag{3}$$

for a homogeneous equation and

Translated from Atomnaya Énergiya, Vol. 44, No. 4, pp. 319-323, April, 1978. Original article submitted January 20, 1977.

0038-531X/78/4404-0364$07.50

$$L\Phi(r) = Q(r), \tag{4}$$

for an inhomogeneous equation, we set up a functional F for problems (3) and (4) and the boundary conditions (1) and (2), respectively:

$$F[\Phi] = \frac{1}{\Delta}\left\{\left(\Phi^+(r),\ M\Phi(r)\right)_V + \int \gamma(r)\,\Phi^+(r)\,\Phi(r)\,d\Gamma\right\};$$

$$F[\Phi] = \Delta + \left(\Phi(r), Q^+(r)\right)_V - \left(\Phi^+(r), Q(r)\right)_V - \int \gamma(r)\,\Phi(r)\,\Phi^+(r)\,d\Gamma,$$

where $\Delta = (\Phi^+, L\Phi)_V$ is the scalar product of the phase variables in the volume V made symmetrical with the aid of conditions on the inner boundaries and $\Phi^+(r)$ is a weighting (coupling) function.

It is well known that (1) and the continuity conditions of the solution of the diffusion problem are dominant in the variational formulation; therefore, they stand out as the principal requirements on the coordinate functions. The boundary conditions (2) and the continuity of $D(r)[\partial\Phi(r)/\partial\nu]$ are natural conditions, and this means that they are optional for coordinate functions. The exact fulfillment of these conditions is usually achieved only in the limit.

Let us cite as an illustration the calculation of the neutron distributions $\Phi(r)$ in a sector of a reactor (Fig. 1) on two boundaries Γ_1 and Γ_2 of which symmetry conditions [a particular case of the condition (2)] are specified, and on whose third boundary Γ_3 the null Dirichlet conditions are specified:

$$\Phi(r)|_{\Gamma_3} = 0;\quad \frac{\partial\Phi(r)}{\partial\nu}\Big|_{\Gamma_1,\,\Gamma_2} = 0. \tag{5}$$

The macroscopic constants of the sector are given in Table 1. The system to be calculated is divided into twelve elements: OCD, ABCD, D'C'CD, ABC'D', A'B'C'D', ABB'A', OBA, ONN', K'KNN', OKK', N'NBA, and zone IV in the form of a circle. It is expected that the azimuthal neutron flux density distribution (Fig. 2) will be altered most significantly along the curve LL' (see Fig. 1). Let us consider the two cases:

$$S_{ABCD} = 2;\quad S_{OAB} = 2;\quad S_n = 0$$

and

$$S_{ABCD} = 2;\quad S_{OAB} = 4;\quad S_n = 0,$$

where S_n is the degree of the polynomial in the element n. Normalization of the approximate solution Φ of the homogeneous equation is performed on the value of the flux density at the point L' $[\widetilde{\Phi}(L') = 5, 4]$. The increase in the accuracy of fulfillment of the boundary conditions (5) is appreciable upon an increase of just the degree of the polynomials S_{OAB}.

The MIE scheme used in this example [1, 2] is directed towards fulfillment of only the principal conditions, which simplifies significantly the computational algorithm. However, for a satisfactory description of the distributions near the boundaries it is necessary in such schemes to use sufficiently many coordinate functions (and this means coefficients to be determined). Methods exist for the construction of coordinate functions within the framework of MIE which satisfy exactly all (including the natural ones) boundary conditions and the "matching" conditions of the solution on the inner boundaries of the reactor zones. As a rule, the MIE schemes in which such functions are used are complicated, require a lot of computational effort, but are eco-

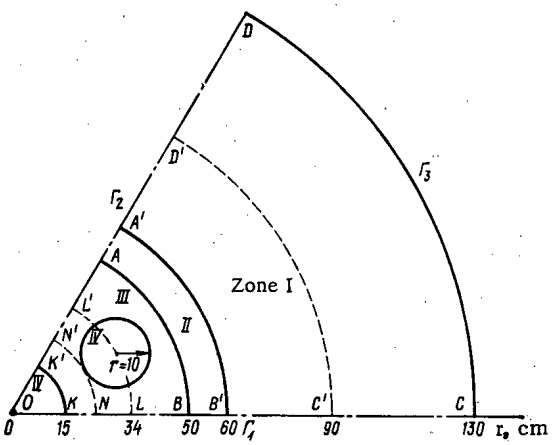

Fig. 1. Reaction model.

TABLE 1. Zone Properties

Group	Macroscopic constants	Zone I	Zone II	Zone III	Zone IV
1	D, cm	1,368	0,976	1,580	2,581
	Σ_{ad}, cm^{-1}	0,026	0,00776	0,0182	0,00672
	$\nu\Sigma_f$, cm^{-1}	0	0	0	0,0098
2	D, cm	0,940	0,281	0,957	0,891
	Σ_{ad}, cm^{-1}	0,000213	0,00246	0,00000118	0,0124
	$\nu\Sigma_f$, cm^{-1}	0	0	0	0,0143
	$\Sigma^{1\to 2}$, cm^{-1}	0,026	0,00626	0,0182	0,00228

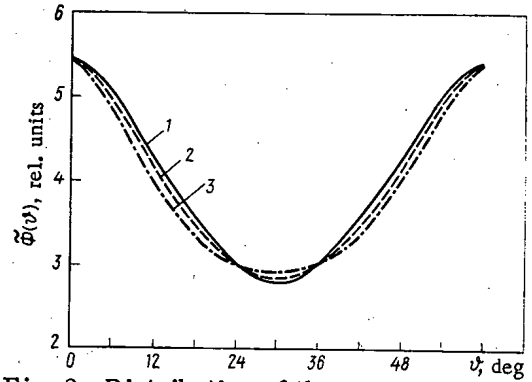

Fig. 2. Distribution of the approximate and asymptotic neutron flux density (group 2) along the curve LL': 1) asymptotic solution of the problem ($S_n\to\infty$; n = 1, 2, . . ., 12); 2) $S_{OAB}=2$; and 3) $S_{OAB}=4$.

nomical with respect to computer memory requirements due to the lower dimensionality of the matrix operators and vectors, which consist of the polynomial coefficients.

Let us proceed to an exposition of methods for the construction of coordinate functions which satisfy exactly the boundary conditions on the external boundary of the reactor. In order that an approximate solution in MIE satisfy the boundary conditions (both the principal ones and the natural ones), it is necessary to select in the outer element the appropriate approximating function $\Phi_0(r)$ which ensures fulfillment of the specified conditions. In constructing such a function we use the following structure [3]:

$$R_0=\varphi_0-\tilde{\omega}_0 D_1\varphi_0+\tilde{\omega}_0\psi, \tag{6}$$

where $\tilde{\omega}_0$ is the normalized equation of the external boundary of the region Ω_0, $\tilde{\omega}_0|_{\Gamma_0}=\frac{\partial^n\tilde{\omega}_0}{\partial\nu^n}\Big|_{\Gamma_0}=0$; $n=2,\ 3,\ldots$; $\frac{\partial\tilde{\omega}_0}{\partial\nu}\Big|_{\Gamma_0}=1$; ν is the inner normal to Γ_0; $D_1\equiv\frac{\partial\omega_0}{\partial x}\frac{\partial}{\partial x}+\frac{\partial\tilde{\omega}_0}{\partial y}\frac{\partial}{\partial y}$. The structure (6) takes the values

$$R_0|_{\Gamma_0}=\varphi_{0\ \Gamma_0}\text{ and }\ \frac{\partial R_0}{d\nu}\Big|_{\Gamma_0}=\psi|_{\Gamma_0} \tag{7}$$

on the boundary Γ_0.

Let the boundary Γ_0 be divided into N smooth segments, and let Γ_0 not necessarily be a smooth curve. Then the "splicing" formula

$$\varphi=\frac{\varphi_1\tau_1^{m_1}+\ldots+\varphi_N\tau_N^{m_N}}{\tau_1^{m_1}+\ldots+\tau_N^{m_N}}, \tag{8}$$

which provides for fulfillment of the conditions

$$\varphi|_{\Gamma_k}=\varphi_k|_{\Gamma_k};\quad \frac{\partial^i\varphi}{\partial\nu^i}\Big|_{\Gamma_k}=\frac{\partial^i\varphi_k}{\partial\nu^i}\Big|_{\Gamma_k};$$
$$i=1,\ 2,\ldots,m_N-1;\quad k=1,\ 2,\ldots,N.$$

is another useful relation. Here $\tau_k = 1/\tilde{\omega}_k$, where $\tilde{\omega}_k$ is the normalized equation of the part of the boundary Γ_k.

In the general case the "splicing" formula and structure of the form (6) are simultaneously used in connection with the construction of functions satisfying different conditions on various segments Γ_k of the boundary. One can distinguish two approaches in the use of the "splicing" formula and the structure (6) in construction of the required function $\Phi_0(r)$:

1) the function $\Phi_0(r)$ is selected in the form (8), and the unknown functions φ_k are sought in the form

$$\varphi_k = \tilde{\varphi}_{0k} - \tilde{\omega}_k D_1 \tilde{\varphi}_{0k} + \tilde{\omega}_k \psi_k$$

so that the φ_k ensure fulfillment of the specified conditions on the segment Γ_k of the boundary; and

2) the function $\Phi_0(r)$ is taken in the form (6), and the unknown functions φ_0 and ψ are sought in the form (8) so that φ_0 and ψ ensure fulfillment of the specified conditions on the entire boundary.

Using the first approach for the reactor illustrated in Fig. 1, let us construct a function $\Phi_0(r)$ which ensures fulfillment of the conditions (5) on the segments Γ_1, Γ_2, and Γ_3, the normalized equations of which one can represent respectively as

$$\tilde{\omega}_1 = y; \quad \tilde{\omega}_2 = x \sin\theta - y\cos\theta \,(\theta = 60°); \quad \tilde{\omega}_3 = \frac{1}{2R}(R^2 - x^2 - y^2). \tag{9}$$

We seek the function $\Phi_0(r)$:

$$\Phi_0(r) = \frac{\varphi_1\tau_1^2 + \varphi_2\tau_2^2 + \varphi_3\tau_3}{\tau_1^2 + \tau_2^2 + \tau_3},$$

and the unknown functions φ_1 and φ_2 are represented as

$$\varphi_1 = \tilde{\varphi}_{01} - \tilde{\omega}_1 D_1 \tilde{\varphi}_{01} + \tilde{\omega}_1 \psi_1;$$
$$\varphi_2 = \tilde{\varphi}_{02} - \tilde{\omega}_2 D_1 \tilde{\varphi}_{02} + \tilde{\omega}_2 \psi_2,$$

and φ_3 is determined immediately from the boundary conditions (5):

$$\varphi_3|_{\Gamma_3} = 0.$$

Let us require of φ_1 and φ_2 the fulfillment of the conditions $\varphi_1|_{\Gamma_3} = \varphi_2|_{\Gamma_3} = 0$ and $\varphi_1 = \varphi_2$ at the point O having the coordinates $x = y = 0$. To this end let us take $\tilde{\varphi}_{01} = \varphi_{01}\tilde{\omega}_3$, $\tilde{\varphi}_{02} = \varphi_{02}\tilde{\omega}_3$. In addition it is evident from the conditions (5) and the properties of the structure (7) that ψ_1 and ψ_2 should be equal to zero: $\psi_1|_{\Gamma_1} = \psi_2|_{\Gamma_3} = 0$. After substitution of φ_1, φ_2, and φ_3 into $\Phi_0(r)$ we obtain

$$\Phi_0(r) = [(\tilde{\varphi}_{01} - \tilde{\omega}_1 D_1 \tilde{\varphi}_{01})\tau_1^2 + (\tilde{\varphi}_{02} - \tilde{\omega}_2 D_1 \tilde{\varphi}_{02})\tau_2^2](\tau_1^2 + \tau_2^2 + \tau_3)^{-1}.$$

It is evident that $\Phi_0(r)$ ensures fulfillment of the conditions (5) for any values of the functions φ_{01} and φ_{02}. One can select the latter in the form

$$\varphi_{01} = C + \sum_k A_k \eta_k; \quad \varphi_{02} = C + \sum_k B_k \eta_k,$$

where η_k are coordinate functions which one can select in the form of power functions, and C, A_k, and B_k are unknown coefficients.

For the reactor model illustrated in Fig. 1 the function $\Phi_0(r)$ takes the form

$$\Phi_0(r) = \frac{\left(\tilde{\varphi}_{01} - y\frac{\partial\tilde{\varphi}_{01}}{\partial y}\right)\frac{1}{y^2} + \left[\tilde{\varphi}_{02} - (x\sin\theta - y\cos\theta)\left(\sin\theta\frac{\partial\varphi_{02}}{\partial x} - \cos\theta\frac{\partial\varphi_{02}}{\partial y}\right)\right]\frac{1}{(x\sin\theta - y\cos\theta)^2}}{\frac{1}{y^2} + \frac{1}{(x\sin\theta - y\cos\theta)^2} + \frac{2R}{R^2 - x^2 - y^2}}$$

when the properties of the operator D_1 are taken into account. As has already been pointed out, the approximation that the function $\Phi_0(r)$ is of the form

$$\Phi_0(r) = \varphi_0 - \omega_0 D_1 \varphi_0 + \omega_0 \psi$$

lies at the basis of the second approach.

It follows from the boundary conditions (5) that the function $\Phi_0(r)$ takes null values on Γ_3 and is unknown on Γ_1 and Γ_2. Let us introduce the unknown function φ, which coincides with $\Phi_0(r)$ on all segments of the boundary. Then we have

$$\varphi|_{\Gamma_3}=0;\quad \varphi|_{\Gamma_2}=\varphi_0|_{\Gamma_2};\quad \varphi|_{\Gamma_1}=\varphi_0|_{\Gamma_1};$$
$$\psi|_{\Gamma_1}=0;\quad \psi|_{\Gamma_1}=0.$$

from the conditions (5) and the properties of the structure. Having applied the "splicing" formula to the determination of φ_0 and ψ, we find

$$\varphi_0=\frac{\varphi_1\tau_1+\varphi_2\tau_2+0\tau_3}{\tau_1+\tau_2+\tau_3}=\varphi f;$$
$$f=\frac{\tau_1+\tau_2}{\tau_1+\tau_2+\tau_3};\quad \psi=0.$$

After substitution of φ_0 and ψ into $\Phi_0(r)$ we obtain

$$\Phi_0(r)=\varphi f-\tilde{\omega}_0 D_1(\varphi f)=\varphi f-\tilde{\omega}_0\varphi\left(\frac{\partial\tilde{\omega}_0}{\partial x}\frac{\partial f}{\partial x}+\frac{\partial\tilde{\omega}_0}{\partial y}\frac{\partial f}{\partial y}\right)-$$
$$-\tilde{\omega}_0 f\left(\frac{\partial\tilde{\omega}_0}{\partial x}\frac{\partial\varphi}{\partial x}+\frac{\partial\tilde{\omega}_0}{\partial y}\frac{\partial\varphi}{\partial y}\right).$$

Here $\tilde{\omega}_0$ is the normalized equation of the boundary consisting of the segments Γ_1, Γ_2, and Γ_3; it can be determined with the aid of the R-operations $\wedge_0$ [3]:

$$\tilde{\omega}_0\equiv[y\wedge_0(x\sin\theta-y\cos\theta)]\wedge_0\frac{1}{2R}(R^2-x^2-y^2)=0,$$

where $\wedge_0$ is determined by the expression $x\wedge_0 y=x+y-\sqrt{x^2+y^2}$.

And so we have

$$\tilde{\omega}_0\equiv y+(x\sin\theta-y\cos\theta)-\sqrt{y^2+(x\sin\theta-y\cos\theta)^2}+[(R^2-x^2-y^2)/2R]-$$
$$-\sqrt{[y+(x\sin\theta-y\cos\theta)-\sqrt{y^2+(x\sin\theta-y\cos\theta)^2}]^2+[(R^2-x^2-y^2)^2/4R^2]}.$$

The function constructed $\Phi_0(r)$ ensures the fulfillment of the conditions (5) for any values of the function φ, which can be selected as before in the form of a series $\varphi=\sum_k A_k\eta_k$. One can often simplify $\Phi_0(r)$ by using peculiarities of the geometry of the problem. Thus it is easy to note that the normal derivative of $\tilde{\omega}_3$ on the segments Γ_1 and Γ_2 is equal to zero. Let us construct a function $\tilde{\Phi}_0(r)$ which satisfies only the conditions that the normal derivatives on Γ_1 and Γ_2 be equal to zero without imposing any conditions on it along Γ_3. By multiplying $\tilde{\Phi}_0(r)$ by the equation of the boundary Γ_3 we obtain the function $\Phi_0(r)=\tilde{\Phi}_0(r)\tilde{\omega}_3(r)$, which ensures fulfillment of the conditions (5) and has a simpler form than in the previous method of construction $\Phi_0(r)$. One should note that the function $\Phi_0(r)$ constructed in the second approach is differentiable everywhere except the angular points. However, the function $\Phi_0(r)$ constructed in the first approach does not have this inadequacy, and it is interesting to note that the derivative of $\Phi_0(r)$ with respect to any direction within the limits of the angle θ at point O is equal to zero, which agrees with the properties of the exact solution.

Let us proceed to the construction within the framework of MIE of a structure which ensures fulfillment of the continuity conditions of $D(r)[\partial\Phi(r)/\partial\nu]$ on the inner boundaries of the reactor.

We will assume that the element with index i+1 lies completely in the element with index i and that no elements intersect and they are not in contact with each other. Then the coupling conditions on the boundary Γ_{i+1} are of the form

$$D_i(r)\frac{\partial\Phi_i(r)}{\partial\nu}\Big|_{\Gamma_{i+1}}=D_{i+1}(r)\frac{\partial\Phi_{i+1}(r)}{\partial\nu}\Big|_{\Gamma_{i+1}};$$
$$\Phi_i(r)|_{\Gamma_{i+1}}=\Phi_{i+1}(r)|_{\Gamma_{i+1}}.$$

Here $\Phi_i(r)$ is the solution in the element i and $D_i(r)$ is the diffusion coefficient in the element i.

As before, we will seek $\Phi_{i+1}(r)$ in the form

$$\Phi_{i+1}(r)=\varphi_{i+1}-\tilde{\omega}_{i+1}D_{1,\,i+1}\varphi_{i+1}+\tilde{\omega}_{i+1}\psi_{i+1}.$$

Here $D_{1,\,i+1}\equiv\frac{\partial\tilde{\omega}_{i+1}}{\partial x}\frac{\partial}{\partial x}+\frac{\partial\tilde{\omega}_{i+1}}{\partial y}\frac{\partial}{\partial y}$; $\tilde{\omega}_{i+1}$ is the normalized equation of the boundary of the element i+1, and φ_{i+1} and ψ_{i+1} are unknown functions.

It is not difficult to see that the conditions

$$\Phi_{i+1}(r)|_{\Gamma_{i+1}} = \varphi_{i+1}|_{\Gamma_{i+1}} \tag{10}$$

are fulfilled, i.e., $\varphi_{i+1}|_{\Gamma_{i+1}} = \Phi_i(r)|_{\Gamma_{i+1}}$;

$$\frac{\partial \Phi_{i+1}(r)}{\partial \nu}\Big|_{\Gamma_{i+1}} = \frac{D_i(r)}{D_{i+1}(r)} \frac{\partial \Phi_i(r)}{\partial \nu},$$

whence

$$\psi_{i+1}|_{\Gamma_{i+1}} = \frac{D_i(r)}{D_{i+1}(r)} \frac{\partial \Phi_i(r)}{\partial \nu}\Big|_{\Gamma_{i+1}},$$

or in more general form

$$\psi_{i+1}|_{\Gamma_{i+1}} = \frac{D_i(r)}{D_{i+1}(r)} \frac{\partial \Phi_i(r)}{\partial \nu} + \tilde{\omega}_{i+1}\tilde{\eta}_{i+1}. \tag{11}$$

Here $\tilde{\omega}_{i+1}\tilde{\eta}_{i+1}$ is some unknown function which vanishes on the boundary Γ_{i+1} and can be selected in the form $\tilde{\omega}_{i+1}\sum_k A_k\eta_k$. After substitution of φ_{i+1} and ψ_{i+1} in the form in which they are determined in Eqs. (10) and (11) into the equation for $\Phi_{i+1}(r)$, we find

$$\Phi_{i+1}(r) = \Phi_i(r) + \left[\frac{D_i(r)}{D_{i+1}(r)} - 1\right]\tilde{\omega}_{i+1}D_{1,\,i+1}\Phi_i(r) + \tilde{\omega}_{i+1}^2\tilde{\eta}_{i+1}.$$

Let us recall that within the framework of MIE the approximate solution in the element i+1 is determined as a sum:

$$\Phi_{i+1}(r) = \Phi_i(r) + P_{i+1}(r),$$

where $P_{i+1}(r)$ is a polynomial which differs from zero only in the element i+1.

It is evident that $P_{i+1}(r)$ has the form

$$P_{i+1}(r) = \frac{D_i(r) - D_{i+1}(r)}{D_{i+1}(r)}\tilde{\omega}_{i+1}D_{1,\,i+1}\Phi_i(r) + \tilde{\omega}_{i+1}^2\tilde{\eta}_{i+1}.$$

LITERATURE CITED

1. I. S. Slesarev and A. M. Sirotkin, At. Energ., 38, No. 6, 419 (1975).
2. I. S. Slesarev and A. M. Sirotkin, Zh. Vychisl. Mat. Mat. Fiz., 16, No. 2, 399 (1976).
3. V. L. Rvachev and A. P. Slesarenko, Logic Algebra and Integral Transformations in Boundary-Value Problems [in Russian], Naukova Dumka, Kiev (1976).

SUBGROUP METHOD FOR TAKING ACCOUNT OF THE SPATIAL DISTRIBUTION OF UNSCATTERED AND SINGLY SCATTERED NEUTRONS IN MULTIGROUP SHIELDING CALCULATIONS

V. F. Khokhlov, V. D. Tkachev, V. L. Reitblat, and I. N. Sheino

UDC 621.039.51.12

The group-averaged neutron cross sections in resonance media generally vary spatially since the structure of the neutron spectrum over which the neutron cross sections are averaged has a spatial dependence [1]. It is practically impossible to take account of this dependence within the framework of the multigroup procedure. The spatial dependence of the group-averaged cross sections has a very important effect on the spatial distribution of unscattered and singly scattered neutrons. Therefore, it is particularly important to take correct account of this dependence for such neutrons.

In multigroup calculations the spatial distribution of unscattered radiation $\varphi^j_{un}(x, \mu)$ and the source of scattered radiation from the unscattered $F^j_p(x, \mu)$ generally obeys an exponential law*:

$$\varphi^j_{un}(x, \mu) = Q^j(\mu) \exp\left[-\int_0^{x/\mu} \Sigma^j(x')\, dx'\right] = Q^j(\mu)\, T^j(x/\mu), \tag{1}$$

$$F^j_p(x, \mu) = \sum_{q=1}^{j} \int_{-1}^{+1} d\mu' Q^q(\mu')\, w_s^{q\to j}(x, \mu' \to \mu) \sum_s^q (x) \exp\left[-\int_0^{x/\mu'} \Sigma^q(x')\, dx'\right] =$$

$$= \sum_{q=1}^{j} \int_{-1}^{+1} Q^q(\mu')\, w_s^{q\to j}(x, \mu' \to \mu)\, \Sigma^q_s(x)\, T^q(x/\mu')\, d\mu', \tag{2}$$

where μ is the cosine of the angle with the shield normal, $Q^j(\mu)$ is the angular distribution of the source of neutrons of the group at the shield surface $x = 0$, $\Sigma^j(x)$ is the average total cross section of neutrons of group j, $T^j(x/\mu)$ is the transmission function (the probability of a neutron of group j moving in the direction μ reaching point x without making a collision), $w_s^{q\to j}(x, \mu' \to \mu)$ is the neutron scattering indicatrix, and $\Sigma^q_s(x)$ is the average cross section for the scattering of neutrons of group q.

If the shielding material contains elements whose cross sections have a resonance structure, or if the cross sections vary significantly within the group limits, even though they are monotonic, the spatial dependence of the unscattered radiation and the source of scattered radiation from the unscattered in these groups differs from exponential. This is a result of self-shielding of cross sections, and therefore in such cases it is impossible to choose an effective group-averaged total cross section to describe the spatial distribution of unscattered radiation over a sufficiently broad range of shield thicknesses [2].

In the present paper we propose to calculate the unscattered radiation and the spatial distribution of first collisions in the subgroup approximation [3]. In this case the transmission function is approximated by a sum of exponentials. In particular, for a homogeneous medium

$$\varphi^j_{un}(x, \mu) = Q^j(\mu) \sum_{p=1}^{n} a^j_p \exp(-\Sigma^j_p x/\mu), \tag{3}$$

where a^j_p is the fraction of subgroup p in group j, Σ^j_p is the total cross section in subgroup p of group j, and n is the number of subgroups in the j-th group.

It is shown in [3, 4] that the error of approximation (3) does not exceed 3% when using two or three subgroups. The necessary subgroup parameters can either by obtained from experiment [4] or by analyzing the calculated transmission functions [3].

*For simplicity we consider a plane one-dimensional problem without azimuthal dependence.

Translated from Atomnaya Énergiya, Vol. 44, No. 4, pp. 324-327, April, 1978. Original article submitted March 23, 1977.

0038-531X/78/4404-0370$07.50

The scattered component of the neutron flux is determined by solving the kinetic equation with the source $F_p^j(x, \mu)$ from unscattered radiation in each energy group. If the cross sections are not constant within the group limits, the correlation of the energy dependences of the total and scattering cross sections must be taken into account in calculating this source. Then if it is assumed that the scattering indicatrix varies slowly with neutron energy within the group limits, the source will have the form

$$F_p^j(x, \mu) = \sum_{q=1}^{j} \int_{-1}^{+1} d\mu' Q^q(\mu') w_s^{q \to j}(x, \mu' \to \mu) \times$$

$$\times \int_{\Delta u_q} du' \Sigma_s(x, u') \exp\left[- \int_0^{x/\mu'} \Sigma(x', u') dx' \right] = \sum_{q=1}^{j} \int_{-1}^{+1} d\mu' Q^q(\mu') w_s^{q \to j}(x, \mu' \to \mu) T_s^q(x/\mu'), \quad (4)$$

where Δu_q is the lethargy range of group q, and $T_S^q(x/\mu)$ is the transmission function for scattering, i.e., the probability that a neutron of group q moving in the direction μ will reach point x and be scattered there.

Thus the problem is reduced to a correct calculation of the transmission function of the shielding medium. In practice it is generally necessary to deal with multilayer shields composed of different chemical elements and with the same chemical elements in different layers. When a shield layer consists of different elements, the transmission functions are calculated as products of the transmission functions of the layers. If the same elements are present in separate layers of the shield the correlation of the cross sections of these elements must be taken into account.

By considering the transmission of neutrons by each element in the shield composition general formulas can be obtained for calculating transmission functions in the subgroup approximation. For point x_k of the k-th shield layer these formulas have the form

$$T_s^j(x_k/\mu) = \sum_{p_1=1}^{n_1} \sum_{p_2=1}^{n_2} \dots \sum_{p_N=1}^{n_N} a_{p_1}^j a_{p_2}^j \dots a_{p_N}^j \left(\sum_{l=1}^{N_k} \rho_l^k \sigma_{s, p_l}^{j, k} \right) \exp\left(- \sum_{i=1}^{N} \sigma_{p_i}^j \tau_i^k / \mu \right); \quad (5)$$

$$T^j(x_k/\mu) = \sum_{p_1=1}^{n_1} \sum_{p_2=1}^{n_2} \dots \sum_{p_N=1}^{n_N} a_{p_1}^j a_{p_2}^j \dots a_{p_N}^j \exp\left(- \sum_{i=1}^{N} \sigma_{p_i}^j \tau_i^k / \mu \right); \quad (6)$$

$$\tau_i^k = \sum_{m=1}^{k-1} \rho_i^m \Delta x_m + \rho_i^m \left(x_k - \sum_{m=1}^{k-1} \Delta x_m \right), \quad (7)$$

where N_j is the number of elements in the first k layers of the shield, a_{pi}^j is the fraction of subgroup p in the j-th group of the i-th element, N_k is the number of elements in the k-th layer of the shield, p_i^k is the nuclear density of the i-th element in the k-th layer, σ_{s, p_l}^{jk} is the microscopic scattering cross section in subgroup p of the j-th group of the l-th element in the k-th layer, σ_{pj}^j is the total microscopic cross section in subgroup p of j-th group of the i-th element, τ_i^k is the reduced thickness of the i-th element in the first k layers of the shield, n_i is the number of subgroups of the i-th element in the j-th group, and Δx_m is the thickness of the m-th layer of the shield.

Equations (5) and (6) enable one to take account of the correlation of the cross sections of identical elements in various layers of the shield. This is ensured by the introduction of the reduced thickness τ_i for each i-th element in the shield composition. From the definition of τ_i (Eq. (7)) it follows that the reduced thickness of the i-th element in each layer of the shield is computed from the reduced thicknesses of the preceding layers containing the i-th element. The usual multigroup calculations do not take account of the correlations of the cross sections of identical elements in various layers of the shield, since the transmission function of a multilayer medium is determined by the product of the transmission functions of the separate layers. For example, in calculating the transmission functions of 0.4-0.8-MeV neutrons through a three-layer shield of iron, water, iron with each layer 10 cm thick, neglecting the correlation of the iron cross sections in the first and last layers leads to an error of ~63%. The algorithm for calculating the transmission functions (5) and (6) was realized in the complex OBRAZ program [5].

The proposed method of taking correct account of the spatial distribution of singly scattered neutrons was realized in a specially developed program ALGOL ROZA-T for a Minsk-22 computer. The basic scheme of numerical solution of the kinetic equation was taken from [6]. The unscattered radiation was separated out for an arbitrary angular distribution of the neutron source. To do this the angular distribution of the source in each energy group where self-shielding of the cross sections of the medium under consideration is important is represented as a superposition of plane monodirectional sources

$$Q^j(\mu) \approx \sum_{i=1}^{N} Q_i^j \delta(\mu - \mu_i). \quad (8)$$

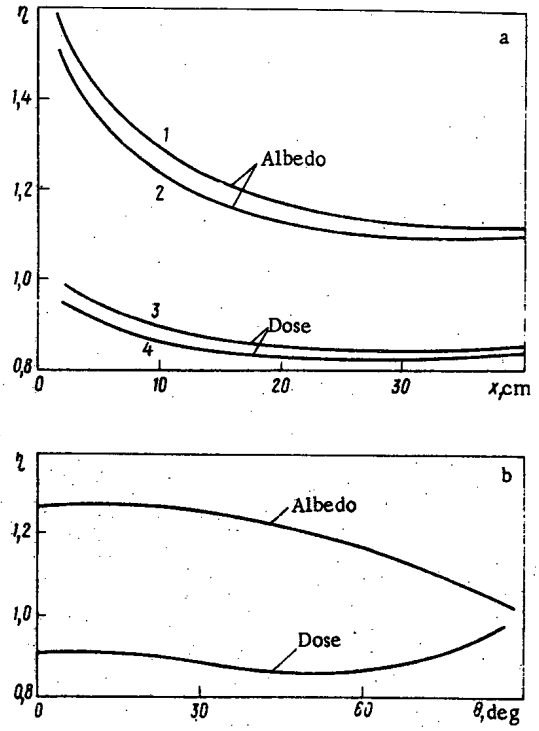

Fig. 1. Ratios of integral dose albedo and transmitted neutron dose for $Q(\mu) = \delta(\mu - 1)$ (1, 3), and $Q(\mu) = \mu$ (2, 4).

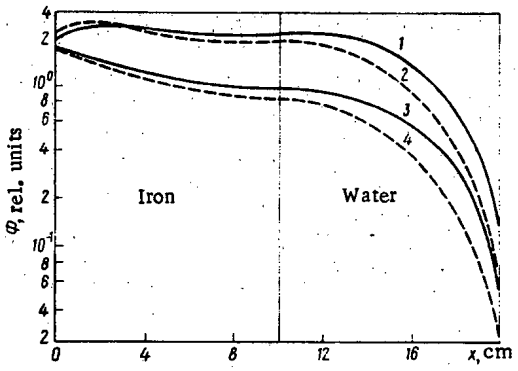

Fig. 2. Spatial distributions of neutron fluxes in a two-layer shield calculated by taking account of the unscattered radiation in the group (——) and subgroup (---) approximations for $Q(\mu) = \delta(\mu - 1)$ (1, 2) and $Q(\mu) = \mu$ (3, 4).

The coefficients Q_1^i are determined automatically in the ROZA-T program. The number N of terms in the sum (8) is chosen to maintain the required accuracy of the approximation. The ROZA-T program runs in combination with the OBRAZ program.

The efficiency of the method was investigated by calculating slab shields of iron, water, and combinations of them. The calculations were performed in the $2D_5P_5$ approximation (the $2D_5$ approximation in the flux and the P_5 approximation in scattering) for a neutron source with an energy spectrum of the BR-5 fast reactor [7] in a 21-group approximation [5]. All the necessary constants were calculated using the OBRAZ combination program.

Figure 1 shows the ratios of the integral dose albedo and the transmitted neutron dose calculated by taking account of the unscattered radiation in the subgroup and group approximations for: a) layers of iron of

various thicknesses, and b) for various angles of incidence of a plane beam of neutrons on a 10-cm-thick layer of iron. These data show that the effect of a more accurate treatment of the unscattered radiation, which is maximum for monodirectional radiation at $\theta = 0$, is preserved for a distributed source. The behavior of the ratios (Fig. 1a) for the albedo for a small thickness is determined by the singly scattered radiation, which is proportional to the transmission function for scattering [4]. As $x \to 0$ the exact function $T_S(x)$ approaches $\langle \Sigma_S \rangle$, the unblocked cross section; in the usual group approximation it approaches $\overline{\Sigma}_S$, the blocked cross section. Therefore the usual group approximation underestimates the albedo in the resonance region since $\langle \Sigma_S \rangle > \overline{\Sigma}_S$. The penetration of neutrons through small thicknesses of matter is determined mainly by the unscattered radiation, which in both cases has a distribution which approaches that of the external source as $x \to 0$; therefore the ratio of the transmitted doses approaches unity. As the angle of incidence of a plane beam of neutrons is increased, the albedo and dose ratios (Fig. 1b) approach unity, since in this case the effect of the unscattered radiation can be neglected, and the spatial distribution of singly scattered neutrons is equivalent to a plane source of scattered neutrons at $x = 0$, with the albedo and transmission determined by the same constants in the subgroup and usual group calculations.

Figure 2 shows the spatial distributions of neutron fluxes in a two-layer iron–water shield. Taking account of the unscattered radiation has a significant effect on the distribution of neutrons in water, mainly because of the change in spectrum of resonance neutrons transmitted by iron. As they emerge from this system the neutron fluxes being compared differ by about a factor of two for both sources.

The correct account of the unscattered radiation in few-group calculations when the shielding medium consists of elements with monotonically varying cross sections is particularly important, since in this case the effect of self-shielding of the cross sections increases with an increase in the energy range of the group. For example, the transmission of fast neutrons which have a fission spectrum with energies $E > 0.8$ MeV through a layer of water 80 cm thick calculated in the one-group approximation is $\approx 10^3$ times smaller than the transmission calculated in the five-group approximation. In such cases it is particularly important to take account of the correlation of cross sections of the same elements in separate layers of the shield.

LITERATURE CITED

1. L. P. Abagyan et al., USSR paper No. P/357, Third Geneva Conference (1964).
2. V. G. Khokhlov et al., in: Nuclear Constants, No. 8, Part 4 [in Russian], TsNIIatominform (1972), p. 154.
3. V. F. Khokhlov et al., ibid., Part 2, p. 119.
4. V. V. Filippov et al., Anglo–Soviet Seminar on Nuclear Constants for Reactor Calculations [in Russian], Paper ASS-68/103, Dubna, June 18-22, 1968.
5. V. F. Khokhlov and V. D. Tkachev, in: Abstracts of Papers on an All-Union Scientific Conference on Shielding against Ionizing Radiation from Nuclear Engineering Installations [in Russian], MIFI, Moscow (1974), p. 7.
6. A. A. Dorofeev et al., Solution of the Transport Equation for a Slab (program ROZ-5), Part 1 [in Russian], Inst. Prikl. Mat., Akad. Nauk SSSR (1972).
7. Yu. A. Kazanskii, Physics of Reactor Shielding, Israel Program for Scientific Translations, Jerusalem (1969).

THERMODYNAMIC STABILITY OF URANIUM MONONITRIDE

S. A. Balankin, L. P. Loshmanov,
D. M. Skorov, and V. S. Sokolov

UDC 621.039.544.57

Thermodynamic stability may restrict the use of uranium mononitride as a nuclear fuel in high-temperature reactors, as a result of the change in the composition of the UN and the appearance of free uranium at high temperatures. A change in the composition of the UN is indicated by the reduction in the rate of vaporization when the material is held isothermally at temperatures of 1878 and 1983°K [1]. There are also reports of observed changes in the partial pressures of nitrogen and uranium in the vaporization of UN [2, 3]; however, the reasons for these changes are not discussed in detail. Data on the temperature at which free uranium appears in the UN vary widely: 1773°K according to [4], 1973°K according to [5], and 2073°K according to [1].

To investigate this phenomenon, we measured the rate of vaporization in the 1758-2168°K temperature range. The temperature at which the free uranium appeared was determined by x-ray phase analysis of the specimens after vaporization experiments. The original uranium nitride had the following chemical composition (in % by mass): U, 94.3; N, 5.15; C (total), 0.1; C (free), 0.018; O, 0.25; this corresponds to the formula composition $U(N_{0.94}C_{0.02}O_{0.04})_{0.99\pm0.01}$. The x-ray analysis of the original specimens did not indicate the presence of any phases other than uranium mononitride with a lattice period of 4.890 ± 0.001 Å. The rate of vaporization was investigated in a vacuum of $1 \cdot 10^{-5}$ mm Hg by the Langmuir method in the variant using continuous weighing in a high-temperature apparatus with automatic recording of the measurement results [6]. The measurement error in the vaporization rate was 15%. A specimen having the shape of a plate measuring $7 \times 7 \times 1$ mm, weighed on a quartz microbalance with a tungsten filament, after establishing the necessary temperature, was left in the heating zone, and the changes in the mass of the specimen were then automatically recorded. It follows from Fig. 1 that for isothermal holding, the rate of vaporization decreases, reaching a constant time-independent value. The results of x-ray phase analysis indicate the presence of free uranium in the uranium mononitride specimens held at 1970°K and higher, which is in good agreement with the data of [5].

In order to explain the results on the basis of statistical-thermodynamic theory [7], which was successfully used for UC [8], we calculated the variation of the partial pressures of uranium and nitrogen as functions of the temperature and the composition of the uranium mononitride. According to [7], the expressions for the partial pressures of the components of the phase $A_{1-x}B_x$ have the form

$$\ln \bar{P}_A = \ln P_A^0 - (F_A^+ + 2RT \ln 2\alpha)/2RT + \ln \frac{1-2x}{1-x}; \quad (1)$$

$$\ln \bar{P}_B = \ln P_B^0 - F_B^+/2RT + \ln \frac{x}{1-2x}, \quad (2)$$

where P_A^0 and P_B^0 are the pressure values above the pure components A and B; F_A^+ and F_B^+ are the free energies of formation of the structural vacancies of the components A and B; α is the concentration of thermal vacancies in the metallic or nonmetallic sublattices.

Knowing the partial pressures of the components above a compound of known composition and the pressures above the pure components, we can determine from Eqs. (1) and (2) the values of F_B^+, $F_A^+ + 2RT\ln 2\alpha$ and then obtain expressions for the partial pressures in the region of homogeneity of the compound.

Substituting the experimentally determined partial pressures of uranium and nitrogen over $UN_{0.99}$ into Eqs. (1) and (2), using the most reliable values of the pressure above pure uranium [9], we can determine the desired values:

$$F_{U^+} + 2RT \ln 2\alpha = 60400 - 80.0T, \text{ J/mole}; \quad (3)$$

$$F_{N^+} = 583000 - 99.4T \text{ J/mole}, \quad (4)$$

Translated from Atomnaya Énergiya, Vol. 44, No. 4, pp. 327-329, April, 1978. Original article submitted February 17, 1977.

0038-531X/78/4404-0374$07.50

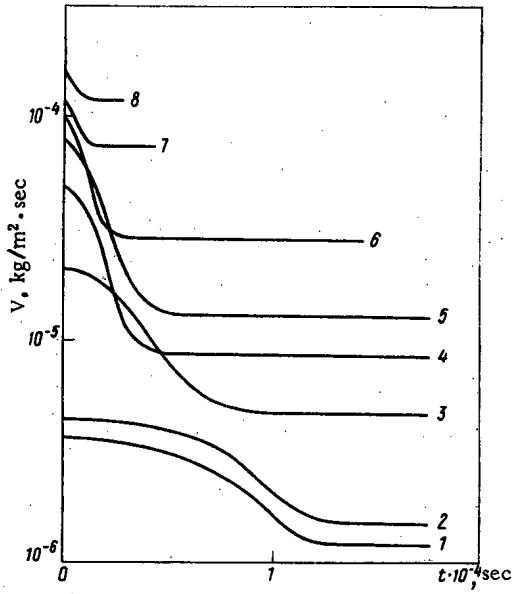

Fig. 1. Rate of vaporization as a function of holding time at various temperatures, °K: 1) 1758; 2) 1873; 3) 1938; 4) 1970; 5) 2020; 6) 2073; 7) 2133; 8) 2168.

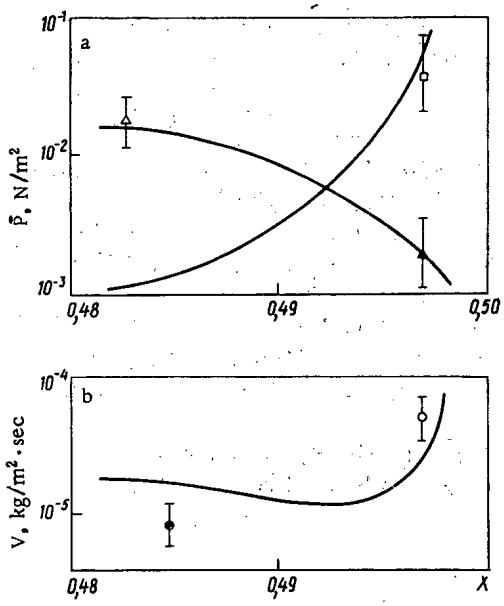

Fig. 2. Variation with composition $U_{1-x}N_x$ at 1970°K: a) partial pressures of nitrogen (□) and uranium (▲, △) [2, 8]; b) rate of vaporization of original (○) and congruent (●) compositions.

and find the variation with temperature of the partial pressures of uranium and nitrogen above uranium mononitride specimens of various compositions:

$$\lg \overline{P}_U = 12.9 - \frac{26850}{T} + \lg \frac{1-2x}{1-x}, \text{ N/m}^2; \quad (5)$$

$$\lg \overline{P}_{N_2} = 10.2 - \frac{30460}{T} + 2\lg \frac{x}{1-2x}, \text{ N/m}^2. \quad (6)$$

Making use of the vaporization congruence condition and expressions (5) and (6), we can represent the temperature variation of the compositions of congruent vaporization (x_k) of the UN in the form

$$\frac{x_h}{1-x_h} = 1.03 - 4.22 \cdot 10^{-5} T. \quad (7)$$

Figure 2 shows the calculated variations of the partial pressures of uranium and nitrogen and also of the total rate of vaporization as functions of the composition $U_{1-x}N_x$ at 1970°K. At compositions close to stoichiometric the partial pressure of nitrogen is considerably higher than the partial pressure of uranium (see Fig. 2), which must lead to nitrogen depletion of the uranium mononitride, as shown by (7). The partial pressure of the nitrogen and the rate of vaporization decrease, while the partial pressure of uranium increases until congruent vaporization is achieved. The foregoing explains the experimentally observed changes [1-3] in the rate of vaporization and the partial pressures of uranium and nitrogen when UN vaporizes.

In accordance with Eq. (7), the higher the temperature the closer the composition of congruent vaporization will be to the lower limit of the region of homogeneity of the UN. At a certain temperature (1970°K) the composition of the congruent vaporization reaches the lower limit of the homogeneity region.

For comparison with the calculations, we show in Fig. 2 the published data on partial pressures of nitrogen and uranium, as well as the experimental results on the rate of vaporization. Since in [8] the UN specimens, before the investigation, were subjected to prolonged annealing at the maximum experimental temperature, the composition of the specimens varied. Therefore we applied a correction obtained from [8] to the composition which, according to Eq. (7), corresponds to the annealing temperature. Fig. 2b shows the experimental data on the rate of vaporization of the original composition and the composition of congruent vaporization of the UN. The data for the original composition corresponds to the rate of vaporization at the initial instant of time at 1970°K (see Fig. 1). The final, time-independent value of the rate of vaporization relates to the composition of the congruent vaporization, calculated from Eq. (7). The calculated, experimental, and published data are in good agreement.

Thus, we have established that the experimentally observed decrease in the rate of vaporization in the process of isothermal holding is due to nitrogen depletion of the uranium mononitride and also to the appearance of free uranium as a second phase at 1970°K.

LITERATURE CITED

1. C. Alexander, J. Ogden, and W. Pardue, J. Nucl. Mater., 31, 13 (1969).
2. K. Gingerich, J. Chem. Phys., 51, No. 10, 4433 (1969).
3. Y. Ikeda, M. Tamaki, and G. Matsumoto, J. Nucl. Mater., 59, No. 2, 103 (1976).
4. H. Inouye and J. Leitnaker, J. Am. Ceram. Soc., 51, No. 1, 6 (1968).
5. P. Evans and T. Davies, J. Nucl. Mater., 10, No. 1, 43 (1963).
6. D. M. Skorov, S. A. Balankin, and V. S. Sokolov, in: Physicochemical Analysis of Alloys of Uranium, Thorium, and Zirconium [in Russian], Nauka, Moscow (1974), p. 164.
7. L. Kaufman and E. Clougherty, in: Metallurgy at High Pressures and High Temperatures, AIME, New York (1964), p. 322.
8. R. A. Andrievskii et al., At. Energ., 26, No. 6, 494 (1969).
9. E. K. Storms, Refractory Carbides, Academic Press (1967).

NEUTRON MULTIPLICATION IN URANIUM BOMBARDED WITH 300-660-MeV PROTONS

R. G. Vasil'kov, V. I. Gol'danskii,
B. A. Pimenov, Yu. N. Pokotilovskii,
and L. V. Chistyakov

UDC 621.039.54

Research on neutron multiplication in massive (quasi-infinite) blocks of heavy elements, such as Pb, Bi, Th, and U, bombarded with particles accelerated to hundreds and thousands of mega-electron-volts is of interest for the solution of various scientific and applied problems. For example, high-current beams of accelerated protons, deuterons, and possibly helium nuclei, may offer a convenient method, frequently called electronuclear, of producing free neutrons which may turn out to be a useful supplement to the self-sustaining chain process of nuclear fission and controlled thermonuclear fusion for the large-scale production of neutrons in general, and for nuclear power engineering in particular. The idea of producing free neutrons by using proton or deuteron accelerators was suggested in the late 1940s by N. N. Semenov in the USSR and independently by E. O. Lawrence in the U. S., and was subsequently developed in the U. S. and Canada to the level of technical designs of electronuclear devices [1, 2]. The possible role of such devices was discussed in [2-9].

To aid the development of these plans, and also for other reasons, many calculations and measurements of neutron yields from targets of various geometries and compositions were performed in several laboratories [10-15]. In particular, in 1963-1969 the authors studied neutron multiplication in massive targets of uranium metal bombarded with 300-, 400-, 500-, and 660-MeV protons at the synchrocyclotron of the Nuclear Problems Laboratory at Dubna.

Method of Measurement. The absorption of protons in a uranium target leads to the production of fast cascade and evaporation neutrons and also fission neutrons with energies ~1-100 MeV which are scattered by uranium nuclei and degraded to energies in the range where their radiative capture occurs:

$$^{238}\mathrm{U}\,(n,\,\gamma)\,^{239}\mathrm{U} \xrightarrow{\beta^-} {}^{239}\mathrm{Np} \xrightarrow{\beta^-} {}^{239}\mathrm{Pu}.$$

During slowing down, the neutrons are further multiplied as a result of uranium fission. By measuring the (n, γ) capture-density distribution over the volume of the target A(z, r, φ) and integrating this distribution, normalized to one absorbed accelerated proton and one gram of target material, we obtain the total number of captures (the ^{239}Pu yield) per high-energy proton:

$$Y = \rho \int_V A\,(z,\,r,\,\varphi)\,dv,$$

where z is in the direction of the proton beam and ρ is the density of the uranium metal. A cylindrical coordinate system (r, φ, z) is used since the neutron-density distribution must be axisymmetric in a homogeneous target. Since the fast-neutron source is axisymmetric, the measured distributions do not depend on φ, and therefore it is sufficient to measure them in any half-plane of the target passing through the axis of the proton beam. Then the expression for the total yield takes the form

$$Y = 2\pi\rho \int_S A'\,(z,\,r)\,dS.$$

The number of fissions is determined in a similar way. The (n, γ) capture-density distribution was measured by the yield of ^{239}Np separated radiochemically from uranium samples irradiated at various points in the target, and the uranium fission-density distribution was found by using miniature silicon surface-barrier counters covered with a layer of uranium. The uranium samples in the radiochemical experiments and the fissionable layers for the counters were made of the target material.

Primary Proton Beam. The experiments were performed with a 660-MeV extracted proton beam. For experiments with 300-, 400-, and 500-MeV bombarding particles the primary protons were slowed down in

Translated from Atomnaya Énergiya, Vol. 44, No. 4, pp. 329-335, April, 1978. Original article submitted April 6, 1977.

0038-531X/78/4404-0377$07.50

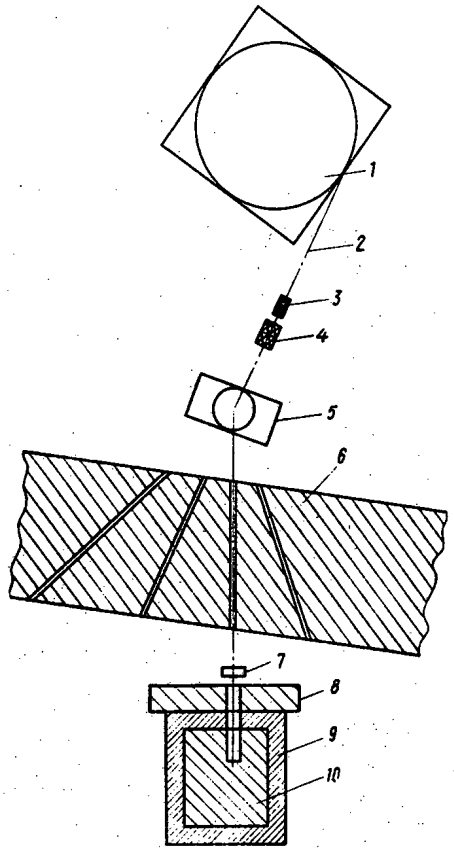

Fig. 1. Schematic diagram of target arrangement in JINR synchrocyclotron research room: 1) accelerator; 2) trajectory of extracted proton beam; 3) polyethylene attenuator; 4) magnetic lens; 5) bending magnet; 6) iron shielding wall with collimators; 7) ionization chamber; 8) supplementary shielding wall (60 cm of concrete and 40 cm of iron); 9) lead casing; 10) uranium.

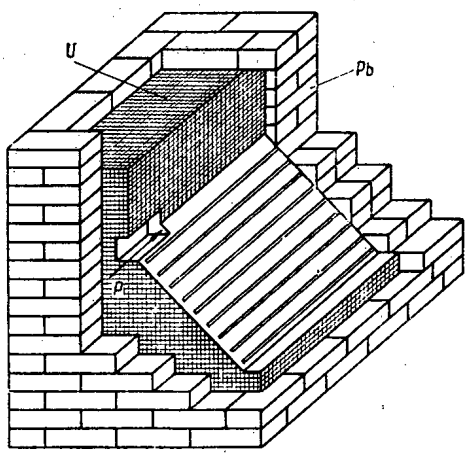

Fig. 2. General view of a portion of the uranium target in its lead shield showing the location of channels for detectors and the opening for introducing the proton beam into the target.

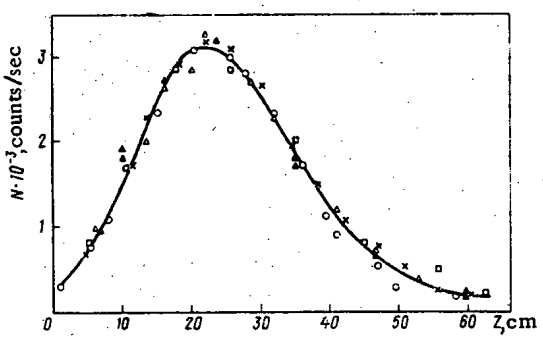

Fig. 3

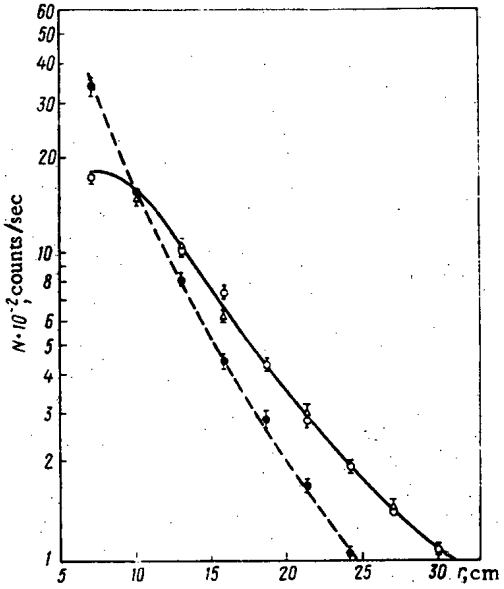

Fig. 4

Fig. 3. Distribution of activity of various detectors irradiated in channel 2 of a natural uranium target: □) ^{239}U; ○) Al; ×) Cu; △) In; ▲) In in cadmium cover.

Fig. 4. Radial dependence of the activity of various detectors irradiated in a natural uranium target at points corresponding to the maximum of the longitudinal distributions: △) ^{239}U; ●) Cu; ○) Al.

polyethylene attenuators placed in the beam before it entered the magnetic quadrupole lens. The required thicknesses of the attenuators and the energy dispersion of the slowed-down protons were determined from data in [16].

By using magnetic probes, a focusing quadrupole, and a bending magnet, the proton beam was brought through a 2-cm steel collimator in a 4-m iron shielding wall onto the target located ≈ 5 m behind this wall. The diamater of the proton beam at the target entrance was 4-5 cm (Fig. 1).

In the work with semiconductor fission-fragment counters the intensity of the proton beam at the target entrance was measured with a helium-filled ionization chamber calibrated by the $^{27}Al(p, 3pn)^{24}Na$ reaction. Its cross section was taken from [17]. In experiments on the measurement of the ^{239}Pu yields when the uranium detectors were irradiated for several hours, the total number of protons incident on the target during the time of exposure was determined directly from the activity of the aluminum foil induced during this same time.

The absolute ^{24}Na activity of the irradiated foil was measured with a spectrometer using a NaI(Tl) crystal. The error in determining the number of protons absorbed by the target was ± 7%.

Target. The targets were built up of rectangular bars of natural (2 × 4 × 8 cm) and depleted (8 × 8 × 16 cm) uranium. The total mass of each target was ≈ 3.5 tons, and its linear dimensions were 56 × 56 × 64 cm. The background of high-energy scattered neutrons was reduced by surrounding the targets on all sides by a 10-cm-thick layer of lead. This lead casing also decreased the neutron leakage from the target somewhat.

The proton beam was introduced into the central part of the target through an opening 8 × 8 cm in cross section and 16 cm deep. As a result the neutron source was, so to speak, displaced into the interior of the target, and this decreased the neutron leakage through its front face.

The detectors and silicon counters could be moved along a system of channels 2 × 0.3 cm in cross section and 60 cm long made in a diagonal plane of the target passing through the axis of the proton beam. The channels were about 3 cm apart, parallel to the proton beam, and from 6 to 45 cm from it. A portion of the target is shown in Fig. 2.

The background was measured by removing the part of the target in which the protons were slowed down, so that the beam passed freely through the 8 × 8-cm channel in the target to a concrete shielding wall about 13-14 m away.

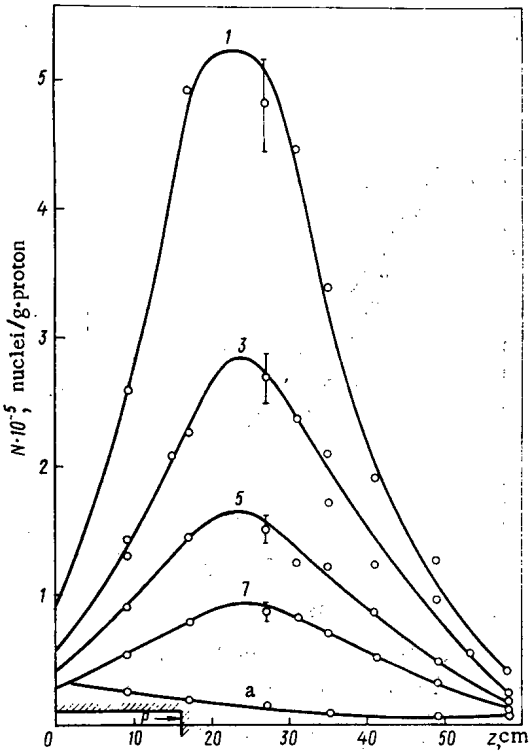

Fig. 5

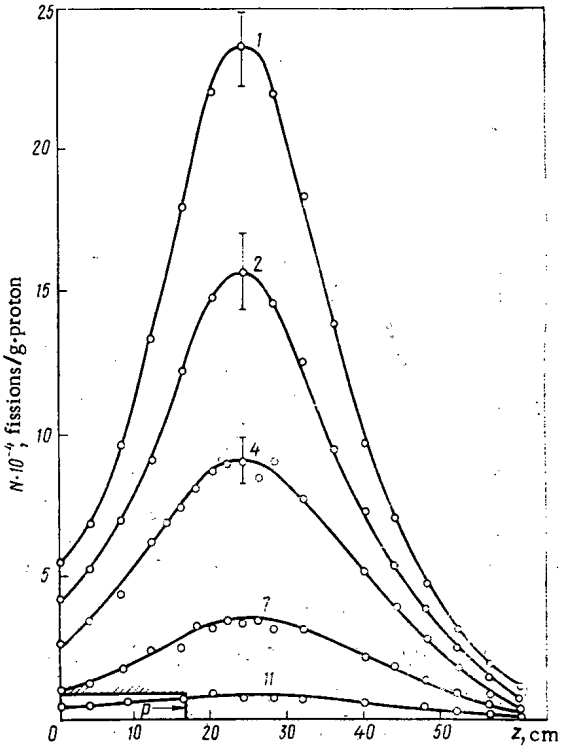

Fig. 6

Fig. 5. Distribution of (n, γ) capture density (i.e., of ^{239}Np nuclei) measured in channels 1, 3, 5, and 7 in a natural uranium target. The distribution is normalized to 1 g of natural uranium and one primary proton. Curve a is the background in a channel.

Fig. 6. Distribution of ^{235}U fission density measured in channels 1, 2, 4, 7, and 11 in a depleted uranium target. The distribution is normalized to 1 g of ^{235}U and one primary proton.

Detectors. The ^{238}U(n, γ) capture-density distribution in the target was measured with small uranium samples of the same isotopic composition as the target. These samples were 1 × 1 × 0.1 cm in size and had masses of 1.5-2 g. The samples were irradiated in the target channels for several hours and then allowed to cool a day or two before the ^{239}Np was separated from them radiochemically. The absolute activity of the ^{239}Np was then measured with a proportional-flux counter every 2 or 3 days for 16-25 days. After the ^{239}Np had decayed there remained an activity with a half-life of about 70 days, which contributed from 1-20% depending on the length of the irradiation of the uranium sample and the cooling time before the measurements of the ^{239}Np activity were begun. The chemical yield of neptunium was at least 99.5%.

In addition, in the initial phase of the research the spatial distribution of the various groups of neutrons was studied by recording them with aluminum, copper, natural uranium, and indium detectors with and without cadmium covers. Figures 3 and 4 show how the activities of such detectors as ^{24}Na, ^{64}Cu, ^{239}U, and ^{116m}In vary along a channel. In experiments with the depleted uranium target the number of time-consuming radiochemical operations was reduced by using the fact that the relative distributions measured with ^{239}U and ^{64}Cu detectors are very nearly the same (cf. Figs. 3 and 4), and therefore in determining the total ^{239}Pu yield the relative (n, γ) capture-density distributions were established from the absolute yield of ^{239}Np measured in the first six target channels. Similar capture-density distributions were obtained directly in natural uranium from the ^{239}Np yield in the first 12 target channels.

The uranium fission-density distribution in the target was measured with miniature fission chambers – n-type silicon surface-barrier fission-fragment counters covered with aluminum foils with layers of uranium deposited on them. In each series of experiments with natural or depleted uranium targets a set of 10 counters was used. Five counters recorded fission fragments from a uranium layer of the same isotopic composition as the target, and the other five "looked through" a layer of uranium of a different isotopic composition. Two counters with uranium layers of different isotopic composition were located simultaneously at the same point in each channel. For a known concentration of ^{235}U and ^{238}U nuclei in the detector layers and in the target, an inspection of the two fission-density distributions obtained with a pair of counters calibrated in a standard thermal-neutron flux permitted the determination not only of the sum of the ^{235}U and ^{238}U fissions, but also their partial contributions to this sum.

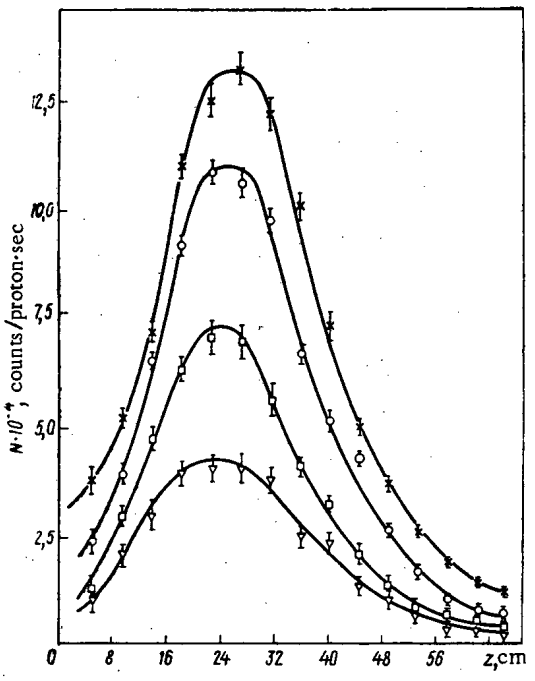

Fig. 7

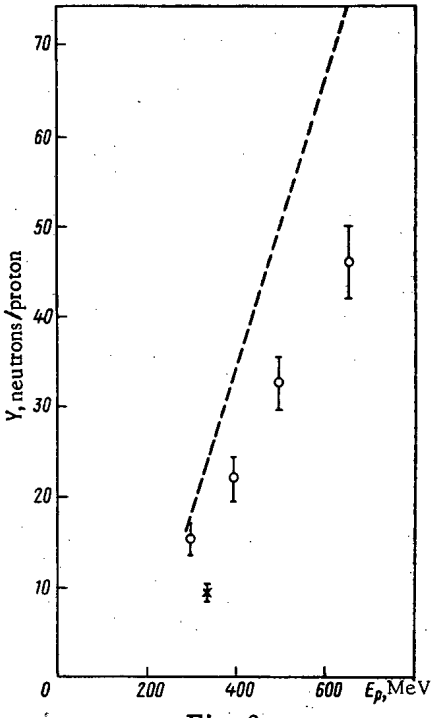

Fig. 8

Fig. 7. Fission-density distribution measured in channel 2 of a natural uranium target at various energies of the primary protons: ▽) 300; □) 400; ○) 500; ×) 660 MeV.

Fig. 8. Dependence of total ^{239}Pu yield in a natural uranium target on the energy of the bombarding protons: ---) [18]; ×) [20]; ○) our results.

In the experiments with a uranium target irradiated at the synchrocyclotron the counting rate of a fragment detector is

$$N_y = \Pi \alpha p \varepsilon,$$

where Π is the proton flux, α is the number of fissions in the counter layer per gram per absorbed proton, p is the mass of the uranium layer, and ε is the efficiency of counting fission fragments. The counting rate of this same detector in a neutron flux with a Maxwellian spectrum at the normal temperature of the moderator is given by the expression

$$N_p = \frac{\sqrt{\pi}}{2} \varphi_T \sigma_T \zeta_{35} \frac{N_A}{A} p \varepsilon.$$

The combination of these two expressions gives a value for the interesting quantity α which does not contain the product $p\varepsilon$:

$$\alpha = \frac{\sqrt{\pi}}{2} \frac{N_y}{N_p} \frac{N_A}{A} \frac{\varphi_T \sigma_T \zeta_{35}}{\Pi}.$$

Here ζ_{35} is the relative concentration of ^{235}U in the counter layer, φ_T is the neutron flux in the thermal column of the reactor, σ_T is the cross section for the fission of ^{235}U by thermal neutrons, N_A is Avogadro's number, and A is the mass number of the fissioning nucleus.

The values of N_p for all counters were measured in the thermal column of the F-1 reactor at the I. V. Kurchatov Institute of Atomic Energy, and the isotopic composition of the fissionable enriched and depleted uranium counter layers was checked with an alpha spectrometer. As a rule the thickness of the layers was 250–300 μg/cm^2 and the area was 0.5 cm^2.

Results and Discussion. Figures 5 and 6 show typical distributions of ^{239}Np yields and ^{235}U fission densities obtained for 660-MeV protons. The distribution in natural uranium is similar to that in depleted uranium and differs only slightly in ordinate. Such distributions were observed in almost all the 15 channels (in some of them several times) under various operating conditions of the accelerator which significantly changed the intensity of the proton beam, and thus the constants cited below are averages over the data of 10 separate

TABLE 1. Yield of ^{239}Pu and Number of Fissions of Uranium Nuclei in Targets of Natural and Depleted Uranium

Constant	E_p			
	300	400	500	660
Y	14,7±1,8 (12,2±1,4)	22,1±2,4 (18,2±0,2)	32,6±3,3 (27,0±2,7)	46±4 (38±4)
η	5,9±0,8 (4,4±0,6)	8,9±1,1 (6,6±0,8)	13,1±1,4 (9,7±1,1)	18,5±1,7 (13,7±1,2)
η_{38}	4,7±0,6 (3,9±0,5)	7,0±0,8 (5,8±0,7)	10,4±1,1 (8,7±1,0)	14,6±1,3 (12,2±1,1)
η_{35}	1,2±0,2 (0,48±0,06)	1,9±0,2 (0,72±0,09)	2,8±0,3 (1,06±0,12)	3,9±0,4 (1,5±0,1)

Note: Numbers in parentheses refer to depleted uranium.

experiments. The ^{239}Pu yield yield per 660-MeV proton, found by integrating the ^{239}Np distributions over the volume of the target, is 46 ± 4 in natural uranium and 38 ± 4 in depleted uranium. Extrapolation of the measured distributions beyond the limits of the target shows that the neutron leakage from targets of the dimensions used does not exceed 10-12%, but this leakage is not included in our values of the plutonium yields and the number of fissions.

Integration of the fission-density distributions obtained for the same proton energy gives the following values of the total number of uranium fissions η in the target and the numbers of ^{235}U and ^{238}U fissions:

in natural uranium $\eta = 18.5 \pm 1.7$; $\eta_{35} = 3.9 \pm 0.4$; $\eta_{38} = 14.6 \pm 1.3$;

in depleted uranium $\eta = 13.7 \pm 1.2$; $\eta_{35} = 1.5 \pm 0.1$; $\eta_{38} = 12.2 \pm 1.1$ fissions per proton.

These values do not take account of nuclear fissions in the part of the target where the bombarding protons are slowed down and a cascade of nuclear reactions is initiated by high-energy nucleons, i.e., in the fast-neutron source. For 660-MeV primary protons the number of inelastic interactions in the cascade can reach five to six [18], and taking 0.75-0.8 for the fissionability of uranium by nucleons with energies of hundreds of mega-electron-volts [19], these lead to approximately three or four fissions in the source [18].

The dependence of the quantities cited above on the energy of the bombarding protons was also established in the experiments. To do this the distribution (Fig. 7) similar to that shown in Fig. 6 was observed in the second and third target channels at proton energies of 300, 400, and 500 MeV by using counters. The ratio of the areas under these curves to the area under the curve measured at 660 MeV is a measure of the change in the neutron source strength which occurs as the energy of the primary protons is varied. It was assumed that the neutron-source spectrum varies slowly with the energy of the bombarding particles in the region where the detectors were located. The relative values δ of the neutron-source strengths measured in this way for $E_p = 300$, 400, 500, and 660 MeV were 0.33 ± 0.03, 0.48 ± 0.04, 0.71 ± 0.04, and 1, respectively.

Table 1 lists the values of the ^{239}Pu yields and the fission yields for natural and depleted uranium targets at proton energies of 300, 400, and 500 MeV, obtained by multiplying the corresponding values measured at 660 MeV by δ. The errors given take account of the errors at 660 MeV. The mean-square error of the values of the ^{239}Pu yields is ± 8% at $E_p = 660$ MeV, and increases to ± 12% at $E_p = 300$ MeV. The loss of statistical accuracy at lower energies is due to the sharp decrease in the intensity of the proton beam which results from its scattering in the attenuators.

The error in the measurements of the number of fissions is ± 9% at $E_p = 660$ MeV, and increases to ± 13% at $E_p = 300$ MeV. The largest contributions to the total error come from errors in determining the proton flux, or the total number of them, (± 7%) and in determining the thermal-neutron flux in the reactor for calibrating the counters (± 3%). The statistical accuracy of the measurement of the fission-density distributions (captures) reached ± 2% and ± 8% at $E_p = 660$ and 300 MeV, respectively, and the error in determining the absolute number of ^{239}Np nuclei did not exceed ± 2%.

In addition, the decrease in neutron yields for 660-MeV protons was measured in several target channels by replacing the uranium in the central part of the target, where the protons are slowed down, by a lead block of the same size (8 × 8 × 48 cm). The ratio of neutron yields for lead–uranium and natural uranium targets was 0.48 ± 0.2.

Except for the results of [18, 20] the authors know of no calculated or experimental data on neutron yields and the number of fissions for infinite (quasi-infinite) uranium targets bombarded with accelerated protons with energies in the interesting range 300-700 MeV. Figure 8 compares data from [18], the present work, and [20] obtained at the Chicago synchrocyclotron for 340-MeV protons. The calculations in [18] were performed for quasi-infinite uranium targets 120 cm in diameter and 90 cm thick; the results in [20] were obtained in experiments with a depleted uranium target. To within ± 5% such a target (30 × 30 × 20 cm) emits approximately nine neutrons per absorbed proton into the manganese sulfate solution surrounding it. This number represents the outside value of the yield and does not include neutrons absorbed in the target itself.

It is difficult to compare other experimental data [2, 11, 15] with our results since there are large differences in target sizes. Our experiments used uranium cylinders 10-15 cm in diameter and 30-60 cm long. Therefore it is proposed that a joint analysis of all the known results be performed later. In conclusion we note that the measured numbers of fissions enable us to set up an energy balance in quasi-infinite uranium targets, since the energy release in them is determined essentially by the fission energy of uranium nuclei.

LITERATURE CITED

1. LRL-102 (1954).
2. AECL-2600 (1966); AECL-2750 (1967).
3. A. Weinberg, in: Proceedings of the International Conference on Isochronous Cyclotrons, Gatlinburg (1966).
4. AECL-2177 (1965).
5. A. P. Aleksandrov, At. Energ., 25, No. 5, 356 (1968).
6. W. Lewis, AECL-3190 (1968).
7. V. A. Kirillin and M. A. Styrikovich, Nauka Zhizn, No. 4, 12 (1970).
8. V. A. Davidenko, At. Energ., 29, No. 3, 158 (1970).
9. R. G. Vasil'kov et al., At. Energ., 29, No. 3, 151 (1970).
10. D. West and E. Wood, Canad. J. Phys., 49, 2061 (1971).
11. R. Fullwood et al., LA-4789 (1972).
12. L. Veeser et al., Nucl. Instrum. Methods, 117, 509 (1974).
13. R. Madey and F. Waterman, Phys. Rev. C, 8, 2412 (1973).
14. V. S. Barashenkov, V. D. Toneev, and S. E. Chigrinov, At. Energ., 37, No. 6, 475 (1974).
15. V. S. Bychenkov et al., Preprint RIAN K-859 (1973).
16. V. V. Vasilevskii and Yu. D. Prokoshkin, At. Energ., 7, No. 3, 225 (1959).
17. J. Cumming, Ann. Rev. Nucl. Sci., 13, 261 (1963).
18. V. S. Barashenkov and V. D. Toneev, At. Energ., 35, No. 3, 163 (1973).
19. N. A. Perfilov, O. V. Lozhkin, and V. M. Ostroumov, Nuclear Reactions Initiated by High-Energy Particles [in Russian], Izd. Akad. Nauk SSSR, Moscow–Leningrad (1962), p. 228.
20. W. Crandall and G. Millburn, J. Appl. Phys., 29, 698 (1958).

A TURBULENT PLASMA BLANKET

N. N. Vasil'ev, A. V. Nedospasov,
V. G. Petrov, and M. Z. Tokar'

UDC 533.9:621.039.61

In future D–T tokamak power reactors the thermal fluxes from the plasma to the wall will be 0.4-1 MW/m^2. With a plasma temperature of 10-20 keV at the axis of the reactor, a density $n \approx 10^{20}$ m^{-3}, and a small fraction of multiply charged impurity ions, radiation may play only a second-order role in the removal of energy from the reactor. The required thermal fluxes may occur if turbulence develops in the plasma volume due, e.g., to the trapped particle instability which is characterized at high temperatures by large transport coefficients [1]. The reactor walls would then be in contact with a hot plasma ($T \approx 3$ keV) and be bombarded by particles with energies greatly in excess of the sputtering threshold of the wall material. Thus, power reactor designs include the use of divertors which attenuate the flux of particles and energy to the first wall by two orders of magnitude.

Another means of protecting the first wall that has been discussed previously [2] is to artificially induce turbulence in the plasma near the wall to ensure that the required thermal fluxes are transported at relatively low plasma temperatures. Here we consider a model of a turbulent plasma blanket assuming that Bohm diffusion, with $D = 1/16(cT/eB)$ and thermal diffusivity $\chi_i = \chi_e = 3D/2$ is produced in some fashion in a layer ≈ 10 cm thick. It is shown that such a blanket can replace a divertor and remove helium and unburnt fuel from the reactor to ensure a low impurity content in the plasma.

Derivation of Equations. The model used here for the physical processes in the region near the wall is as follows. Electrons and ions diffusing perpendicular to the magnetic field strike the wall where they recombine and are thermalized. Because of desorption from the wall a flux of neutral atoms with a temperature $T_M = 1$ eV enters the plasma [3]. It is assumed that their concentration is low and their mutual collisions may be neglected. The following basic physical processes take place: ionization and excitation of the atoms by electron impact, and charge exchange of atoms with ions. Since the probabilities of charge exchange and ionization are comparable, a substantial fraction of the atoms return to the wall.

Part of the neutrals escape through apertures or windows in the walls and are absorbed, e.g., by cryopanels. Thus, it is possible to remove the helium that is formed along with unburnt fuel for regeneration in a steady-state reactor. It seems that the area of these apertures must be small.

The thickness of the region with the neutrals is small compared to the radius of the vessel and the behavior of the neutral atoms may be described by the one-dimensional kinetic equation

$$v_x \left(\frac{\partial f_a}{\partial x}\right) = -(k_{ion} + k)\, n f_a + k f_i n_a, \tag{1}$$

where x is the distance from the wall; n and n_a are the plasma and atomic density; f_i and f_a are the velocity distributions of the ions and neutral atoms; $k_{ion} = \langle \sigma_{ion} | v_e | \rangle$; $k_{ex} = \langle \sigma_{ex} | v_e | \rangle$, $k = \langle \sigma_{ce} | v_a - v_i | \rangle$; σ_{ion} is the ionization cross section; σ_{ex} is the excitation cross section; σ_{ce} is the charge exchange cross section; and, $\langle\ \rangle$ denotes averaging over a Maxwellian distribution. In the definitions of k_{ion} and k_{ex} it is assumed that $v_e \gg v_a$; k is taken to be a constant equal to the average value for the region being considered here.

The boundary conditions for Eq. (1) are the distribution function f_M of the atoms desorbed from the wall (x = 0) and the absence of neutral atoms as $x \to \infty$. f_M and f_i are assumed to correspond to a single velocity in the x direction and to Maxwellian distributions in the other directions; i.e.,

$$f_M = \frac{\Gamma_M}{\sqrt{2T_M/\pi m}}\, \delta\left(v_x - \sqrt{\frac{2T_M}{m\pi}}\right) \frac{m}{2\pi T_M t} \exp\left\{-\frac{m v_\perp^2}{2T_M t}\right\} \tag{2}$$

and

$$f_i = \frac{n}{2}\left[\delta\left(v_x - \sqrt{\frac{2T}{\pi m}}\right) + \delta\left(v_x + \sqrt{\frac{2T}{\pi m}}\right)\right] \frac{m}{2\pi T t} \exp\left\{-\frac{m v_\perp^2}{2Tt}\right\}, \tag{3}$$

Translated from Atomnaya Énergiya, Vol. 44, No. 4, pp. 336-339, April, 1978. Original article submitted March 30, 1977.

0038-531X/78/4404-0384 $07.50

where m is the deuteron mass; T is the plasma temperature; $t = 3/2 - 1/\pi$ is a coefficient chosen because the average energy equals $3T/2$; and Γ_M is the flux of neutral atoms from the wall.

Equation (1) can be transformed into the integral equation [4]

$$f_a = f_M \exp\left\{-\int_0^x \frac{[k_{ion}(x')+k]\, n(x')}{v_x} dx'\right\} + f_+ + f_-. \tag{4}$$

Here, f_-, the distribution function of the charge exchange neutrals moving toward the wall ($v_x < 0$), and f_+, the distribution function of the neutrals moving away from the wall ($v_x > 0$), are given by

$$f_- = \int_\infty^x \frac{kn_a(x')}{v_x} f_i(x', v) \exp\left\{\int_x^{x'} \frac{[k_{ion}(x'')+k]\, n(x'')}{v_x} dx''\right\} dx' \tag{5}$$

and

$$f_+ = \int_0^x \frac{kn_a(x')}{v_x} f_i(x', v) \exp\left\{\int_x^{x'} \frac{[k_{ion}(x'')+k]\, n(x'')}{v_x} dx''\right\} dx'. \tag{6}$$

Integrating Eq. (4) with respect to the velocities, we obtain an integral equation for the density n_a and average energy ε_a of the atoms.

The plasma is treated in the hydrodynamic approximation and the magnetic field is directly parallel to the wall surface. It is assumed that the collision frequency is large, the ion and electron temperatures are equal, and the plasma diffusion is ambipolar.

The particle balance equation including ionization has the form

$$\frac{d\Gamma}{dx} = \frac{d}{dx}\left(D\frac{dn}{dx}\right) = k_{ion} n n_a. \tag{7}$$

In the energy balance equation for the plasma we include the energy loss due to ionization and excitation of atoms, the exchange of energy between ions and atoms due to charge exchange, and the passing of the energy of the ionized atoms into the plasma:

$$\frac{dQ}{dx} = \left[-(Ik_{ion} + I_{ex}k_{ex}) + k\left(\varepsilon_a - \frac{3}{2}T\right) + \varepsilon_a k_{ion}\right] n n_a, \tag{8}$$

where I and I_{ex} are the ionization and excitation energies of the atoms (13.6 and 11 eV, respectively); $Q = q + (3T + I)\Gamma$ is the total thermal flux transported by the plasma; and, $q = (\chi_i + \chi_e) n (dT/dx)$ is the thermal conductivity flux.

Boundary Conditions. We now describe the choice of boundary conditions for Eqs. (7) and (8). For $x \to 0$ ($x \ll \lambda$, where λ is the mean free path of the atoms) heat transport is due to a flux of particles and the thermal conductivity flux q is equal to zero. We can use the estimate $n_w \approx \sqrt{\frac{\Gamma}{T/m}}$ to determine the plasma density right next to the wall. The hydrodynamic description of a plasma is valid when the characteristic distance over which the density changes, $l = n/\nabla n$, is greater than the ion cyclotron radius ρ_i. Using the Bohm diffusion coefficient, for $x \ll \lambda$ we can write $D\Delta n = \frac{1}{16}\rho_i \sqrt{T/m}$; $n/l = n_w \sqrt{\frac{T}{m}}$, from which it follows that $n = 16(l/\rho_i) n_w$. The limiting density for applicability of hydrodynamics is $n_H > n_w$; thus, there must be a point $x = x_H$ when $n = n_H$ and $n_H/(\nabla n)_H = \rho_i$. In the following it is assumed that $x_H = 0$. The change in density from n_H to n_w takes place in a kinetic region of thickness of order $\rho_i \ll \lambda$; that is, setting $\Gamma = \text{const}$ and $q = 0$ in this region is valid. As boundary conditions for Eqs. (7) and (8) at the wall (more precisely, at the boundary of the kinetic region) we take $q = 0$ and

$$\frac{n_H}{(\Delta n)_H} = \rho_i. \tag{9}$$

The flux of slow atoms from the wall, Γ_M, is determined by the condition for the problem to be steady-state. The values of σ_{ion}, σ_{ex}, and σ_{ce} are taken from [5-7].

The region with an artificial turbulence is chosen to be large enough (10 cm) that the flux of neutrals at the inner boundary is small. The plasma density and thermal flux expected in future power reactors are specified at this inner boundary: $n_0 = 10^{20}\ m^{-3}$, $Q_0 = 1\ MW/m^2$. The plasma flow out of the reaction zone is such that the loss of particles due to diffusion is much (e.g., about 100 times) greater than the fuel consumption. This regime can be produced by trapped particle turbulence and will cause a small fraction of helium to appear in the reaction zone [1]. For concreteness it was assumed that $\Gamma_0 = Q_0/3.5\ MeV \cdot 100 = 2 \cdot 10^{20}\ m^{-2} \cdot sec^{-1}$.

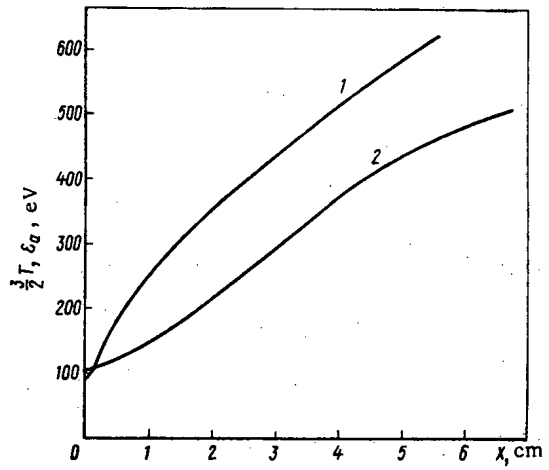

Fig. 1

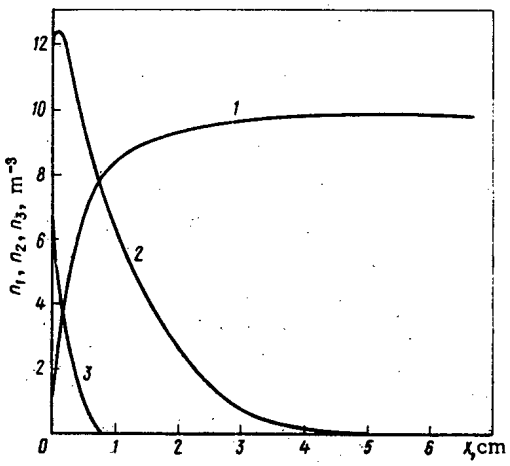

Fig. 2

Fig. 1. Profiles of the average energy of the plasma (1) and of the charge exchanged atoms (2).

Fig. 2. Profiles of the densities of the plasma, $n_1 \cdot 10^{19}$ (1), of the charge exchanged atoms, $n_2 \cdot 2 \cdot 10^{16}$ (2), and of the cold atoms, $n_3 \cdot 10^{18}$ (3).

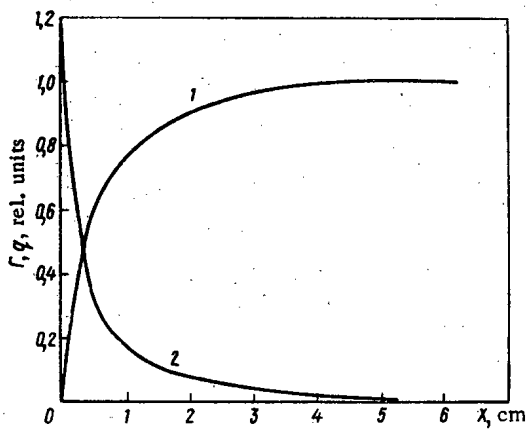

Fig. 3

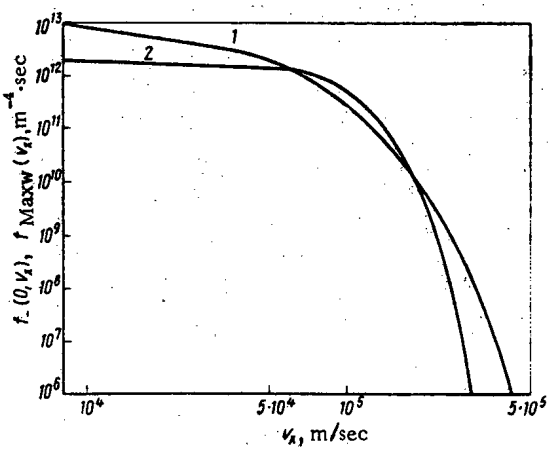

Fig. 4

Fig. 3. Profiles of the thermal conductivity energy flux q (1) and of the plasma particle flux Γ (2).

Fig. 4. The velocity distribution of the charge exchanged atoms incident on the wall (1) and the Maxwellian distribution (2) for equal particle fluxes and average energies.

Results. This system of equations was solved by the method of successive approximations. The results of the numerical calculation are shown in Figs. 1-3. The thickness of the region into which the neutrals penetrate is about 10 cm. The accommodation coefficient of the atoms by the plasma is 0.6. The neutrals carry off 30% of the energy and the luminous energy flux due to emission from excited atoms is insignificant. A few estimates justify the neglect of interatomic collisions. The plasma temperature at the wall is 60 eV and the approximation $T_e = T_i = T$ is valid over the entire region of interest, except in the zone where cold charge exchanged atoms exist. The flux of charge exchanged neutrals to the wall is almost two orders of magnitude greater than Γ_0, which makes it possible to maintain a steady state with the aid of apertures whose area is a few percent of the entire surface.

In order to find the rate of sputtering of the wall by atoms and ions incident on it, the corresponding velocity distributions must be known. It was shown in [4] that the dependence of the density of atoms on x is similar for Maxwellian and one-velocity model ion distribution functions. Thus, using the plasma and atom density profiles obtained here, it is possible to find the distribution function of the atoms for Maxwellian ions. This function will not differ greatly from the case when the densities themselves have been evaluated assuming that the ion distribution function is close to Maxwellian. Figure 4 shows the distribution function $f_-(0, v_x)$ of

the neutrals incident on the wall integrated over v_y and v_z. Knowledge of the distribution function $f_-(0, v_x, v_\perp)$ makes it possible to evaluate the sputtering of the wall by the atoms and ions incident on it:

$$S_a = \int_{-\infty}^{0}\int_{0}^{\infty} f(\varepsilon) f_-(0, v_x, v_\perp) v_x dv_x 2\pi v_\perp dv_\perp, \tag{10}$$

$$S_i = \int_{-\infty}^{0}\int_{0}^{\infty} \Gamma(0) \left(\frac{m}{2\pi T_a}\right)^2 \exp\left\{-\frac{m}{2T_a}(v_\perp^2 + v_x^2)\right\} f(\varepsilon) v_x dv_x 2\pi v_\perp dv_\perp, \tag{11}$$

where $\varepsilon = (m/2)(v_\perp^2 + v_x^2)$; $Ta = 2\varepsilon_a(0)/3$; and $f(\varepsilon)$ is the sputtering coefficient of the wall by fuel ions and atoms of energy ε. For molybdenum $f(\varepsilon)$ has the form [8]

$$\begin{aligned} &f(\varepsilon) = 0 \text{ for } \varepsilon < 60\,\text{eV or } \varepsilon > 52.25\ \text{keV};\\ &f(\varepsilon) = 5.2\cdot 10^{-3}(\ln\varepsilon - 4.1)\\ &\qquad \text{for } 60\,\text{eV} < \varepsilon < 5.25\ \text{keV};\\ &f(\varepsilon) = 1.04\cdot 10^{-2}(11 - \ln\varepsilon)\\ &\qquad \text{for } 5.25\ \text{keV} < \varepsilon < 52.25\,\text{keV}. \end{aligned} \tag{12}$$

(In these formulas the value of the energy ε is in eV.) From the numerical calculation we have $S_a = 8.9\cdot 10^{18}$ $m^{-2}\cdot sec^{-1}$ and $S_i = 6.8\cdot 10^{18}\ m^{-2}\cdot sec^{-1}$.

The steady-state impurity density near the wall can be determined from the balance of entering and escaping particles,

$$\frac{n_{Mo} v_{Mo}}{4} = S_i + S_a. \tag{13}$$

The thermal speed of the impurities may be taken to be 10^4 m/sec, which corresponds to the plasma temperature. In this case $n_{Mo} = 6\cdot 10^{16}\ m^{-3}$. Because of the large turbulent diffusion coefficients (due to trapped particles in the reaction zone and to Bohm diffusion on the periphery), the impurity density distribution will be flat over the cross section. The amount of self-sputtering of the wall is small compared to sputtering caused by the main components of the plasma.

Therefore, a turbulent blanket can keep the impurity density much lower than the "lethal" amount dangerous for thermonuclear burn [9]. Artificially creating the conditions for Bohm diffusion of the plasma in the wall layer will greatly ease the extreme conditions at the first wall of a thermonuclear reactor and reduce wall sputtering without using a divertor.

LITERATURE CITED

1. B. Badger, et al., Report UWFOM-150 University of Wisconsin Nucl. Engineering Dept. (1967).
2. A. Nedospasov, in: Proceedings of the Seventh European Conference on Controlled Fusion and Plasma Physics, Lausanne (1975), p. 129.
3. A. B. Izvozchikov and M. P. Petrov, Fiz. Plazmy, 2, 212 (1976).
4. S. Rehker and H. Wobig, Plasma Physics, 15, 1083 (1973).
5. B. M. Smirnov, Atomic Collisions and Elementary Processes in Plasmas [in Russian], Atomizdat, Moscow (1968), p. 65.
6. E. McDaniel, Collision Phenomena in Ionized Gases [Russian translation], Mir, Moscow (1967), p. 224.
7. D. R. Bates (editor), Atomic and Molecular Processes, Academic Press (1962).
8. V. M. Gusev et al., Preprint IAÉ-2545, Moscow (1975).
9. V. I. Gerdvids and V. I. Kogan, Preprint IAÉ-2722, Moscow (1976).

CAMAC ELECTRONIC HARDWARE FOR HIGH-ENERGY PHYSICS

I. F. Kolpakov

UDC 539.107.5

The electron spectrometer operating in a particle beam from an accelerator and on-line with a computer is the principal type of hardware in high-energy physics. The electron spectrometer usually is a multipurpose setup for studying several types of events with elementary particles and comprises detectors, electronics for receiving and recording information, and a computer for preliminary analysis of events. An event is expressed by the simultaneous recording of several words by the setup.

A distinctive feature of the electronic hardware of high-energy physics, operating on-line with a computer, as compared to the automatic control systems for technological processes is that the requirements on a number of parameters are more stringent. This hardware boasts: a high rate of data accumulation in the computer (up to 10 Mbit/sec); a large volume of recorded data (number of parameters, channels), up to 10^5-10^6 words/sec; pulsed accumulation of events which are randomly distributed in time; reliability (continuous operation for several hundred hours); and a high level of external noise (high-frequency induction from the accelerating electrical field and pulsed high-voltage discharges, and a magnetic field rapidly varying at the rate of up to 5 T/sec). These features of spectrometers make the experience from their construction and operation extremely attractive for both experimental facilities for scientific research and for control tasks.

The requirements placed on equipment for high-energy physics lead to an unequivocal need to employ modular structure for systems and to build these systems from separate functional modules. The CAMAC system, which today is an international standard (standard MÉK482), was chosen in 1970 as the basis for the execution of such modular structures.

In this system any electronic equipment is built from standard modules mounted in a crate (Fig. 1), a unified chassis with a power supply unit in a system of parallel bus-lines on connector sockets at the back panel. Exchange of data is effected through the bus-lines. The first crates at the Joint Institute for Nuclear Research (JINR) were made in 1970 and, moreover, crates of the Transrack company (France) were also used. At first, 86-way connector sockets of the R 5000148 type were used (Carr Fastener Co., Ltd. and UECL, Gt. Britain). In 1971 the Institute began using WK 46579-80 connectors (mfd. by Tesla Lanskroun, exported by KOVO, Czechoslovakia). In 1972-1973 production of crates was started in Poland* and Hungary.† These crates contain a dataway made with multiple-wire cable and requiring power supplies. They now comprise the bulk of the crates used at JINR.

Individual systems are built from functional modules mounted in a crate. The exchange of data between modules takes place through the extreme right-hand module, the controller, which occupies two mounting stations. If the command source is connected to the controller or built into it, then it is possible to organize an autonomous system (Fig. 2) to execute an individual program, e.g., output to a digital printer, perforator, or indicator. The source of programs may consist, in particular, of a computer connected through an interface module mounted in the crate. Up to 368 words can be obtained from such autonomous systems.

Some autonomous systems were built, viz., a timer for controlling the Krion ion source, a system for recording the parameters of an SKM-200 2-m streamer chamber, the beam indication system of the Lyudmila 2-m hydrogen chamber, and an output system to drive a digital printer, tape puncher, and indicators. One such autonomous system, which takes data from ten 8-decade scalers with a counting rate of up to 160 MHz and outputs these data into a digital printer, is used in a spectrometer for studying relativistic nuclei; this system is shown in Fig. 3.

In 1970-1976 the High-Energy Physics Laboratory developed more than 120 different types of CAMAC modules [1-3], which can be divided functionally into the following groups.

*Polon Enterprises (Warsaw), type 002 or 012, power supply unit type 041 or GZC-10, respectively; exported by METRONEX.
†TsIFI Enterprises (Budapest), type CAM 9.01, exported by METRIMPEX.

Translated from Atomnaya Énergiya, Vol. 44, No. 4, pp. 339-347, April, 1978. Original article submitted December 28, 1976.

 0038-531X/78/4404-0388$07.50

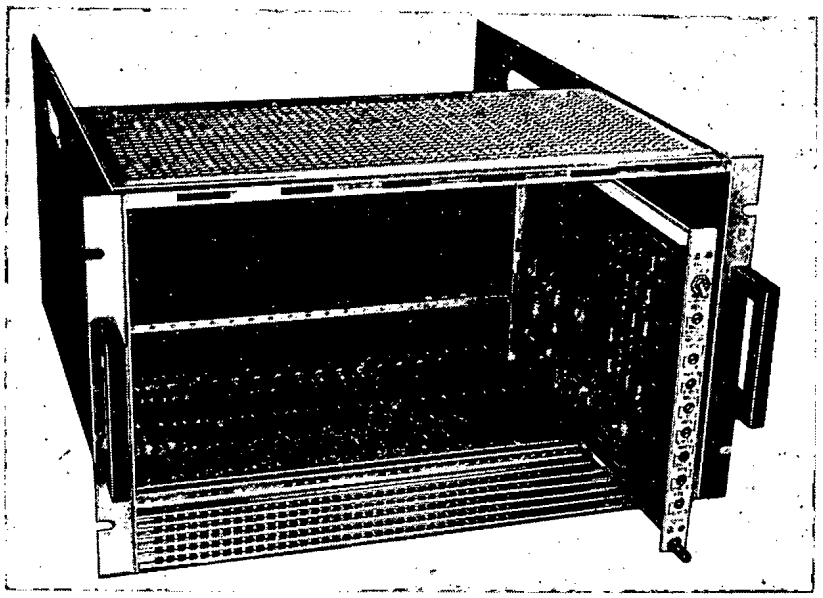

Fig. 1. Functional modules in CAMAC crate.

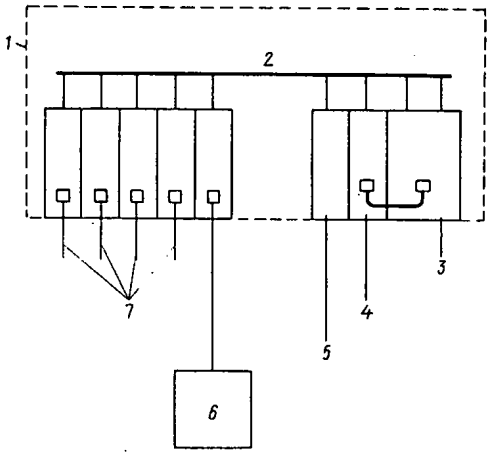

Fig. 2

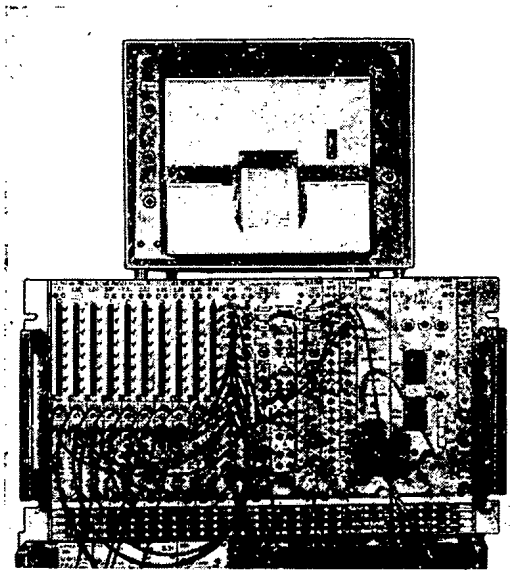

Fig. 3

Fig. 2. Schematic of autonomous one-crate system: 1) crate; 2) crate dataway (EUR, 4100e); 3) controller used to read from command memory; 4) permanent memory; 5) binary-to-binary-decade converter; 6) peripherals; 7) functional modules.

Fig. 3. System for output from decade scalers to digital printer.

1. Controllers of existing computers, in particular, for EC1010, Hp2116B, TPA1001, TPA-i, TPA-70, and BÉSM-4; an autonomous controller; a type A controller for the organization of large systems on the basis of an external cable dataway or branch and other modules for branch organization.

2. Counters and registers: binary scalers with a capacity of 16×4 and 24×2; decade counters with a capacity of 10^8 ($2 \cdot 10^4$); parallel input and output registers of various types; etc.

3. Converters: 9-digit analog-to-digital (ADC) with a conversion time of 8 μsec; digital-to-analog (DAC); charge-to-digital; time-to-digital (TDC); etc.

4. Interfaces (connection module) for peripherals: punches, teletypes, digital printers, modems, digital voltmeters, etc.

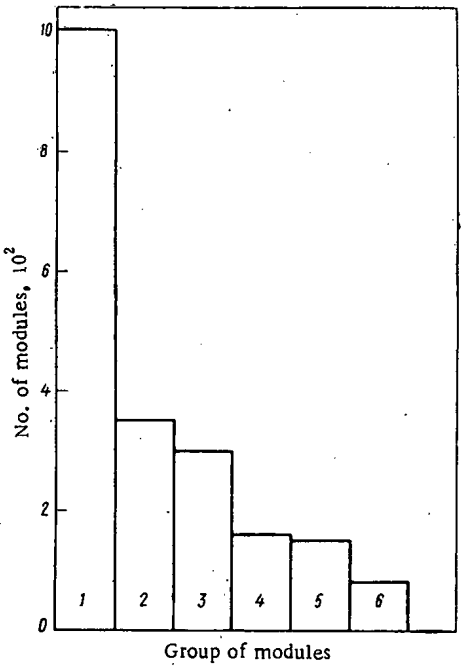

Fig. 4

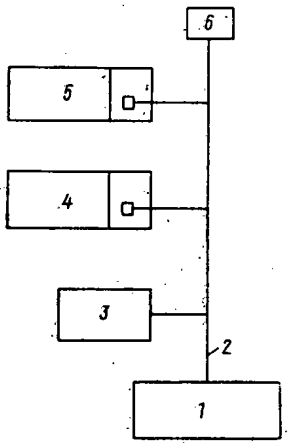

Fig. 5

Fig. 4. Distribution of individual modules according to type: 1) scintillation counter electronics; 2) wire chamber electronics; 3) ADC, TDC, and DAC; 4) counters; 5) controllers; 6) interfaces for peripherals.

Fig. 5. Schematic of radial connection of multicrate systems: 1) computer; 2) dataway to computer; 3) peripheral; 4) crate 1; 5) crate 2; 6) matcher.

5. Modules for recording data from detectors used in high-energy physics: wire proportional chambers, spark chambers, and scintillation counters.

It should be noted that analog and nanosecond circuits as well as digital modules have been made from the outset in the CAMAC system.

Figure 4 shows the total number of CAMAC modules of various types which are used in the experimental facilities of the Laboratory. All told, 179 crates and roughly 2000 CAMAC modules are used. This is a significant part of the CAMAC modules in JINR; 75% of the modules were built in the Institute and 25% were obtained from Hungary and Poland. In particular, most of the type A controllers and the 12-digit precision ADC were supplied by TsIFI (modules of types CAM 1.01 and CAM 4.05). The proportional chamber modules and part of the modules with the scintillation counter electronics were developed in the Laboratory and put into production by Polon, which then supplied them to JINR.

The exchange of hf signals between modules, peripherals, and detectors in physical installations is executed through MK-50 connectors.* Earlier, before production of these connectors began in Czechoslovakia, similar connectors of the 00250 type (mfd. by LEMO, Switzerland) were used. For lf signals transmitted through multiple cables to CAMAC modules, use is made of RP-15 multiple-pin connectors and connectors with 50, 37, 25, 15, and 9 pins (type 871/881 Unitra-Electra, Poland) the equivalent of type DB† (DB52, DB25, etc.). The most suitable for systems with a large number of inputs is type 2DB (2DB52, 2DB25, etc.).

An intercrate interface which has a capacity for up to 704 words is used to organize autonomous systems containing two crates.

The capabilities of each facility can be characterized by the number of CAMAC crates used in it since each crate holds a certain number of functional modules.

*Exported by KOVO, Czechoslovakia.
†Cannon Co., U. S. A.

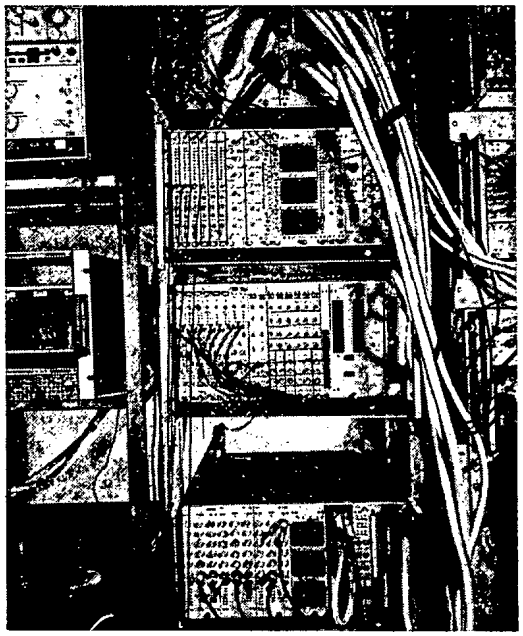

Fig. 6

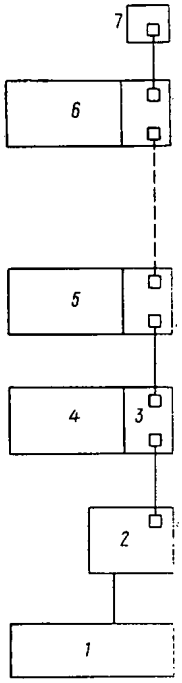

Fig. 7

Fig. 6. CAMAC electronics of Foton facility.

Fig. 7. Schematic of CAMAC branch: 1) computer; 2) branch controller; 3) type A crate controller; 4) crate 1; 5) crate 2; 6) crate 7; 7) branch matcher.

The following spectrometers and control systems on-line with a computer are the main, and largest, facilities of the Laboratory.

1. The Foton magnetic spark Čerenkov spectrometer with 100 spectrometric channels and 40 wire chambers (eight crates, system with radial multiplexer connection to Hp2116B computer).

2. The Al'fa magnetic spectrometer with proportional chambers with 2500 wires (13 crates, 2 branches, system crate, and BÉSM-4 computer).

3. Control system for slow synchrophasotron beam extraction (11 crates, branch for seven crates, system crate, and EC1010 and EC1010B computers).

4. The large BIS-2 magnetic spectrometer with proportional chambers with 7500 wires (43 crates, two branches, system crate, and EC1040 and TPA-i computers).

The first spectrometer on-line with an Hp2116B computer with CAMAC apparatus was the multipurpose Foton system built in 1972-1973 for research on hadron physics [4]. The system contains eight crates and a computer with 32K 16-digit words and a complete set of peripherals. The organizational principle of the connections between the system and the computer is illustrated in Fig. 5. Here, the controllers of individual crates are connected directly to the computer channel through a multiplexer-driver. The driver is connected to the computer through two channels, a command channel and a data channel. A channel consists of an interface card in the input–output system of the computer and a cable connection to the driver. The signals of each channel are separated in the driver in parallel to seven connectors in accordance with the number of the crate controllers connected to the driver. Three crates hold the recording electronics for spark chambers (two crates) and proportional chambers (one crate) as well as the monitoring and control modules (Fig. 6). These modules make it possible to record, per useful start, 642 words of 16 bits which contain 640 coordinates of 32 spark chambers. This information is transmitted in an exact format along the direct access channel to the memory in 7.2 msec. The crate containing the proportional chamber electronics records 20 words of 16 bits from six proportional chambers. The remaining four crates hold ADC and scalers for recording data from a 90-channel Čerenkov spectrometer. It should be noted that this system is an economic alternative to the branch described below which presents another way of organizing large systems. It uses an external cable-connector dataway and special crate controllers type A (CCA) which constitute a so-called branch

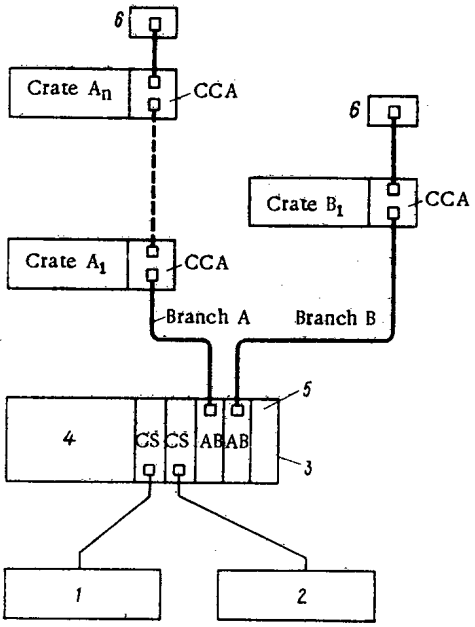

Fig. 8. Schematic of multibranch systems based on system crate: 1) computer; 2) second control source; 3) system crate; 4) CAMAC module; 5) executive controller; branch matcher.

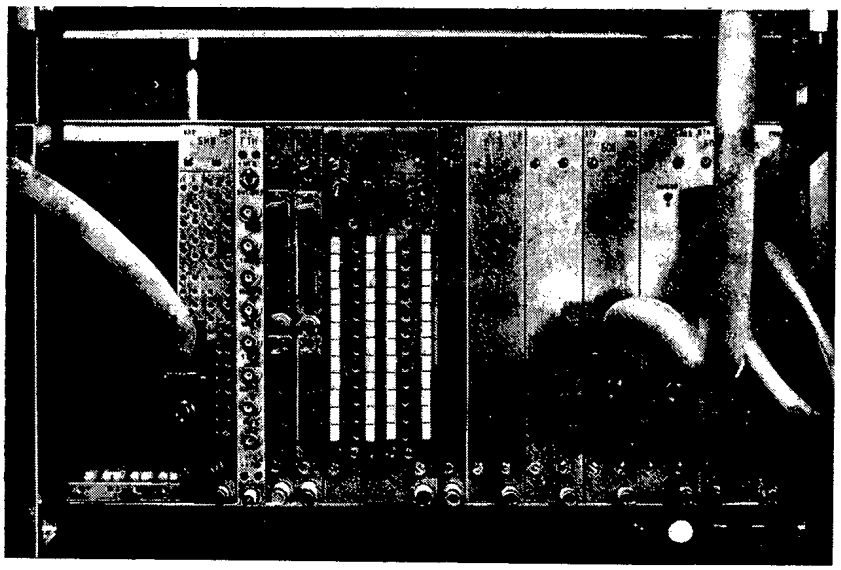

Fig. 9. System crate.

(Fig. 7) containing as many as seven crates. Such a system can record up to 2576 words. A type 132PE189* flexible multiple cable of 66 twisted pairs of wire and a type WSS 132† high-density 132-contact connector were used to organize the branch.

A special system of crates [5], enabling up to 10 branches or up to 20 command sources (computers) to be connected, were used to construct arrangements containing more than one branch (Fig. 8). The system crate is made in the form of a set of specialized modules which are mounted in an ordinary CAMAC crate. This set contains a control module, a priority module or LAM grader, a branch interface module (AB), and an interface module to the command source (CS) (Fig. 9). A computer or a manual control unit (during align-

*Preciable Bour, France.
†Hughes Microelectronics and EMIHUS Microcomponents, Gt. Britain.

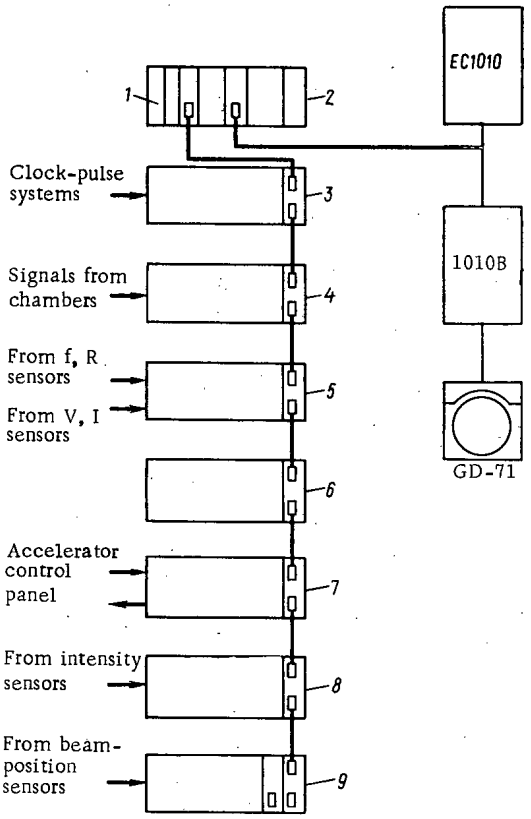

Fig. 10. Schematic of control system for slow beam extraction from synchrophasotron: 1) autonomous control source; 2) system crate; 3) time-measurement crate; 4) measurement of beam profile and position; 5) measurement of parameters of accelerator and elements of extraction system; 6) correction of beam position, timing modules; 7) interface crate to control panel; 8) measurement of nuclear intensity; 9) measurement of beam orbit.

Fig. 11. Electronics of synchrophasotron control system.

ment) may be control sources. When there are several command sources their look-at-me requests to the control module are organized by the LAM grader. Unlike other systems of this type, a system crate does not require an additional external dataway; it can simultaneously operate not only with several branches but also with several command sources (computers) and thus makes it possible to build systems comprising up to 70 crates.

Three large systems based on a system crate have been built. For example, the Alfa magnetic spectrometer, with 2500-wire proportional chambers [6] for research with relativistic α particles, contains 13 crates organized in two branches on-line with a BÉSM-4 computer (at a distance of 1.2 km from the experimental facility) or EC1010 computer. Transfer to the computer is carried out by 24-bit CAMAC driver-receivers through a parallel communications link based on 70 twisted pairs of hf telephone cable and an appropriate system crate.

Another example of large systems is that of a system for recording the parameters and controlling slow beam extraction from the synchrophasotron [7] (Fig. 10). The system includes an EC1010 computer with a memory with a capacity of 32K words of 16 bits and a complete set of peripherals and, connected with it by a program channel, a computer with a memory with a capacity of 16K words of 8 bits, the second computer serving as the display processor of a GD-71 graphical display. The electronics of the system is mounted in two CAMAC racks (Fig. 11). All told, 11 crates are used, including a branch comprising seven crates which is connected to an EC1010 computer through a system crate. Exchange of information (about 10K words) takes place along the program channel at the rate of 30,000 24-bit words/sec through an interface card into the input–output system of the computer. In each acceleration cycle the system measures and monitors the spatial characteristics of the extracted beam, representing the information about the beam profiles in two planes and about the integrated profiles on all these segments, and in between cycles stabilizes the spatial characteristics of the beam and provides the necessary information to the control panel about the operating regimes of the system. The beam profiles are shown on the GD-71 graphical display. The system of programs of exchange between two computers (rate of exchange up to 30 kbite/sec) is controlled by means of a light pen and command symbols on the display screen. Output to the display occurs when a certain symbol is drawn with the light pen.

The CAMAC equipment for measuring the spatial characteristics of the beam contains six fast 8-bit ADC, a buffer store module with a capacity of 256 words of 24 bits, and an autonomous controller in a system crate. Because the EC1010 computer has no direct-access channel, fast retrieval of information is effected at first in the buffer store module and then in the computer. Measurement of the spatial characteristics of the beam was synchronized by varying the magnetic field of the accelerator, the frequency of the accelerating voltage, and the radial position of the beam in the accelerating chamber. Moreover, the equipment of the system includes parallel registers for the link with the operator's control panel, 12-bit ADC for measurements of the intensity and radical deflection of the beam, timers, interfaces for four- and five-digit voltmeters for measuring the induction of the magnetic field, and binary and decade counters. The intensity curve during the acceleration cycle is shown on the graphical display. Digital information is put on the screens of four VT 340 alphanumerical displays, where useful and omitted cycles are counted according to the azimuth in the vertical and horizontal planes on an alphanumerical display. This crate contains two 8-bit ADC, a 10×16-bit-word memory, and other modules.

A large magnetic spark spectrometer with 7500-wire proportional chambers on line with EC1010 and TPA-i computers is installed at the present time on the beam of the 76-GeV accelerator of the Institute of High-Energy Physics (IFVÉ) at Serpukhov [8]. The facility contains 43 crates and two branches, organized through a system crate. The software of all the systems described above was based on the manufacturer's control programs and the program drivers of the CAMAC equipment was based on the assemblers of the respective computers.

Large systems for high-energy physics can serve as prototypes for some data systems for controlling technological processes on the basis of present-day CAMAC electronics. As shown by the experience of foreign companies, however, the construction of commercial CAMAC modules requires such components as R AO302 and F 302* connectors for twisted pairs, R A303 and F 303 as well as R A1303 and F 1303* (high-voltage) connectors for shielded twisted pairs, and AMP20, AMP6,† 2DB52, 2DC79, and DB25‡ multiple-way connectors. It is also necessary to have special-design cabinets, protected from the ambient conditions.

*LEMO, Switzerland.
†Amphenol, U. S. A.
‡Cannon, U. S. A.

It proved possible to supply the CAMAC electronics for the needs of high-energy physics in a comparatively short time, in many ways because of the collaboration with institutes of the socialist member-countries of the Joint Institute for Nuclear Research (JINR), especially with the Polon and TsIFI enterprises.

In the construction of on-line facilities for high-energy physics the period of disappointment when the computer was put on-line, a period which usually follows the great enthusiasm after the decision to use a computer, was reduced to a considerable degree. The comparatively rapid and successful start-up of these facilities was due in no mean measure to the enormous work done on creating the system of CAMAC modules and interfaces. The extension of the experience gained to other areas of application is one piece of evidence of the great influence that basic scientific research in high-energy physics has on advances in modern technology.

Large electronic systems for physics have attained such a size that it is advisable to consider their further development towards miniaturization (increasing the number of functions in an individual module) and improving and simplifying data exchange. The application of special-purpose hybrid integrated circuits for modules of detector electronics and analog modules is one of the promising ways of increasing the reliability and miniaturization of this equipment. The prospect of using microprocessors and distributed control on the basis of these microprocessors will permit computers to be relieved of many secondary tasks and to limit the cost of such systems.

LITERATURE CITED

1. V. A. Aref'ev et al., in: Proceedings of the Sixth International Symposium on Nuclear Electronics [in Russian], D13-6210, JINR, Dubna (1972), p. 218.
2. V. Arefiev (Aref'ev) et al., CAMAC Bull., No. 10, 13 (1974).
3. S. Basiladze et al., Nucl. Instr. Methods, 106, 157 (1973).
4. E. Chernykh et al., CAMAC Bull., No. 10, 21 (1974).
5. Nguyen Phuc and V. A. Smirnov, in: Proceedings of the Eighth International Symposium on Nuclear Electronics [in Russian], D13-9287, JINR, Dubna (1975), p. 190.
6. V. G. Aref'ev et al., in: Proceedings of the All-Union Meeting on Automation of Nuclear Physics Research (Digests of Papers) [in Russian], Izd. IYaI Akad. Nauk Ukr. SSR, Kiev (1976), p. 187.
7. E. Chernykh et al., in: Proceedings of the Second International Symposium on CAMAC, Brussels, Oct. 14-16, 1975, p. 463.
8. G. Aikhner et al., in: Proceedings of the All-Union Meeting on Automation of Nuclear Physics Research (Digest of Papers) [in Russian], Izd. IYaI Akad. Nauk Ukr. SSR, Kiev (1976), p. 98.

ONE POSSIBLE WAY OF MEASURING DOSES FROM ACCIDENTAL IRRADIATION

I. A. Alekhin, S. P. Babenko,
I. B. Keirim-Markus, S. N. Kraitor,
and K. K. Kushnereva

UDC 539.12.08

Interest has recently grown in the use of radiolyoluminescence (RLL) for the dosimetry of ionizing radiation. This term denotes the luminescence which arises when previously irradiated solids are dissolved. It was first observed back in 1895 [1] during dissolution of chlorides of alkali metals and it was then proposed to call it lyoluminescence (from the Greek lyo, to dissolve). This term is still in use today although in the case of organic substances, e.g., saccharose (mannose, glucose, etc.) the emission of light occurs in a complicated manner and is associated not only with the dissolution of the solid but also with chemical reactions between it and the solvent.

The radiolyoluminescence of organic and inorganic substances in water was studied in [2, 3]. It was shown that the considerable RLL yield, the tissue-like composition of saccharides, the slight drop in the effect with time after irradiation, the availability of substances, and the simplicity of observation of the luminescence make it possible to construct lyoluminescence dosimeters for ionizing radiation. At the same time, comparison with familiar dosimeters such as thermoluminescence [4] (γ-ray) or track dosimeters with fissionable isotopes [5] (neutrons) shows that lyoluminescence dosimeters have poorer reproducibility of readings and a large spread of characteristics during fabrication, and sensitivity to moisture and other climatic factors, and permit only one-time use.

It might be interesting and useful to create new personal dosimeters, e.g., for neutron or x-ray radiation, in which case the requirement of minimum energy dependence is difficult to meet. The principal advantage of RLL, in our opinion, lies in the fact that because of dissolution and liberation of the energy stored under irradiation light is emitted by substances in which no radioluminescence of any sort is ordinarily observed. This substantially extends the range of substances accessible for use in such a widespread, tried and tested dosimetric method as luminescence dosimetry.

Radiolyoluminescence is possible not only in saccharides but also in other organic substances, especially in biological human tissue. Samples of such tissue as hair, nails, and a keratic layer of skin can always be taken from a person subjected to accidental irradiation and the radiation dose can be determined from the RLL yield of these samples. The RLL data obtained about samples from various areas of the body surface can supplement the existing system of emergency personal monitoring based on the use of IKS-A and GNEIS personal dosimeters [6] and can be the sole sources of information about the dose in accidental irradiation when there are no personal dosimeters at all.

The RLL of biological tissue was detected with a scintillation detector (Fig. 1) with an FÉU-29 photomultiplier (dark current on photomultiplier $\sim 6 \cdot 10^{-7}$ A with an anode sensitivity of 1000 A/lm). Above the photocathode is a glass cuvette containing solvent. The biological tissue samples were contained in a dish on a shaft and dropped into the cuvette when the shaft was turned. The pulse of photomultiplier current caused by the luminescence as the samples dissolved was fed into a measuring unit to determine the parameters of the lyoluminescence.

The schematic of the measuring unit is presented in Fig. 2. The pulse is fed into a dc amplifier with a small time constant and a delay line ($\tau_d = 1$ msec) at its output. A 50-Hz mercury relay connects the line to a load whose resistance is equal to the wave resistance of the line. As a result, pulses are formed on the load, their length being $2\tau_d$, frequency 50 Hz, and amplitude proportional to the running value of the RLL current at the instant that the load is connected. Thus, instead of a comparatively weak varying current due to the RLL, there is a pulse train whose envelope coincides with the time dependence of the RLL. After the converter changing amplitude to pulse count this pulse train arrives at the time analyzer and the spectrum from the analyzer is fed into the digital printer or recorder.

Translated from Atomnaya Énergiya, Vol. 44, No. 4, pp. 347-350, April, 1978. Original article submitted March 21, 1977.

0038-531X/78/4404-0396$07.50

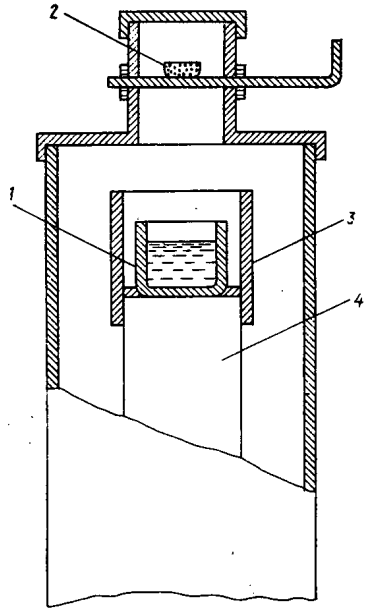

Fig. 1. Scintillation detector for radiolyoluminescence: 1) cuvette with solvent; 2) dish for samples; 3) reflector; 4) photomultiplier.

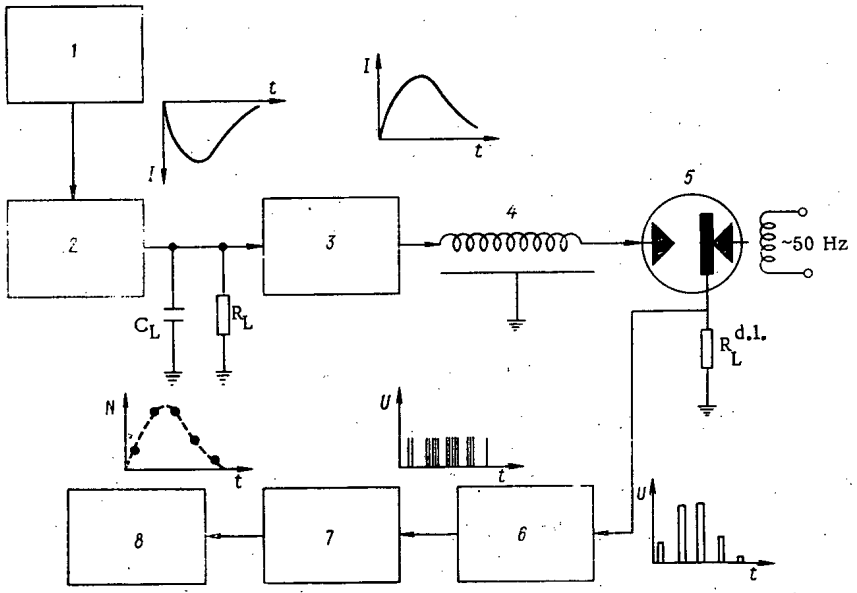

Fig. 2. Schematic of unit for measuring characteristics of radiolyoluminescence: 1) high-voltage rectifier; 2) photomultiplier; 3) dc amplifier; 4) delay line; 5) mercury relay; 6) amplitude-to-count converter; 7) time analyzer; 8) recorder (digital printer).

We detected radiolyoluminescence in such biological tissue as hair, nails, and the keratic layer of skin irradiated with neutrons from an IRT reactor [7] and ^{60}Co γ rays. The solvent used was an aqueous solution of sodium sulfide and the samples weighed about 10 mg. The radiolyoluminescence intensity for γ-ray-neutron irradiation is such that a dose of 1 and 3 krd for hair and nail, respectively, corresponds to the amplitude of the anode current pulse from the photomultiplier of $6 \cdot 10^{-7}$ A. If photomultipliers with a dark current 100 times smaller (e.g., FÉU-37, FÉU-71) are used, then a neutron dose of 10-30 rd is equivalent to such a current and the minimum detectable doses will be even smaller; this is perfectly acceptable for emergency dosimetry.

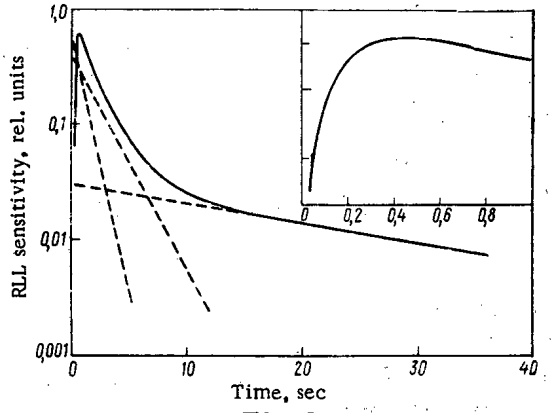

Fig. 3

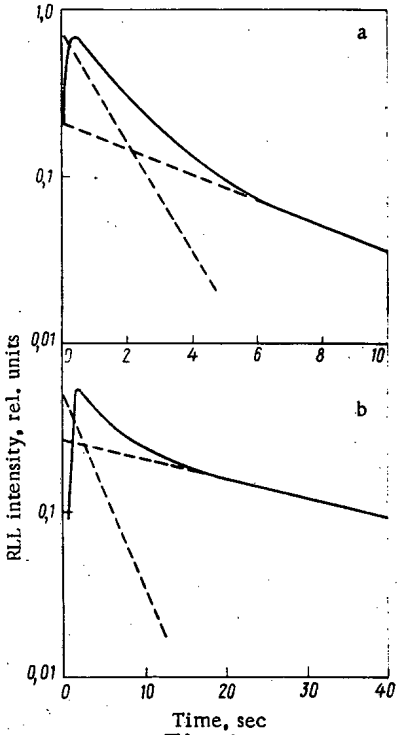

Fig. 4

Fig. 3. Pulse of radiolyoluminescence from hair (—) and its resolution into components (---).

Fig. 4. Radiolyoluminescence pulses from a) cotton and b) paper (—) and their resolution into components (---).

A further increase in sensitivity can be ensured by increasing the weight of the samples and counting the photons emitted during RLL instead of measuring the photomultiplier anode current.

The mechanism by which RLL occurs in biological tissue is evidently the same as in other organic substances [3]. Irradiation of tissue produces radical R which are in the bound state and, therefore, remain stable for a certain time. When the samples are dissolved the radical become mobile and interact with the oxygen of the solvent, $R+O_2 \rightarrow RO_2$. Next, the molecules combine, forming a bimolecular group of oxygen in the excited state:

$$RO_2 + RO_2 \rightarrow R-R + O_2^* . \qquad (1)$$

When this group goes into the ground state luminescence ensues in the visible portion of the spectrum with wavelength of ~4800 Å. In the solvent used sodium sulfide ensures dissolution of the biological tissue and mobility of the radicals whereas the water is the medium in which the radicals interact with oxygen.

Since radicals with different rates of the reactions indicated are formed during irradiation and since individual components of hair may dissolve in different ways, several components are also observed in RLL. In Fig. 3 they are seen in the RLL pulse of neutron-irradiated hair. The pulse shape I(t) can be approximated by the sum of exponents

$$I(t) = [1 - \exp(-t/\tau_r)] \sum_i a_i \exp(-t/\tau_i), \qquad (2)$$

where τ_r and τ_i are the growth and decay constants, respectively; a_i is the intensity of the i-th component; and t is the time. Three components are observed with a decay constant of 0.8, 3, and 30 sec. The growth constant of luminescence is 0.1 sec. When the samples are dissolved at a slower rate these times are roughly ten times the values for mannose which dissolves quickly in water [3].

Biological tissue does not exhaust the range of organic substances which are also exposed along with humans during accidental irradiation; their lyoluminescence can be measured and used to determine the radiation use. The clothing and documents of the individual are also irradiated and we detected RLL in them when they were dissolved in organic solvents. Figure 4 shows a photomultiplier current pulse resulting from the

RLL of the cotton fabric of overalls and smocks as well as paper under irradiation with γ rays. Two components are observed in the RLL decay curve; the constants characterizing them differ in absolute value by a factor of 4-7 for these two samples. They are 1 and 5 sec for the fabric and 4 and 35 sec for the paper, respectively, although cellulose is the basis of both materials. Evidently, different chemical modifications of the cellulose in these two cases dissolve at various rates and have different mobilities. For this reason the RLL growth rate proves to be different and, consequently, the RLL pulse maximum grows in 0.5 sec for the fabric and in 2 sec for the paper. Their dose sensitivity is 5-7 times lower than for biological tissue but when a lyoluminescence intensifier such as luminol (concentration $\sim 10^{-2}\%$) is added to the solvent, the sensitivity increases by more than one order of magnitude [8]. The RLL of biological tissue and accompanying objects of organic substances gradually decreases after irradiation since the radical concentration drops with time [9]. Although some types of radicals disappear in the first few minutes after irradiation, there are some radicals with long lifetimes. They make it possible to initiate RLL a long time after the irradiation (> 1.5 yr). It thus follows, firstly, that corrections must be introduced for the time decay of RLL when determining the dose for a concrete case of accidental irradiation. Secondly, the existence of long-lived RLL components gives reason to hope that it will be possible to establish the level of radiation received by victims during radiation accidents from inadequate dosimetric information if irradiated samples of biological tissue (hair, nails), clothing, documents, etc. are conserved. It is necessary to get such evidence for an objective characterization of the development of acute radiation sickness in the victims.

The results presented here show that it is possible on the basis of the RLL of human tissue and accompanying objects of organic substances to determine the dose received under accidental irradiation at any point of the body surface. This possibility exists even in the absence of personal dosimeters, which is an extremely important feature under real conditions when the irradiation may be highly uneven and when there may be cases of accidental irradiation without dosimetric monitoring.

LITERATURE CITED

1. E. Wiedemann and G. Schmidt, Ann., 54, 618 (1895).
2. N. Atary and K. Ettinger, in: Proceedings of the Fourth International Conference on Luminescence Dosimetry, Vol. 2 (1974), p. 395.
3. N. Atary and K. Ettinger, in: Proceedings of the Fourth International Conference on Luminescence Dosimetry, Vol. 2 (1974), p. 417.
4. I. A. Bochvar et al., Prib. Tekh. Eksp., 5, 208 (1969).
5. I. B. Keirim-Markus et al., At. Energ., 34, No. 1, 11 (1973).
6. I. B. Keirim-Markus, V. A. Knyazev, and S. N. Kraitor, in: Papers on Some Aspects of Dosimetry and Radiometry of Ionizing Radiation [in Russian], No. 5, Dimitrovgrad (1974), p. 5.
7. Yu. I. Bregadze et al., At. Energ., 12, No. 6, 537 (1962).
8. N. Atary and K. Ettinger, Rad. Effects, 20, 135 (1973).
9. Y. Nakajima and S. Watanabe, Nucl. Sci. Tech., 11, 575 (1974).

POSSIBILITIES OF PURIFYING THE PRODUCTS OF CHEMONUCLEAR SYNTHESIS, WITH ESTIMATES OF THE COST OF SUCH OPERATIONS

V. A. Bessonov and E. A. Borisov

UDC 621.039.72

The synthesis of chemical compounds in a nuclear reactor requires the solution of a number of scientific-technical problems [1, 2], important among which is the removal of radioactive impurities from the products. When the synthesis is carried out with the use of the kinetic energy of fission fragments from nuclear fuel (chemonuclear synthesis), the reaction mass and the synthesis products will be contaminated to a considerable degree by radioactive substances. The activity of the reaction mixture in the production of ethylene glycol (EG) in a 500-MW reactor at the initial instant of time after removal reaches values of the order of 10^6 Ci/ton.

We investigated the possibility of removing radioactive impurities from a reaction mixture of products obtained in the synthesis of ethylene glycol from methanol in the liquid phase. The decontamination factors for the reaction mixture reach values of several thousand with respect to individual radionuclides and depend strongly on the method of decontamination and the composition of the radioactive impurities. Thus, for centrifuging at an acceleration of 7000g and filtration through a Petryanov LSF-2 filter, the decontamination factors for the removal of cerium, lanthanum, and zirconium range from 2 to 50; the removal of ruthenium is poor. Coagulation with aluminum hydroxide concentrated to 0.5 g/liter and a pH of 7.0 makes it possible to remove these elements with decontamination factors of 2-100.

The highest decontamination factors (up to 10^4) are obtained by distillation of the reaction mixture. Iodine is satisfactorily removed only by the ion-exchange resin AV-17 in the OH form. Calculated data on the amount and composition of the radioactive wastes of a hypothetical plant producing EG by the chemonuclear method at the rate of 36,000 tons/yr (a 500-MW reactor) indicate that the main activity will be found in the wastes of the first decontamination stage (in our calculations this means the coagulation assembly) a few hours after removal from the reactor. After 1 month the radioactivity of the wastes from this assembly decreases to $4 \cdot 10^3$ Ci. The specific radioactivity of the wastes may be reduced to 10^3-10^4 Ci/liter.

On the basis of an economic appraisal of an entire EG production complex using a 1500-MW chemonuclear reactor, we can say that the capital expenditures for the decontamination system will be $\approx 11\%$ of the total capital expenditures, and the cost of processing in the decontamination stage will be $\approx 9\%$ of the total processing costs. In the calculations the cost of burying the highly active wastes of a 500-MW chemonuclear reactor amounts to about 160 rubles/m^3. The cost of burial of radioactive wastes, on the basis of the data published in [3, 4], is estimated at about 360 rubles/ton, which is considerably higher than the burial costs obtained by direct calculation. The increased expenditure is due mainly to the severe shielding requirements, the use of expensive structural materials, remote control of the waste-processing operation, and steps required to remove heat from the burial sites. A large proportion of these expenditures were taken into account in the calculations performed to estimate the cost of capital construction of the decontaminating installations and burial systems, and therefore it may be assumed that the expenditure figures for the processing and burial of highly active wastes as obtained by the direct calculation gives a more accurate picture of the possible cost of processing highly active wastes in a future chemonuclear reactor.

Despite the optimistic overall picture found in the calculations on capital expenditures and reduced EG production costs in a chemonuclear reactor of high productivity, the realization of such a process will require a great deal of new scientific, technological, and design work.

LITERATURE CITED

1. E. A. Borisov and V. D. Timofeev, Zh. Vses. Khim. Ova. 18, No. 3, 323 (1973).
2. V. I. Gol'danskii et al., Izotopy v SSSR, No. 12, 7 (1968).
3. Economics of the Processing and Removal of Radioactive Wastes [in Russian], TsNIIatominform, Moscow (1971), AINF 102(P).
4. N. V. Krylova and V. V. Kulichenko, At. Tekh. Rubezhom, No. 2, 37 (1974).

Translated from Atomnaya Énergiya, Vol. 44, No. 4, pp. 351-354, April, 1978.

0038-531X/78/4404-0400$07.50

THE RECONSTRUCTION OF A NEUTRON SPECTRUM WITH A PRIORI INFORMATION

A. A. Shkurpelov, V. F. Zinchenko, and B. A. Levin

UDC 621.039.512.44

Consideration is given to the question of taking account of a priori information when solving the incorrect problem of reproducing a neutron spectrum from activation measurements. The problem reduces to finite-dimensional form with the use of a system of effective constants obtained in the paper by generalizing the method of effective cross sections [1] to a large number of groups. The measured activation integrals are written as

$$\underset{k=1,\ldots,M}{A_k}=\sum_{j=1}^{N}\sigma_{k,j}\varphi_j(1+\delta_k);\quad M<N;$$
$$\varphi_j=\int_{E_j}^{E_{j+1}}\varphi(E)\,dE, \tag{1}$$

where δ_k is the relative error of the activation measurements.

A priori information about the sought spectrum is given in the form of a set of integrated fluxes $\Phi^{(\nu)}$, $\nu = 0, 1, \ldots, L$; $\{\Phi = [\Phi_j = \int_{E_j}^{\infty}\varphi(E)\,dE]$, which, with some degree of reliability, characterize the integrated flux Φ_j from the sought spectrum. This set incorporates the results of measurements, the spectra of reactors of similar design, the results of measurements by other methods, etc. From the given set we choose a reference spectrum $\Phi^{(0)}$ which, in respect of energetic behavior, occupies an intermediate position among the others. Constructing the matrix

$$f_j^{(\nu)}=\frac{\Phi_j^{(\nu)}}{\Phi_j^{(0)}}-1\left\{\begin{array}{l} j=1,\ \ldots,\ N \\ \nu=1,\ \ldots,\ L\end{array}\right.$$

and applying the simplest method in accordance with the algorithm given in [2], in matrix $f_j^{(\nu)}$ we can optimally isolate the given number of trial vectors $\{\Pi_p\}$ characterizing the general laws in the behavior of the integrated fluxes from the set. In this case

$$f_j^{(\nu)}=\sum_{p=1}^{Q}X_p^{(\nu)}\Pi_{p,j}\pm\Delta_j^{(\nu)}\left\{\begin{array}{l} j=1,\ \ldots,\ N \\ \nu=1,\ \ldots,\ L\end{array}\right., \tag{2}$$

where the number Q is taken to be smaller than the number of measurements M and $\Delta_j^{(\nu)}$ are the resulting errors of the expansion. It is assumed that the sought spectrum can also be expanded in the basis vectors $\{\Pi_p\}$, i.e.,

$$f_j=\frac{\Phi_j}{\Phi_j^{(0)}}-1=\sum_{p=1}^{Q}X_p\Pi_{p,j}\pm\Delta_j;\ j=1,\ \ldots,\ N, \tag{3}$$

where $\Delta_j \geqslant \max_{\nu=1,\ldots,L}\{\Delta_j^{(\nu)}\}$ and the coefficients X_p are subject to determination from the integrated experiments (1). Writing the errors Δ_j and δ_k as $\Delta_j = P_j\Delta$ and $\delta_k = \omega_k\delta$ ($P_j = \max_{\nu=1,\ldots,L}\Delta_j^{(\nu)}/\Delta_0$; $\Delta_0 = \max_{\nu=1,\ldots,L;\ j=1,\ldots,N}\Delta_j^{(\nu)}$; $\delta = \min_{k=1,\ldots,M}\delta_k$), we can find the sought solution Φ_j and X_p by minimizing the functional

$$I=\sum_{k=1}^{M}\frac{1}{\omega_k^2}\left[1-\frac{\sum_{j=1}^{N}(\sigma_{k,j}-\sigma_{k,j-1})(f_j+1)\Phi_j^{(0)}}{A_k}\right]^2+\frac{\delta^2}{\Delta^2}\sum_{j=1}^{N}\left(f_j-\sum_{p=1}^{Q}X_p\Pi_{p,j}\right)^2\Big/P_j^2;\quad f_j=\frac{\Phi_j}{\Phi_j^{(0)}}-1. \tag{4}$$

If the solution Φ_j^1, $j = 1, \ldots, N$ obtained by minimizing functional (4) is to satisfy the system of measurements (1) within the limits of experimental error, the error Δ of the expansion is varied from the value $\Delta = \Delta_0$ with a gradual increase. As soon as the solution begins to satisfy the system (1), the corresponding value of Δ is taken to be the optimal and the matrix of errors for the sought solution is found by minimizing functional

(4). The matrix can be used to evaluate the error in various functionals from the sought spectrum, including those characterizing the efficiency of radiation damage of materials. The paper gives the results of processing of the data from actual experiments which testify to the efficacy of the proposed method. As $\Delta \to 0$ or $\Delta \to \infty$, the method is in agreement with methods published earlier [3, 4].

LITERATURE CITED

1. D. J. Hughes, Pile Neutron Research, Addison-Wesley, Cambridge, Mass. (1953).
2. V. A. Daugavet, Zh. Vychisl. Mat. Mat. Fiz., 11, No. 2, 289 (1971).
3. G. Cola and A. Rota, Nucl. Sci. Eng., 23, 344 (1965).
4. V. A. Dulin, At. Energ., 9, No. 4, 318 (1960).

γ-ADSORPTION ANALYSIS OF A SUBSTANCE WITH ALLOWANCE FOR EFFECT OF HEAVY IMPURITIES

I. A. Vasil'ev, Ya. A. Musin, and P. I. Chalov

UDC 539.106

The modification of the γ-absorption method of analysis presented in the paper enables the concentration of an element or a group of elements in samples to be determined in the presence of impurities with higher atomic numbers than those of the elements being determined. The γ-ray source is chosen with an energy such that: 1) the lower energy (E') lies between the values of the K-absorption edge of the heaviest element determined and the lightest of the heavy impurity elements; and 2) the highest energy (E") lies beyond the K-absorption edge of the heaviest impurity element.

The concentration of the sum of the sought elements is found from the simple relation

$$C=(\ln\frac{I_0'}{I'}-P\ln\frac{I_0''}{I''}-m)/M,$$

where I is the intensity of γ-ray beam after passage through a layer of the sample of thickness x; I_0 is the initial intensity; and M and m are determined during calibration of the setup or by calculation from the formulas

$$M=x\sum_{i=1}^{k}\frac{C_i}{C}(\mu_i'-P\mu_i'');$$

$$m=x\sum_{i=k+1}^{n}C_i(\mu_i'-P\mu_i'').$$

Here C_i and μ_i are, respectively, the concentration of the i-th element in the sample and the coefficient of γ-ray attenuation in the i-th element; and C_i/C is the relative concentration of the i-th element being determined in the sum. (All of the quantities refer to a γ-ray energy of E' or E", respectively.)

The coefficient C is chosen from the condition of minimum variation

$$P=\sum_{i=k+1}^{n}(\Delta C_i)^2\mu_i'/\sum_{i=k+1}^{n}(\Delta C_i)^2\mu_i'',$$

where ΔC_i is the real variation of the concentration of the i-th impurity element in the sample.

The method has been introduced in a plant producing rare-earths, where it is used for operative monitoring of the technological process.

ESTIMATION OF THE STEADY-STATE ISOTOPIC COMPOSITION OF PLUTONIUM IN A MODEL OF AN EXPONENTIALLY GROWING NUCLEAR POWER INDUSTRY

A. N. Shmelev, L. N. Yurova,
V. V. Kevrolev, and V. M. Murogov

UDC 621.039.5

The paper considers a three-component model of a developing nuclear power industry (including fast breeders, thermal reactors, and hybrid thermonuclear reactors as auxiliary producers of plutonium) as well as steady-state conditions of exponential development of the nuclear power industry with a close uranium–plutonium cycle. The approach proposed by A. I. Leipunskii et al. (Third Geneva Conference, 1964, USSR, Rep. No. 369) was used to formulate equations for the variations in the contents of higher plutonium isotopes with allowance for losses and delays in the external fuel cycle. The relations obtained make it possible to calculate the steady-state isotopic composition of plutonium as a function of the structure, the growth rate of the nuclear power industry, the losses and delays in the external fuel cycle, and the critical charge of the fast breeders. The isotopic composition obtained can be used to get more precise physical characteristics for the reactors. The following conclusions were reached.

1. In the one-component model of the nuclear power industry, containing fast breeders, with allowance for an increase in its growth rate the steady-state content of the higher plutonium isotopes in the fuel may drop appreciably in comparison with the asymptotic content. For example, for a BN-600 fast breeder operating on oxide fuel (the estimated asymptotic content of $^{239-242}$Pu was 64.1, 26.4, 5.8, and 3.7%, respectively) with allowance for the development of the nuclear power industry at a rate such that it doubles in size in 5 years, the steady-state composition of $^{239-242}$Pu is 79.3, 17.1, 2.9, and 0.7%, respectively.

2. The two-component model of the nuclear power industry contains fast breeders and thermal reactors, with the proviso that the fuel from the fast breeder cores and shields can be charged into the thermal reactors and then returned to the fast breeders. With a small proportion of fast breeders in the industry, the tendency to use the "cleanest" possible plutonium in the thermal reactors makes it preferable to choose the layout of the fast breeders so that to an appreciable extent the charged fuel would burn out and new fuel would accumulate in various areas of the fast breeder cores. In this case the fast breeder cores will be provided with "dirtier" plutonium since the plutonium burned up in them will be made up to a great extent by plutonium from thermal reactors and not by their own production of ^{239}Pu.

3. In the two-component model of the nuclear power industry, containing hybrid thermonuclear reactors and thermal reactors, the steady-state composition of the plutonium in the thermal reactors will be determined by their own repeatedly regenerated plutonium and supplementary charges from the thermonuclear reactors. Such plutonium will be found to contain a noticeable quantity of higher isotopes. The inclusion of fast breeders in the nuclear power industry can make the plutonium used in the thermal reactors "cleaner."

OPTIMIZATION OF THE CYCLICAL OPERATING REGIME OF AN ATOMIC POWER PLANT REACTOR

V. I. Pavlov and V. D. Simonov

UDC 621.039.516:139.566

The maximum principle* is used to optimize the operating regime of an atomic power plant reactor whose power is periodically reduced for several hours according to the load chart of the energy system. The problem is solved for maximum operating time at nominal power U_{nom} in a cycle of period T for a reactor with an operational reactivity margin smaller than the non-steady-state poisoning with xenon which accumulates during the fuel discharging time τ.

Since the operating regime of the reactor in the interval $T - \tau$ consists of a phase at nominal power and a preparatory phase which makes it possible for nominal power to be attained after the discharging time, the problem reduces to one of minimizing the duration of the second phase. When the allowable values of the power and concentration of ^{135}Xe nuclei are limited from above, a reactor operating cycle satisfying the indicated criterion is guaranteed by a three-stage sequence of change in power during the preparatory phase: $U(t) = 0$, $U(t) = var$, and $U(t) = U_{nom}$.

The general character of the optimal operating regime and the quantitative characteristics of its individual phases and stages are considered by examining the example of a one-group zero-dimensional model of a water-moderated–water-cooled (VVÉR) power reactor.

Calculations are made for a number of 24-h cyclic regimes, differing as to the extent and duration of the fuel discharging. Relations are obtained for the operating times at nominal power as a function of the operative reactivity margin and minimum reactivity values are determined, in which case the regime need not be optimized since cyclicity is ensured by operation at nominal power in the interval $T - \tau$ and by direct discharging in the time τ. The length of reactor operation at variable power $U(t) = var$ is also calculated as a function of the operative reactivity margin and the reactivity values for which a preparatory phase in this stage ceases to be necessary are calculated.

The method developed and the results calculated can be used to optimize cyclic regimes of reactor operation with partial rechargings of fuel at the end of the run. For reactors with continuous fuel recharging and a constant reactivity margin, in addition to optimizing the cyclic regime with a known reactivity margin, the method makes it possible to calculate the minimum reactivity margin for a 24-h cyclic regime for an atomic power plant in an energy system with an acceptable length of the phase of preparation for a decrease in power.

*L. S. Pontryagin, The Mathematical Theory of Optimal Processes [in Russian], Fizmatgiz, Moscow (1965).

LETTERS

SOME FEATURES OF NICKEL BLISTERING UNDER IRRADIATION WITH HELIUM IONS

V. I. Krotov and S. Ya. Lebedev

UDC 621.039.51

The process by which blisters (swellings) are formed on the surface of various metals and alloys under irradiation with helium and hydrogen ions has been studied in a considerable number of works, especially [1-5].

The present paper gives the results of studies of the surface of polycrystalline specimens of nickel after irradiation with helium ions at various temperatures. Nickel foil 0.2 mm thick was annealed at 800°C for 1 h in a vacuum of 10^{-6} mm Hg and, after electropolishing, specimens with a diameter of 3 mm were cut from the foil. The specimens were then again electropolished to reveal the grain boundaries, placed in a cassette, and irradiated in the ILU-100 accelerator with 20-keV helium ions according to the method described in [6]. The radiation temperatures was varied within the limits 400-700°C, the ion current was 40 $\mu A/cm^2$, and the total dose was $8 \cdot 10^{17}$ ions/cm^2. The irradiated specimens were studied by means of optical microscopy and interferometry.

The outer annular segment of each specimen was shaded from the ion beam by a shielding ring which made possible a direct comparison of the state of the relief and level of the irradiated and unirradiated surface. In all specimens there is a general rise in the level of the irradiated surface in comparison with the adjacent unirradiated segment; this rise depends on the radiation temperature (Fig. 1). With a rise in the radiation temperature, the height of the step gradually decreases, the uniformity of the distribution of blisters over the surface and the area they occupy decrease, and so does the mean size of the blisters. After irradiation at 700°C the blisters are practically indistinguishable under the optical microscope.

Figure 2 gives the plots of the relative area occupied by blisters, their concentration, and their mean size as a function of the temperature. At 400°C practically the entire area is covered comparatively uniformly with blisters (Fig. 3a), at 500°C there is a noticeable difference in the covering of various grains (Fig. 3b), and at 650°C the entire area of the specimen is free and only several grains have blisters (Fig. 3c). In the range 400-450°C traces of completely and partially destroyed blisters can be seen on the surface (Figs. 3a, 4a, and 4b). Thus, in addition to whole blisters in Fig. 4a we can clearly see round unshadowed contours, "bases" which had held the cupolas of the blisters. Figure 4b shows a micrograph of the same segment, taken with the

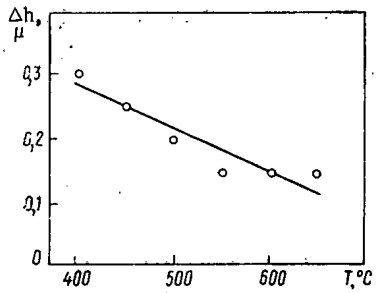

Fig. 1

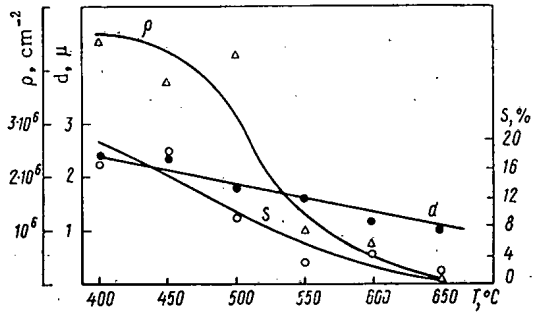

Fig. 2

Fig. 1. Rise Δh in level of irradiated part of specimen as function of radiation temperature.

Fig. 2. Δ) Concentration ρ, ●) mean size d, and O) relative area S occupied by blisters as function of temperature.

Translated from Atomnaya Énergiya, Vol. 44, No. 4, pp. 355-357, April, 1978. Original article submitted January 25, 1977; revision submitted August 22, 1977.

0038-531X/78/4404-0405$07.50

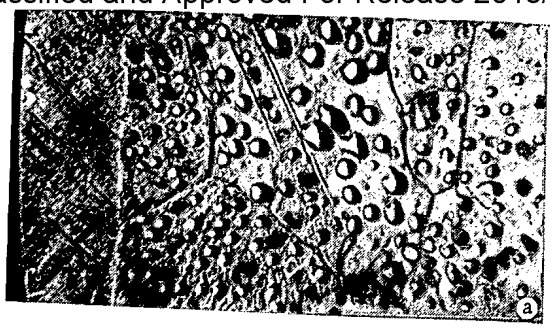

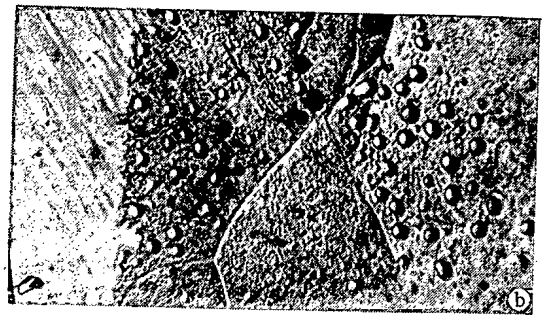

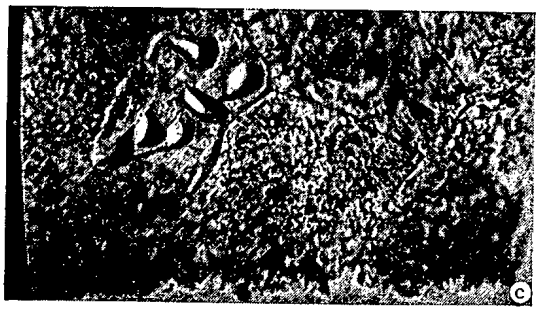

Fig. 3

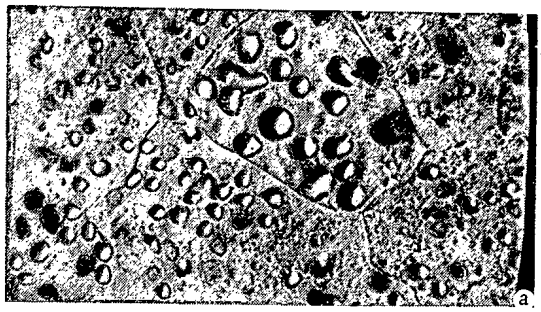

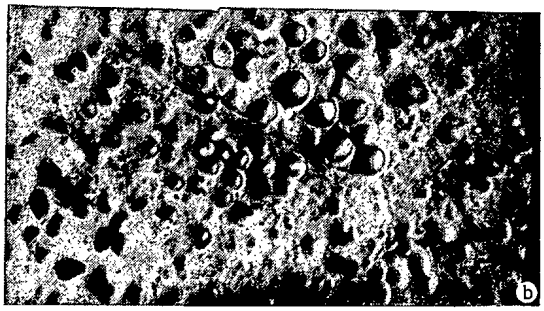

Fig. 4

Fig. 3. Photomicrographs of obliquely illuminated surfaces of nickel specimens irradiated with 20-keV helium ions with a dose of $8 \cdot 10^{17}$ ions/cm^2 (×1350) at: a) 400°C, b) 500°C, and c) 650°C.

Fig. 4. Photomicrographs of obliquely illuminated surfaces of nickel specimens irradiated with 20-keV helium ions at 450°C with a dose of $8 \cdot 10^{17}$ ions/cm^2 (×1350) removed at different focusing objectives: a) on sample surface; b) on cupola blisters.

objective focused on a plane somewhat above the plane of the specimen; this makes it possible to notice cupolas which are beginning to tear away. The dark elongated formations in the micrograph are such cupolas, but already turned almost vertically, which is why the "bases" from which they have partially torn away are visible in Fig. 4a.

The observed pronounced anisotropy which arises in the distribution of blisters between the surfaces of the various grains of the polycrystal with a decrease in temperature is probably related to the anisotropy of the coefficient of helium diffusion in the crystal lattice. The effect of this anisotropy does not manifest itself at low temperatures when the helium diffusion is insignificant.

Note should also be taken of the character of the destruction of the blisters. Thus, on the basis of the expressions obtained for estimating the stresses in the center and along the periphery of the blister cupolas in the process of the lifting of the cupola (proceeding from the model of an edge-clamped round plates) it was concluded [7] that at the instant the cupola begins to lift, when the deflection is smaller than the cupola wall thickness, the stress along the periphery is greater than the stress at the center of the cupola, i.e., in materials with low elastic deformation strain to failure the blister tear should occur along the contour (e.g., for niobium). If the lift of the cupola is commensurate with its thickness, then the inverse relation is observed and more convex blisters (i.e., in more plastic materials) should break at the center of the cupola (e.g., for 1Kh18N9T steel). In the case of nickel, which is a material with a quite high plasticity, judging by the con-

siderations above, one would expect the blisters to break at the cupola center, whereas in Fig. 4 it is seen that the bream occurs along the cupola periphery (as in niobium).

This disparity with calculation can be explained by the fact that the side walls of a quite high cupola will become thinner when the central part sputters more quickly since with oblique incidence the sputtering ratio is high.

It may be that the cupola contour loses strength as the result of its side walls becoming saturated with helium under oblique incidence and whereas the top of the cupola is "shot right through" by ions.

Undoubtedly there should also be a "dimensional" effect due to the fact that the cupola wall thickness is comparable to the distances of the interactions of defects and structural components of the material with the cupola surfaces. Thus, dislocations come out on the surface, phase transformations occur on the surface, etc. [8]. The strength of the material in the zone of cupola-base contact may, therefore, differ from the strength of the material of the cupola itself.

In conclusion, the authors are pleased to thank G. G. Gunin and L. A. Zhdamirov for preparing and irradiating the specimens as well as L. P. Naumov and G. P. Fokin for processing the experimental results.

LITERATURE CITED

1. S. Das and M. Kaminsky, J. Appl. Phys., 44, No. 1, 25 (1973).
2. S. Erents and G. McCracken, Rad. Effects, 18, 191 (1973).
3. S. Das and M. Kaminsky, J. Nucl. Mater., 53, 115 (1974).
4. B. A. Kalin et al., At. Energ., 39, No. 2, 126 (1975).
5. J. Roth, R. Behrish, and B. Scherzer, J. Nucl. Mater., 57, 365 (1975).
6. V. I. Krotov, S. Ya. Lebedev, and S. D. Panin, Preprint FÉI-652 (FÉI – Physics and Power Engineering Institute), Moscow (1976).
7. B. A. Kalin, D. M. Skorov, and V. T. Fedotov, in: Proceedings of the Fourth All-Union Conference "Interactions of Atomic Particles with Solids," Part I [in Russian], Kharkov. State Univ. (1976).
8. P. Hirsch et al., Electron Microscopy of Thin Crystals [Russian translation], Mir, Moscow (1968).

SPATIAL FLUCTUATIONS OF NEUTRON AND POWER DISTRIBUTION IN CRITICAL REACTOR

V. K. Goryunov

UDC 621.039.564.2

In most cases, errors in physical reactor calculations may be attributed to real or hypothetical spatial fluctuations of the macroscopic cross sections. There is a broad class of problems in which the fluctuations of the cross section may be regarded, formally at least, as a random function of the coordinate (e.g., fluctuations due to neglected variations in the fuel enrichment or temperature oscillations). The present work considers the statistical characteristics of spatial fluctuations of the neutron flux in a single-velocity diffusion model of a reactor.

Assume that in a homogeneous initially critical reactor with mass parameter $\varkappa_0^2$ there is a small variation in the physical properties of the active region (e.g., the macroscopic cross sections) according to the law $\varepsilon(\mathbf{r})$ which does not affect the diffusion coefficient. The reactor is restored to an accurately critical state by imposing some (constant over the volume) variation in the property θ, so as to satisfy the equation

$$\Delta\Phi(\mathbf{r}) + \{\varkappa_0^2 + \varepsilon(\mathbf{r}) + \theta\}\,\Phi(\mathbf{r}) = 0 \qquad (1)$$

with the boundary condition $\mathbf{n}\nabla\Phi(\mathbf{r}) + \beta\Phi(\mathbf{r}) = 0$ and the condition that the flux $\Phi(\mathbf{r})$ is not negative in a reactor of volume V.

In the approximation linear with respect to the perturbation $\varepsilon(\mathbf{r}) + \theta$ it is simple to obtain expressions for the fluctuation of the neutron flux

Translated from Atomnaya Énergiya, Vol. 44, No. 4, pp. 357-359, April, 1978. Original article submitted January 25, 1977.

0038-531X/78/4404-0407$07.50

$$\tilde{\Phi}(\mathbf{r}) \equiv \frac{\Phi(\mathbf{r}) - \Phi^{(0)}(\mathbf{r})}{\Phi^{(0)}(\mathbf{r})} = \sum_{m \neq 0} \frac{\int \Phi_m^*(\mathbf{r}')\,\varepsilon(\mathbf{r}')\,\Phi_0(\mathbf{r}')\,d\mathbf{r}'}{(\varkappa_m^2 - \varkappa_0^2)\int |\Phi_m(\mathbf{r}'')|^2\,d\mathbf{r}''} \frac{\Phi_m(\mathbf{r})}{\Phi_0(\mathbf{r})}, \tag{2}$$

and for the first correction to the eigenvalue (which, in the same approximation, is θ)

$$\theta = \frac{\int |\Phi_0(\mathbf{r})|^2\,\varepsilon(\mathbf{r})\,d\mathbf{r}}{\int |\Phi_0(\mathbf{r}')|^2\,d\mathbf{r}'}. \tag{3}$$

Here Φ_m and $\varkappa_m$ are the eigenfunctions and eigenvalues of the unperturbed problem. The subscript $m = 0$ corresponds to the eigenfunction describing the neutron distribution in a homogeneous reactor: $\Phi^{(0)}(\mathbf{r}) = a\Phi_0(\mathbf{r})$.

Consider first of all perturbations of the cross section that have the properties of white noise with zero mean: $\langle \varepsilon(\mathbf{r}) \rangle = 0$. The correlation of these perturbations may be represented by a Dirac δ function

$$K_\varepsilon(\mathbf{r}, \mathbf{r}') \equiv \langle \varepsilon^*(\mathbf{r})\,\varepsilon(\mathbf{r}') \rangle = c\delta(\mathbf{r} - \mathbf{r}'). \tag{4}$$

It follows from Eqs. (2) and (3) that in a linear approximation $\langle \tilde{\Phi}(\mathbf{r}) \rangle = \langle \theta \rangle = 0$. It may be shown that the mean over the realizations of the second correction to the eigenvalue is always negative. This was discussed in detail in [1] for a Markov form of correlation of the perturbations: $K_\varepsilon(\mathbf{r}, \mathbf{r}') = \sigma_\varepsilon^2 \exp(-\alpha |\mathbf{r} - \mathbf{r}'|)$.

Taking into account Eqs. (2) and (4) the self-correlation function (SCF) of the relative fluctuations of the neutron flux $\langle \tilde{\Phi}^*(\mathbf{r}_1)\tilde{\Phi}(\mathbf{r}_2) \rangle$ is

$$K_\Phi(\mathbf{r}_1, \mathbf{r}_2) = \sum_{m,\, n \neq 0} \frac{c\int \Phi_m(\mathbf{r})\,\Phi_n^*(\mathbf{r})\,|\Phi_0(\mathbf{r})|^2\,d\mathbf{r}}{(\varkappa_m^2 - \varkappa_0^2)(\varkappa_n^2 - \varkappa_0^2)} \times$$
$$\times \frac{1}{\int\int |\Phi_m(\mathbf{r}')|^2\,|\Phi_n(\mathbf{r}'')|^2\,d\mathbf{r}'\,d\mathbf{r}''} \frac{\Phi_m^*(\mathbf{r}_1)\,\Phi_n(\mathbf{r}_2)}{\Phi_0(\mathbf{r}_1)\,\Phi_0(\mathbf{r}_2)}. \tag{5}$$

The relative fluctuations of the power distribution $\tilde{N}(\mathbf{r})$, considered in the same single-velocity diffusional model of the reactor, are due to variation both of the neutron flux and of the fission cross section.

Accordingly, the SCF of the power distribution is represented as the sum of the SCF of the neutron flux, the SCF of the cross-sectional perturbations, and an interference term taking into account the correlation of the fluctuations in the flux and the cross section. In fact, taking the same approximation for $\tilde{N}(\mathbf{r})$ as in Eq. (2), the SCF of the power distribution – $\langle \tilde{N}^*(\mathbf{r}_1)\tilde{N}(\mathbf{r}_2) \rangle$ – is obtained in the form

$$K_N(\mathbf{r}_1, \mathbf{r}_2) = K_\Phi(\mathbf{r}_1, \mathbf{r}_2) + \xi^2 K_\varepsilon(\mathbf{r}_1, \mathbf{r}_2) +$$
$$+ \xi c \sum_{m \neq 0} \frac{\Phi_m^*(\mathbf{r}_1)\,\Phi_m(\mathbf{r}_2)}{(\varkappa_m^2 - \varkappa_0^2)\int |\Phi_m(\mathbf{r})|^2\,d\mathbf{r}} \left\{ \frac{\Phi_0(\mathbf{r}_1)}{\Phi_0(\mathbf{r}_2)} + \frac{\Phi_0(\mathbf{r}_2)}{\Phi_0(\mathbf{r}_1)} \right\}, \tag{6}$$

where ξ is the conversion factor from the perturbation of $\varkappa^2$ to the perturbation in the fission cross section (in relative units). For example, $\varkappa_0^2 = \{(\nu - 1)\Sigma_f - \Sigma_c\} D^{-1}$ and Σ_f is varied, $\xi = D\{(\nu - 1)\Sigma_f\}^{-1}$.

Consider the neutron-flux fluctuations over the thickness of an infinite critical plate without a reflector. Substituting the eigenfunctions of the one-dimensional problem into Eq. (5) and integrating gives

$$K_\Phi\left(\frac{H}{\pi}x_1, \frac{H}{\pi}x_2\right) = \frac{cH^3}{\pi^4} \sum_{m=2}^{\infty} \left\{ \frac{\sin mx_1 \sin mx_2}{(m^2-1)^2 \sin x_1 \sin x_2} - \right.$$
$$\left. - \frac{\sin mx_1 \sin (m+2)x_2 + \sin mx_2 \sin (m+2)x_1}{2(m^2-1)[(m+2)^2-1]\sin x_1 \sin x_2} \right\}. \tag{7}$$

Here H is the plate thickness (the correction to the extrapolated limit is neglected); and the coordinate origin is at one boundary of the reactor.

Even the approximation for K_Φ taking into account the first term of the sum in Eq. (7) [$K_\Phi(x, x+\tau) \approx (4/9)(cH^3/\pi^4)\cos(\pi x/H)\cos\pi(x+\tau)/H$] reveals the inhomogeneous behavior of the neutron-flux fluctuations: the dispersion $K_\Phi(x, x)$ has a maximum close to the reactor boundary.

In practice the SCF of the neutron or power distribution is often used to investigate the characteristics of the fluctuations over the height of a reactor as above, and very frequently to investigate the fluctuations in the plan of a cylindrical reactor. The SCF of the neutron-flux fluctuations in the plan of a "bare" cylindrical reactor over the radius of infinite length R may be obtained from Eq. (5) in the form

$$K_\Phi(Rr_1, Rr_2) \approx \frac{c\pi\mu_0^1 R^2}{2\sqrt{2\pi\rho}} \sum_{m=-\infty}^{\infty} \sum_{\lambda=1+\delta_{m0}}^{\infty} \frac{\mu_m^\lambda J_m(\mu_m^\lambda r_1)\,J_m(\mu_m^\lambda r_2)\cos_m\varphi}{(\mu_m^{(\lambda)2} - \mu_0^{(1)2})\,J_0(\mu_0^1 r_1)\,J_0(\mu_0^1 r_2)}, \tag{8}$$

where $J_m(r)$ is a Bessel function of the first kind; μ_m^{λ} is the λ-th nonnegative root of the equation $J_m(r)=0$; $\delta_{mm'}$ is a Kronecker delta; $\rho \approx 1.2$. Since the value of the sum in Eq. (8) is mainly determined by the terms with $m=\pm 1$ and $\lambda=1$, the fluctuations are of the same kind as in the one-dimensional problem, i.e., the dispersion is a maximum close to the reactor boundary.

If the reactor has a reflector, the distribution of the relative fluctuations of the neutron flux will change. It is found that the maximum of the relative fluctuations close to the reactor boundary remains when a reflector is introduced. For example, for the same plate surrounded by an ideal reflector Eq. (5) gives

$$K_{\Phi}(x_1, x_2)=2\frac{cH^3}{\pi^4}\sum_{m=1}^{\infty}\frac{\cos m\frac{\pi}{H}x_1\cos m\frac{\pi}{H}x_2}{m^4}\approx 2\frac{cH^3}{\pi^4}\cos\frac{\pi}{H}x_1\cos\frac{\pi}{H}x_2. \tag{9}$$

Thus, the approximation for Eq. (9) differs from the corresponding approximation for Eq. (7) only by a constant factor.

It is of great convenience for the purposes of mathematical computation to represent the correlation of the perturbations as a δ function. However, many real perturbations of the cross section, for example, those associated with spatial fluctuations of the temperature, are often otherwise correlated. Consider the effects of perturbations of the cross section if K_{ε} is of the form

$$K_{\varepsilon}(r_1, r_2)=\sigma_{\varepsilon}^2\exp(-\alpha|r_1-r_2|), \tag{10}$$

where α is the inverse correlation length; $\sigma_{\varepsilon}^2=\langle\varepsilon^*(r)\varepsilon(r)\rangle$.

The expression for the neutron-flux dispersion over the thickness of a reactor without a reflector is derived by a method different from that for Eq. (5). The random function $\varepsilon(x)$ is approximated by a Stieltjes integral [2] with infinite limits

$$\varepsilon(x)=\int_{-\infty}^{\infty}\exp(i\omega x)\,d\Psi(\omega). \tag{11}$$

The differential $d\Psi(\omega)$ satisfies the relations $\langle d\Psi(\omega)\rangle=0$; $\langle d\Psi^*(\omega)\,d\Psi(\omega_1)\rangle=S_{\varepsilon}(\omega)\,\delta(\omega-\omega_1)\,d\omega\,d\omega_1$, where $S_{\varepsilon}(\omega)=(\sigma_{\varepsilon}^2/\pi)\alpha/(\omega^2+\alpha^2)$ is the spectral density of perturbations with the correlation function in Eq. (10). Substituting Eq. (11) into Eq. (2) and integrating with respect to x' and x'' gives

$$\tilde{\Phi}(x)=\frac{4H^2}{\sin\frac{\pi}{H}x}\sum_{m=2}^{\infty}\frac{m\sin\frac{m\pi}{H}x}{m^2-1}\int_{-\infty}^{\infty}\frac{d\Psi\left(\frac{\Omega}{H}\right)\Omega\{1+\exp(i\Omega+m\pi)\}}{i[\Omega^2-(m+1)^2\pi^2][\Omega^2-(m-1)^2\pi^2]}. \tag{12}$$

As $\alpha\to\infty$, provided that $\lim_{\alpha\to\infty}\sigma_{\varepsilon}^2/\alpha=c/2$, the dispersion obtained from Eq. (12) by forming the average $\langle\tilde{\Phi}^*(x)\tilde{\Phi}(x)\rangle$ transforms asymptotically to Eq. (7) for the δ-correlated perturbations of the cross section at $x_1=x_2=x$. Therefore for large α (more precisely $\alpha H/\pi$), $c=2\sigma_{\varepsilon}^2/\alpha$. Increase in αH leads to decrease in scale of the fluctuations; for example, it follows from Eq. (7) that

$$\langle\tilde{\Phi}^*(x)\,\tilde{\Phi}(x)\rangle\approx\frac{4}{9}\left[\frac{\sigma_{\varepsilon}}{\varkappa_0^2}\right]^2\frac{\cos^2\frac{\pi}{H}x}{\alpha H}. \tag{13}$$

For a two-dimensional problem, equating Eqs. (4) and (10) leads to the result that $c=2\pi\sigma_{\varepsilon}^2/\alpha^2$ for large αR.

In conclusion, the main results of the work are as follows.

1) In the framework of the single-velocity diffusion model of a reactor, expressions have been obtained in general form for the spatial SCF of relative fluctuations of the neutron and power distributions in the case of δ-type correlation of the perturbations of the macroscopic cross sections. The SCF of the neutron flux for reactors with reflectors of different quality is given in analytic form for the one- and two-dimensional formulations most frequently required in practice.

2) It is shown that, regardless of the active-region geometry, reactors without a reflector and those with an ideal reflector ($n\Delta\Phi=0$ at the boundary) are characterized by an increase in fluctuations toward the reactor boundary, with a homogeneous and isotropic distribution of the cross-section perturbations inside the active region.

3) The change in the neutron-flux SCF is considered, in particular, in the limit as the correlation of the perturbations changes from Markov form to δ-type correlation (white noise). It is shown that increase in correlation of the perturbation leads to decrease in the fluctuations of the flux.

The conclusions obtained from the above model are found to contradict the usual assumption that the fluctuations of the neutron and power distribution are homogeneous. On the one hand, this may be a result of the inaccuracy of the single-velocity diffusion approximation; on the other, it may be because the experiments and calculations have been analyzed on the a priori assumption that the secondary fluctuations are homogeneous. Hence, the possibility of replacing averaging over realizations by averaging over the reactor plan requires special proof.

Note finally that, although the analysis has been performed for an initially homogeneous reactor, there is no particular difficulty in transferring the results to other reactors if the relative fluctuations are considered in a linear approximation.

It remains to thank P. N. Svirkunov for numerous useful discussions of the results.

LITERATURE CITED

1. M. Williams, Atomkernenergie, 22, No. 4, 248 (1973).
2. A. A. Sveshnikov, Applied Methods of the Theory of Random Functions [in Russian], Nauka, Moscow (1968), p. 85.

IMPROVING THE CHARACTERISTICS OF LIQUID-METAL FAST BREEDERS USING A MAGNETIC FIELD

A. N. Shmelev, V. G. Ilyunin, and V. M. Murogov

UDC 621.039.5

As is known, magnetic fields are used for various purposes in nuclear reactors, e.g., in electromagnetic pumps [1]. A magnetic field may influence neutron diffusion and hence also the reactivity of the reactor [2].

The known theoretical and experimental investigations of turbulent flow in tubes in a longitudinal magnetic field indicate that the drag coefficient may be reduced by a factor of 5-10 in comparison with turbulent flow in the absence of a magnetic field [3, 4]. Therefore, suppose that a reactor body is surrounded by a solenoid generating a magnetic field, the lines of force of which are parallel to the coolant flow in the active region (Fig. 1). Investigations of the flow around a cylinder and a sphere in the presence of a transverse magnetic field indicate that the hydraulic-drag coefficient may be significantly increased [3]. If, on the basis of these results, it is assumed that applying a longitudinal magnetic field leads to increase in the hydraulic-drag coefficient across the element and decrease in that along the element, then it is possible to replace the walls of the fuel elements in the active region and the blanket by, e.g., a rigid frame. Results of calculations using the ROKBAR optimization complex [5] showed that this leads to increase in the multiplication factor and the energy yield of the fuel while the doubling time may be reduced by 20-25%. Since buckling of the fuel-element casing necessitates an increase in the gaps between them and leads to additional blurring of the neutron spectrum, replacing the casing by a rigid frame would allow these losses to be reduced.

The results of calculations indicate that increase in fast-breeder power is possible mainly by increase in radius of the active region. Increase in height of the active region is limited both by the mechanical stress in the walls of the fuel-element casing and by the accompanying heating of the coolant, which reaches 180-250°C [5, 6]. The heating may be reduced, e.g., by increasing the rate of coolant flow. However, the maximum rate is limited by a number of factors: the erosional effects of the coolant on the fuel-element casing and other structural components; increase in the injection power, which depends on the hydraulic drag; vibrations of the fuel assemblies in the coolant flow. Applying a longitudinal magnetic field may diminish these limiting factors and hence allow the rate of the coolant flow to be increased. The increase in the erosional effects of the coolant with increase in its flow rate is associated with the accompanying reduction in thickness of the laminar boundary layer at the immersed surfaces [7, 8]. Applying a longitudinal magnetic field leads to increase in thickness of the laminar layer [8]. Rise in injection power with increase in the coolant flow rate is impossible on those sections of the fuel assembly where the field is parallel to the coolant flow. This

Translated from Atomnaya Énergiya, Vol. 44, No. 4, pp. 359-360, April, 1978. Original article submitted February 21, 1977; revision submitted October 10, 1977.

 0038-531X/78/4404-0410$07.50

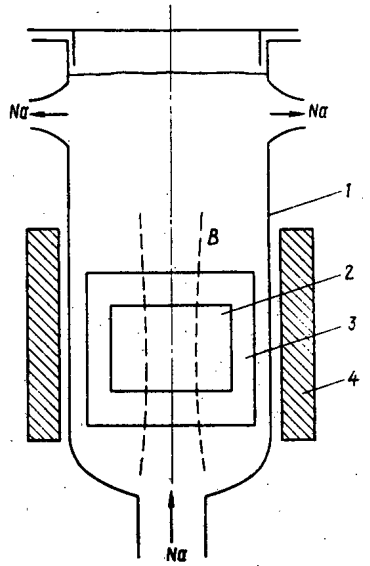

Fig. 1. Nuclear reactor: 1) reactor body; 2) active region; 3) blanket; 4) solenoid generating magnetic field with induction B.

TABLE 1. Reduction in Drag Coefficient and Induction of Magnetic Field

Parameter	v, m/sec					
	10		20		30	
d_{hydr}, mm	2,5	5	2,5	5	2,5	5
$\max_B \frac{\xi\mid_B}{\xi\mid_{B=0}}$	0,14	0,09	0,09	0,05	0,07	0,04
$B_{req}\left(\frac{\xi\mid_B}{\xi\mid_{B=0}}=0,5\right)$	3,6	2,7	5,4	4,3	7,1	5,7

is because applying a longitudinal magnetic field reduces the drag coefficient. On the basis of experimental results for the hydraulic-drag coefficient in turbulent flow along a stainless-steel tube in a longitudinal magnetic field [4] it is possible to estimate the maximum reduction in the drag coefficient $\xi\mid_B$ in the presence of a field in comparison with the drag coefficient $\xi\mid_{B=0}$ in the absence of a field (Table 1) for different sodium flow rates v and tubes of differing hydraulic diameter d_{hydr}.

It follows from Table 1 that applying a longitudinal magnetic field may reduce the drag coefficient by approximately an order of magnitude. It is also found that the required value of the induction is comparable with the induction of the magnetic field considered in programs for the development of tokamak-type thermonuclear reactors [9]. Since the longitudinal magnetic field tends to suppress the transverse turbulent pulsations, it may be expected that applying such a field reduces the vibrations in the fuel-element casing. Increasing the coolant flow rate by a factor of 2-3 allows the power removed from an active region of given diameter to be increased, without significant change in size of the reactor body. Decrease in the heating of the coolant may lead to a reduction in temperature in the fuel elements by 30-50°C or to an increase in the exit temperature. The possibility of increasing the energy yield of nuclear fuel is very important for fast breeders and in the development of high-flux research reactors. Estimates show that the energy consumption of the magnetic system may be compensated by the various effects indicated. However, the implementation of the proposals outlined requires the solution of a number of technical problems.

LITERATURE CITED

1. Yu. E. Bagdasarov et al., Technical Problems of Fast Reactors [in Russian], Atomizdat, Moscow (1969).
2. V. V. Orlov and Yu. N. Kazachenkov, At. Energ., 33, No. 2, 710 (1972).

3. G. G. Branover and A. B. Tsinober, Magnetic Hydrodynamics of Incompressible Media [in Russian], Nauka, Moscow (1970).
4. V. B. Levin and A. I. Chinenkov, Magn. Gidrodin., No. 3, 145 (1970).
5. V. G. Ilyunin et al., Kernenergie, No. 12, 367 (1975).
6. V. V. Orlov et al., State and Prospects of Development Work on APS with Fast Reactors. Paper at a Symposium of COMECON Member Countries [in Russian], Obninsk (1973).
7. B. V. Petunin, Thermoenergetics of Nuclear Reactors [in Russian], Atomizdat, Moscow (1960).
8. I. I. Novikov, Applied Magnetic Hydrodynamics [in Russian], Atomizdat, Moscow (1960).
9. D. Steiner, Proc. IAEA, 63, No. 11, 1568 (1975).

SURFACE BARRIER DETECTOR BASED ON EPITAXIAL GALLIUM ARSENIDE

V. M. Zaletin, I. I. Protasov,
S. P. Golenetskii, and A. S. Mal'kovskii

UDC 535.243

Semiconductor detectors of ionizing radiation based on epitaxial gallium arsenide, operating at normal temperature, hold out promise for use in basic and applied research and are the subject of comprehensive studies at present [1, 2].

The first data on the use of monocrystalline gallium arsenide layers to make spectrometric detectors for x rays and low-energy γ rays were reported in [3]. The present paper gives the results of subsequent investigations.

The low resolution and high noise level in the first such detector based on gallium arsenide [4, 5] were due to the imperfection of the structure and the contamination of the bulk crystals used. This limitation was in great measure eliminated by the application of epitaxial technology. With epitaxy (gaseous or fluid) growth of single crystals occurs at a temperature below the melting point of the given compound: this reduces the diffusion of electrically active impurities in the crystal and considerably simplifies the problem of the container material [6-8].

The monocrystalline layers of gallium arsenide used to fabricate the detectors were grown in a Ga–$AsCl_3$–H_2 system containing components of high purity. The substrates used consisted of n^+-type gallium arsenide, doped with tin or tellurium to a concentration of $(2\text{-}4)\cdot10^{18}$ cm^{-3}. Layers of doped gallium arsenide from 50 to 300 μ thick were used to make the semiconductor detectors.

A detector constituted a surface-barrier diode (Fig. 1) in which the $n-n^+$ structure was produced by growing a pure epitaxial layer (n) on a highly doped substrate and the barrier, by evaporating gold onto the

TABLE 1. Initial Data and Results of Tests with Gallium Arsenide Semiconductor Detectors

Parameter	Initial data of detectors			Results of repeated tests (for 12-14 months)	
	21	31	33	31	33
Barrier area, mm^2	2	3	2		
Epitaxial layer thickness, μ	140	210	300	—	—
Carrier concn., cm^{-3}	$7\cdot10^{12}$	$1\cdot10^{14}$	$1{,}1\cdot10^{14}$	—	—
Operating voltage, V	200	60—80	250	110	250
Reverse current, A	$1{,}1\cdot10^{-8}$	$1{,}2\cdot10^{-8}$	$1{,}2\cdot10^{-9}$	$1{,}2\cdot10^{-8}$	$1{,}4\cdot10^{-9}$
Instrumental energy resolution, keV at 122-keV line	2,7	6,1	1,9	5,1	3,0
59,6	2,4	6,0	1,7	4,7	2,2
22,4	—	—	1,5	4,5	1,9
Quantum detection eff. (%) at 122-keV line	—	—	—	0,05	0,2
59,6	—	—	—	0,35	1,0
26,4	—	—	—	2,0	6,6
14,4	—	—	—	7,4	15,1
6,4	—	—	—	4,6	4,9

Translated from Atomnaya Énergiya, Vol. 44, No. 4, pp. 360-363, April, 1978. Original article submitted March 10, 1977.

 0038-531X/78/4404-0412$07.50

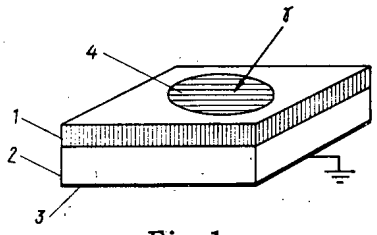

Fig. 1

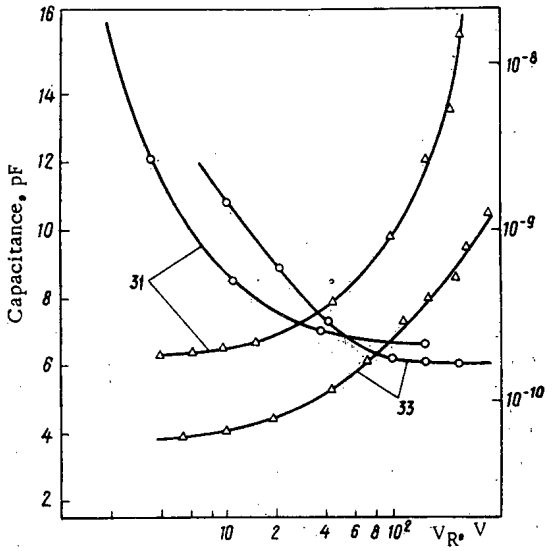

Fig. 2

Fig. 1. Structure of semiconductor detector based on epitaxial GaAs: 1) epitaxial film of GaAs; 2) n^+-type GaAs(Sn); 3) ohmic contact (Ni); 4) sensing area of detector (Au 20 nm).

Fig. 2. Volt–ampere (Δ) and volt–capacitance (○) characteristics of GaAs semiconductor detectors (air, 300°K).

epitaxial surface. The thickness of the gold film was 20 (±3) nm and the sensing area of the detector was 2-3 mm^2. The electrical contact to the n^+-type substrate was made by electrolytic deposition of nickel.

The crystal of the detector was placed in the case of a low-power transistor and was fastened with conductive adhesive to a holder on the case. The signal was taken from the sensing area through a thin copper wire, one end of which was soldered to the gold spot and the other to an insulated output. The detector case was closed with a cover containing a beryllium window (beryllium thickness 200 μ) and was hermetically sealed by cold welding.

The spectrometric properties of the detector were studied with the aid of standard equipment: a PU-2-B charge-sensitive preamplifier, usually employed with a germanium–lithium semiconductor detector; the SÉS2-02 ("Langur") main spectrometric channel; and LP-4840 and NTA-512 B multichannel pulse-height analyzers. For detectors with a leakage current of more than $1 \cdot 10^{-8}$ A the feedback resistance (Rf) in the preamplifier was reduced from 15 to 2 GΩ. The mean energy of the formation of a pair of carriers in GaAs is 4.27 eV as compared to 2.98 eV for Ge [1]. The input noise parameters of the preamplifiers for gallium arsenide detectors, therefore, were somewhat poorer: 1.0 keV + 0.050 and 1.75 keV + 0.055°C keV/pF for Rf equal to 15 and 2 GΩ, respectively.

The photoelectric efficiency of the detectors was determined with standard ^{57}Co and ^{241}Am sources from the OSGI set with long exposures. The instrumental spectra were measured with ^{109}Cd (22.5 keV), ^{241}Am (24.6 and 59.5 keV), and ^{57}Co (14.4 and 122 keV) sources. The sensing area of all detectors was taken equal to 3 mm^2 in the calculations of the solid angle.

In the present study we have investigated the dependence of the reverse current and capacitance of the detector structure on the magnitude of the reverse voltage and the dependence of the photoelectric efficiency of the detector on the radiation energy, measured the energy resolution of the detectors, and established the salient features which appear in the instrumental spectra because of the small thickness of the sensing region of the detectors studied. The parameters of the epitaxial structures used and the detectors prepared from them are given in Table 1.

The operating voltage is 60-250 V, the lower threshold being determined by the minimum detector voltage which ensures charge collection at a given thickness of sensing region and the upper threshold, by the reverse current. The maximum value of the reverse current, allowing spectrometric measurements to be made, was $(3\text{-}4) \cdot 10^{-8}$ A whereas the minimum was $1.2 \cdot 10^{-9}$ A at a voltage of 250 V. The volt–ampere and volt–capacitance characteristics of the detector, taken in air at 300°K, are given in Fig. 2 (for detectors Nos. 31 and 33).

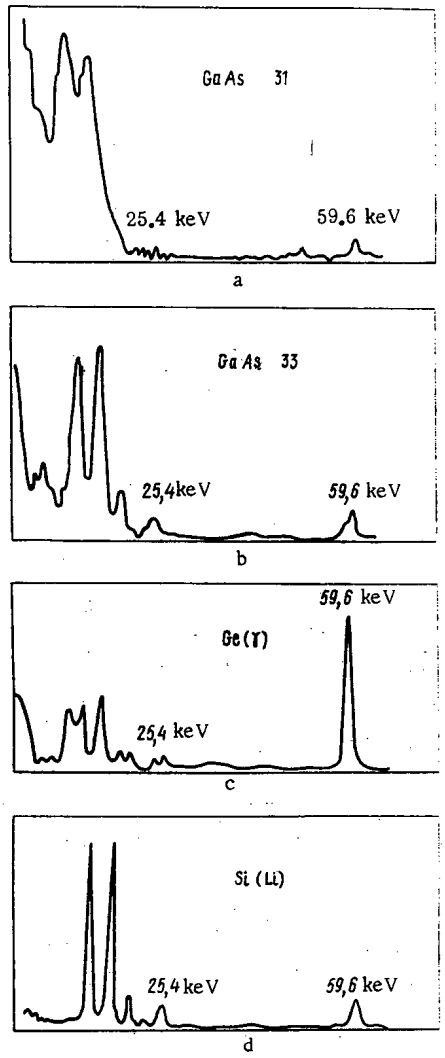

Fig. 3

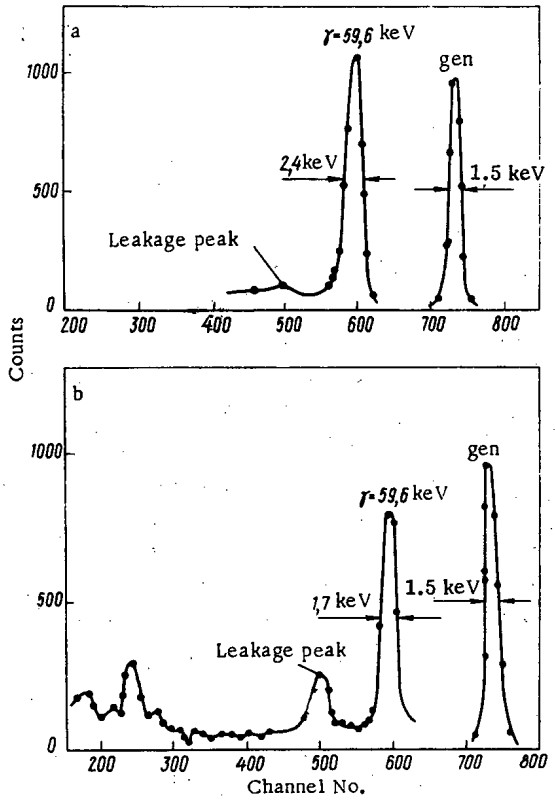

Fig. 4

Fig. 3. Instrumental spectra of characteristic and low-energy γ radiation from ^{241}Am: a, b) Ga—As semiconductor detectors Nos. 31 and 33, respectively; c, d) cooled Ge(γ) and Si(Li) detectors.

Fig. 4. Shape of instrumental spectrum from ^{241}Am source, taken with detectors with a sensing-region thickness of: a) 140 and b) 55 μ.

The growth of the leakage current with the voltage after total depletion of the layer is avalanche-like. The anomalously rapid growth of the detector current at a voltage above the optimal operating voltage is evidently explained by the properties of the epitaxial material.

A resolution of 20.2 keV was attained in the spectrometry of 5.48-MeV α-ray particles from a ^{241}Am source at 300°K. The thickness of the depleted region in all cases was greater than the range of the α particles. Figure 3 gives the instrumental spectra of γ- and x-ray radiation from ^{241}Am, taken with two gallium arsenide detectors. Similar spectra obtained with two types of commercial cooled Ge(γ) and Si(Li) detectors are also given for comparison.

The absolute efficiency of detector No. 33 reaches 15-16% at 14 keV and drops to 1% for 60 keV. At the 122-keV line it is a mere 0.2%. The photoelectric efficiency of this detector has a maximum in the region of 13-16 keV, dropping by half at energies of 7 and 30 keV. Beyond this range the photoelectric efficiency of this detector falls off sharply, by more than two orders of magnitude for 130 keV. In the case of detector No. 31, which has a thinner sensing region, the efficiency maximum is shifted somewhat towards lower energies (9-10 keV) and drops by half at energies of 6 and 21 keV.

The ^{241}Am spectrum of detector No. 21 is shown in Fig. 4a. The thickness of the sensing region in this detector was 140 μ. For comparison Fig. 4b gives the spectrum of the same source, as taken by detector

No. 33 with a sensing-region thickness of 55 μ. A leakage peak is seen in both spectra but, whereas in the case of detector No. 21 the ratio of the photopeak to the leakage peak is 9, for detector No. 33 it is only 3.

Better energy resolution was achieved with detector No. 33. The instrumental resolution at the 59.6-keV line of ^{241}Am was 1.7 keV with a generator-peak width of 1.5 keV and 1.9 keV at the 122-keV line of ^{57}Co.

The instrumental spectra of gallium arsenide detectors are characterized by distinct leakage peaks whose intensity is 15-18% of the main photopeak, practically independent of the energy to which it corresponds. The leakage peaks at 9.2-10.5 keV (the energy of the K-absorption edge of gallium and arsenic) are shifted towards the lower energies and can appreciably increase the background in x-ray radiometric analysis of elements whose characteristic radiation coincides in energy with the leakage peak from exciting radiation quanta singly scattered in the specimen.

This is a mjaor disadvantage, apparently, of all thin-film and gas-discharge detectors, especially from materials with high and intermediate atomic numbers Z. The relative contribution of the leakage peaks falls off rapidly as the sensing-region thickness ($h_{r.0}$) of the detector increases, the decrease in this contribution being from 25-30% for detector No. 31 ($h_{r.0}=45\ \mu$) to 16% for detector No. 33 ($h_{r.0}=55\ \mu$) and 1.1% for detector No. 21 ($h_{r.0}=140\ \mu$).

The energy resolution attained for gallium arsenide detectors in the range of low-energy x-ray and γ radiation is at the level of the resolution of spectrometric proportional counters with an absolute photoelectric efficiency of 5-15%. While they are inferior to semiconductor detectors based on elemental semiconductors (Ge and Si), gallium arsenide detectors do have a great advantage over them as well, viz., a capability for operating at normal temperature.

The sensitivity of spectrometric semiconductors based on epitaxial gallium arsenide in the detection of x-ray and low-energy γ radiation in the range 5-100 keV can be increased by increasing the thickness of the sensing region and employing various versions of circuit layout of the detector structure, e.g., a circuit with a protective ring.

LITERATURE CITED

1. I. Eberhard, R. Ryan, and A. Tavendale, Nucl. Instrum. Methods, 94, 463 (1971).
2. T. Kobayashi et al., IEEE Trans., 3, No. 19, 324 (1972).
3. V. M. Zaletin et al., At. Energ., 39, No. 1, 68 (1975).
4. T. Kabayashi and S. Takayanagi, Nucl. Instrum. Methods, 44, 145 (1965).
5. W. Akutagawa, K. Zanio, and J. Mayer, Nucl. Instrum. Methods, 55, 383 (1967).
6. J. Dilorenzo, J. Crystl. Growth, 17, 189 (1972).
7. H. Miki and M. Otsubo, Jpn. J. Appl. Phys., 10, 509 (1971).
8. Yu. G. Sidorov, S. A. Dvoretskii, and V. M. Zaletin, Electron. Tekh., 21, No. 3, 17 (1974).

INDEPENDENT CONTROL OF NEUTRON FLUX IN EXPERIMENTAL REACTOR CHANNELS

P. T. Potapenko

UDC 621.039.55

Experiments of quite different sorts requiring various reactor powers are commonly performed in experimental channels of a single reactor. Ideally each experimental group needs its own neutron flux in its own experimental channel, varying in time according to its own individual program. It is difficult to make channels independent since the neutron fluxes in all experimental channels are determined mainly by the reactor power, and the possibilities of controlling neutron fluxes in experimental reactors by using absorbing rods are extremely limited [1]. Control of neutron fluxes by using heavy mechanical shielding gates is ineffective and has not been widely used in reactors.

Because of these difficulties it is frequently necessary to operate an experimental reactor at reduced power, which lowers the efficiency of utilization of the reactor. Several papers [2, 3] have considered the use of gaseous neutron absorbers in a reactor to control power or the neutron flux in an in-pile experimental channel. The proposed method of independent control of neutron flux in experimental channels by using a gaseous neutron absorber such as ^{3}He or boron trifluoride outside the core is considerably simpler from the technical point of view.

In an experimental channel (Fig. 1) at least one cell filled with an absorbing gas is located between the core and the target. The pressure in the cells is controlled by means of gas supply lines connected to the high- and low-pressure gas collectors through three-way valves. The required pressure difference between the collectors is maintained by a pump.

The control characteristics of a system with two cells are described by the expression

$$\Phi/\Phi_0 = \gamma = \exp(-\Sigma P_1 l_1)\exp(-\Sigma P_2 l_2) = \gamma_1(P_1)\,\gamma_2(P_2),$$

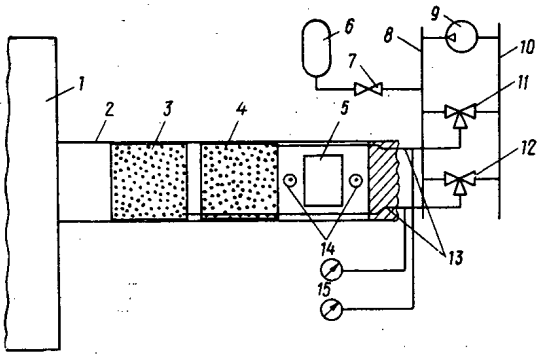

Fig. 1. Schematic diagram of facilities and instrumentation of an experimental channel: 1) reactor core; 2) experimental channel; 3, 4) hollow gas-tight plug-cells with neutron-absorbing gas; 5) irradiation container with samples and instruments; 6) tank of absorbing gas; 7) valve; 8, 10) high- and low-pressure gas collectors; 9) pump; 11, 12) three-way valves; 13) gas supply lines; 14) neutron detectors; 15) manometers.

Translated from Atomnaya Énergiya, Vol. 44, No. 4, pp. 363-364, April, 1978. Original article submitted March 28, 1977.

0038-531X/78/4404-0416$07.50

where Φ_0 and Φ are, respectively, the neutron fluxes at the experimental channel entrance and exit, γ_1 and γ_2 are the attenuations of the flux, Σ is the macroscopic neutron absorption cross section of the gas at normal conditions (e.g., $\Sigma = 0.12$ cm^{-1} for ^{3}He), P_1 and P_2 are the pressures of the absorbing gas in the cells in kgf/cm^2, and l_1 and l_2 are the lengths of the gas cells in cm.

By using two cells of absorbing gas the range and accuracy of the neutron flux control are increased. It is convenient to control the pressure in each cell from 0.1 of nominal and lower to nominal. The total range of control with such a two-decade system is from 0.01 to 1 for constant reactor power. The recommended pressures in the high- and low-pressure gas collectors are 1 and < 0.01 kgf/cm^2, respectively. Then for the cited values of γ_1 and γ_2 the lengths of the cells are $l_1 = l_2 = 23$ cm.

It is convenient to graduate the manometers for measuring the pressures in the gas cells directly in flux attenuation units.

The three-way valves can be turned so as to form an automatic control system for stabilizing the neutron flux at the experimental channel exit. The sensing elements of the system are neutron detectors located at the target. With such a system the neutron flux at the channel exit can be kept within a specified range as the reactor power varies. A computer can easily be programmed to control electrically operated valves so as to ensure automatic programmed control of the neutron flux in experimental reactor channels as the reactor power undergoes programmed variations.

Of course a gaseous absorber has practically no effect on gamma rays at the channel exit. In this sense the proposed device does not replace mechanical gates. The small amount of heat released in a gaseous absorber [1] can be transferred to structures surrounding the channel. The control device can be installed in horizontal or vertical experimental channels. The proposed control method makes it possible to increase the efficiency of utilization of experimental reactors. The method of gaseous control was tested on the IRT-2000 reactor at the Moscow Engineering Physics Institute.

LITERATURE CITED

1. A. N. Kosilov et al., At. Energ., 40, No. 5, 416 (1976).
2. G. T. Potapenko, At. Tekh. Rubezhom, No. 6, 22 (1975).
3. F. M. Arinkin et al., At. Energ., 40, No. 5, 415 (1976).

THERMOKINETICS OF HYDROGEN GENERATION FROM METAL–HYDROGEN COMPOUNDS BASED ON TRANSITION METALS OF GROUP V (V, Nb, Ta)

M. I. Eremina and E. V. Khodosov

UDC 541.44:546.88

In the operation and design of installations using hydride materials, it is important to know the manner in which hydrogen is generated at high temperatures.

The authors of [1] studied the generation of hydrogen and deuterium embedded in niobium by bombardment with H^+ and D^+ ions. This processing results in the formation of hydride and deuteride compounds of various types, which has an important effect on the process of gas generation.

In the present study we investigated the V–H, Nb–H, and Ta–H compounds obtained by the method of cathode saturation with hydrogen in an aqueous solution of fluoric and orthophosphoric acids. The compounds so obtained are hydrides or solid solutions produced by the embedding of hydrogen in the metals, for which the phase diagrams are well known [2, 3].

The experiments were carried out on foils 0.03 mm thick. The hydrogen concentration in the initial specimens was determined by the method of [4], and the phase composition of the initial specimens at room temperature was checked by x-ray structural analysis (Table 1).

Translated from Atomnaya Énergiya, Vol. 44, No. 4, pp. 365-366, April, 1978. Original article submitted April 6, 1977.

0038-531X/78/4404-0417$07.50

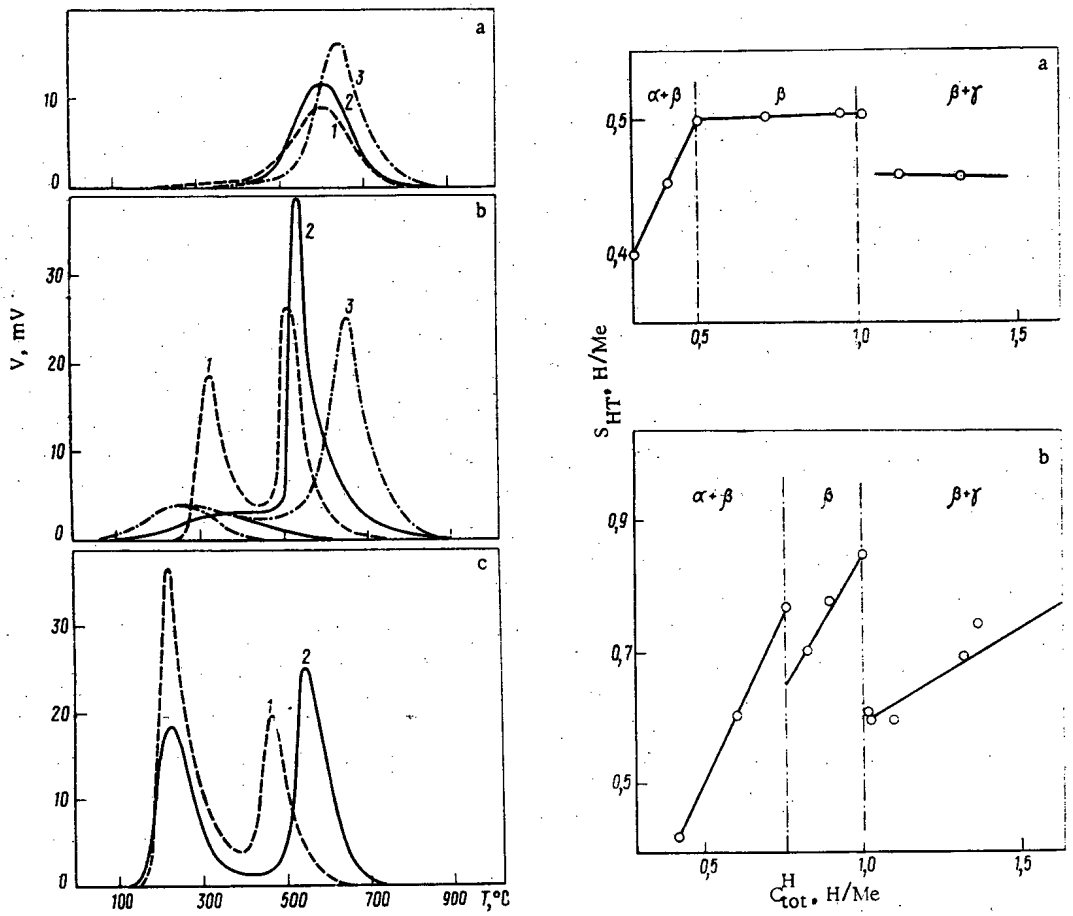

Fig. 1. Thermokinetic curves for hydrogen generation from hydrides of vanadium (1), niobium (2), and tantalum (3) at a heating rate of 20 deg/min: a) $VH_{0.37}$; $NbH_{0.42}$; $TaH_{0.54}$; b) $VH_{0.94}$; $NbH_{0.90}$; $TaH_{0.95}$; c) $VH_{1.22}$; $NbH_{1.10}$.

Fig. 2. The effect of total hydrogen content (C^H_{tot}) in vanadium (a) and niobium (b) on the integral intensity of the high-temperature maximum (S_{HT}) of the thermokinetic curve for hydrogen generation.

The information on the nature of the hydrogen generation was obtained by means of a chromatograph on the basis of the change in the thermal conductivity of the gas mixture formed when the specimens were heated from room temperature to 900°C at rates of 5, 10, and 20 deg/min in an argon stream.

Figure 1 shows the thermokinetic* curves for the generation of hydrogen at a heating rate of 20 deg/min; curves which are similar (in shape) to these were also obtained for heating rates of 5 and 10 deg/min. However, when the heating rate is reduced, we have a displacement of the gas-generation peaks toward lower temperatures. Thus, at a heating rate of 10 deg/min the maxima are displaced by 30-35°C, and at 5 deg/min they are displaced by 60-70°C from their temperature position for a heating rate of 20 deg/min.

It can be seen from Fig. 1a that when we heat specimens which at room temperature have a two-phase ($\alpha+\beta$) structure, the hydrogen generation curves have only one maximum, in the 600-700° C region. The shape of the curves remains similar approximately up to compositions of $VH_{0.5}$, $NbH_{0.7}$, and $TaH_{0.6}$.

In the hydride region we observe second maxima for the hydrogen generation (at 250-350°C) (Fig. 1b). For niobium hydrides and tantalum hydrides with a hydrogen concentration of H/Me < 1, these maxima are small. For vanadium hydrides, in this region of hydrogen concentration we observe an intense and sharply marked peak at 350°C. In niobium hydrides such a peak appears only at concentrations of H/Nb > 1 (Fig. 1c).

*The gas generation curves may be called thermokinetic in the present case, since here we have a time dependence in implicit form: the abscissa axis shows the temperature, but if we divide this by the constant rate of heating, we can obtain the variation as a function of time.

TABLE 1. Experimental Data on the Hydrogen Content and Phase Composition of the Investigated Specimens of Vanadium, Niobium and Tantalum

Metal	Hydrogen content, H/Me	Phase comp.	Type of lattice
V	0,37 0,40 0,45 0,49	$\alpha+\beta$	α solid solution of hydrogen in vanadium, bcc
	0,71 0,94 1,01	β	β hydride of the VH type, bet; γ hydride of the VH_2 type, fcc
	1,22 1,33	$\beta+\gamma$	
Nb	0,42 0,61 0,75	$\alpha+\beta$	α solid solution of hydrogen in niobium, bcc
	0,83 0,90 1,01	β	β hydride of the NbH type, orthorhombic lattice
	1,02 1,03 1,1 1,33 1,36	$\beta+\gamma$	γ hydride of the NbH_2 type, fcc
Ta	0,54	$\alpha+\beta$	α solid solution of hydrogen in tantalum, bcc
	0,95	β	β hydride of the TaH type, orthorhombic structure

Thus, a characteristic feature of the generation of hydrogen from hydrides of Group V metals is the existence of two gas-generation maxima, one at low and one at high temperature, and the intensity of the low-temperature maximum increases with increasing concentration of hydrogen in the hydrides.

An increase in the hydrogen concentration also causes a change in the intensity of the high-temperature peak.* The existence of two gas-generation peaks may presumably be related to the phase composition of the specimens. Thus, the high-temperature gas generation observed (see Fig. 1a) for α solid solutions of hydrogen and two-phase ($\alpha+\beta$) specimens undergoing a transition to a single-phase (α) state above 200°C can be explained by the loss of hydrogen by the α phase. The low-temperature gas generation appears with the transition to the pure hydride β and $\beta+\gamma$ regions and is apparently due to the loss of hydrogen by the β and γ hydrides.

Consequently, the entire process of gas generation takes place in two stages: the first is the decomposition of the hydrogen-enriched hydride phases until the α phase is formed; the second is the loss of hydrogen by the α phase.

In connection with this, it is interesting to note the break-points of the curves in Fig. 2 situated near the tentatively designated boundaries of the phase diagram. It is not impossible that their appearance is due to phase transitions arising when hydrogen is lost by the compounds under investigation.

LITERATURE CITED

1. A. A. Pisarev and V. G. Tel'kovskii, At. Energ., 39, No. 3, 195 (1975).
2. V. I. Mikheeva, Hydrides of Transition Metals [in Russian], Atomizdat, Moscow (1960).
3. R. A. Andrievskii (editor), Metal Hydrides [in Russian], Atomizdat, Moscow (1973).
4. M. I. Eremina, I. A. Novokhatskii, and G. T. Moroz, in: Methods for Determining Gases in Metals [in Russian], Izd. Mosk. Doma Nauchno-Tekhn. Propagandy, Moscow (1971).

*Since the amount of hydrogen is calculated from the area under the gas-generation curve, we can use the expression "integral intensity of the peak."

OPTIMIZATION OF ^{238}Pu PRODUCTION FROM ^{237}Np

A. I. Volovik

UDC 621.039.516.22

A great many studies have been devoted to calculations of the process of obtaining ^{238}Pu from ^{237}Np. In particular, this process was calculated for the purely thermal neutron spectrum in [1], the effect of resonance neutrons was taken into account in [2], the variation of the calculation results with inaccuracies in the initial physical constants was analyzed in [3], the role of the time profiling of the neutron flux was determined in [4], and the effect of enrichment of the initial nuclear fuel was taken into account in [5].

In the present paper we consider the problem of optimizing this process. A target made of ^{237}Np can be placed at various points of a nuclear reactor. These points differ both in their value of thermal-neutron flux density and in the energy spectrum of the neutrons. For a given irradiation time we must find a time regime for moving the target inside the volume of the reactor in such a way as to obtain the maximum total yield of the isotopes ^{238}Np and ^{238}Pu.

If U(t) and $\omega(t)$ are the fluxes of thermal and resonance neutrons, respectively, and $x^{(1)}(t)$, $x^{(2)}(t)$, $x^{(3)}(t)$ are the amounts of the isotopes ^{237}Np, ^{238}Np, and ^{238}Pu, then the burnup equations have the form:

$$\left.\begin{aligned} dx^{(1)}/dt &= f^{(1)} = -(U\sigma_1+\omega I_1)\,x^{(1)};\\ dx^{(2)}/dt &= f^{(2)} = (U\sigma_1+\omega I_1)\,x^{(1)} - \\ &\qquad -[\lambda+(U\sigma_2+\omega I_2)]\,x^{(2)};\\ dx^{(3)}/dt &= f^{(3)} = \lambda x^{(2)} - (U\sigma_3+\omega I_3)\,x^{(3)}. \end{aligned}\right\} \tag{1}$$

Here σ_i are the corresponding thermal cross sections; I_i are the resonance integrals; λ is the decay constant of ^{238}Np. For the sake of simplicity, we assume that the I_i are independent of the $x^{(i)}$. The irradiation time T is given. The following restrictions are imposed on the control functions U(t) and $\omega(t)$:

$$0 \leqslant U(t) \leqslant U_{\max};\quad 0 \leqslant \omega(t) \leqslant \omega_{\max}. \tag{2}$$

The minimized functional is

$$F(U,\ \omega) = -[x^{(2)}(T)+x^{(3)}(T)] = \int_0^T [-U(\sigma_1 x^{(1)} - \sigma_2 x^{(2)} - \sigma_3 x^{(3)}) -$$

$$-\omega(I_1 x^{(1)} - I_2 x^{(2)} - I_3 x^{(3)})]\,dt = \int_0^T f^{(0)}\,dt. \tag{3}$$

In accordance with the maximum principle [6], we construct equations conjugate to those of (1):

$$\left.\begin{aligned} &\psi_0 = -1;\\ &d\psi_1/dt = (U\sigma_1+\omega I_1)(\psi_0+\psi_1-\psi_2);\\ &d\psi_2/dt = (U\sigma_2+\omega I_2)(-\psi_0+\psi_2)+\lambda(\psi_2-\psi_3);\\ &d\psi_3/dt = (U\sigma_3+\omega I_3)(-\psi_0+\psi_3). \end{aligned}\right\} \tag{4}$$

At the start of the irradiation, when t = 0, we assume that we have pure ^{237}Np, i.e., $x^{(1)}(0)=1$, $x^{(2)}(0)=0$, $x^{(3)}(0)=0$. At the end of the irradiation, when t = T, we find from the transversality conditions that $\psi_1(t)=\psi_2(t)=\psi_3(t)=0$. The Hamiltonian

$$\mathcal{H}^0 = \sum_{i=0}^{3} f^{(i)}\psi_i = \varphi^0 U + \chi^0\omega - \lambda(\psi_2-\psi_3) \tag{5}$$

is linear with respect to the control functions, since the switching functions

$$\begin{aligned} \varphi^0 &= -\sigma_1(\psi_0+\psi_1-\psi_2)\,x^{(1)} + \sigma_2(\psi_0-\psi_2)\,x^{(2)} + \sigma_3(\psi_0-\psi_3)\,x^{(3)};\\ \chi^{(0)} &= -I_1(\psi_0+\psi_1-\psi_2)\,x^{(1)} + I_2(\psi_0-\psi_2)\,x^{(2)} + I_3(\psi_0-\psi_3)\,x^{(3)} \end{aligned} \tag{6}$$

do not depend explicitly on U and ω. The integral fluxes are given. This means that in addition to (2), the control functions are subject to the isoperimetric restrictions

Translated from Atomnaya Énergiya, Vol. 44, No. 4, pp. 367-369, April, 1978. Original article submitted April 6, 1977.

0038-531X/78/4404-0420$07.50

$$\int_0^T U(t)\,dt = C_1; \quad \int_0^T \omega(t)\,dt = C_2, \tag{7}$$

where C_1, $C_2 > 0$ are given constants. The increase in the dimension of the phase vector by the introduction of additional variables $x^{(4)}$, $x^{(5)}$ satisfying the equations

$$dx^{(4)}/dt = f^{(4)} = U; \quad dx^{(5)}/dt = f^{(5)} = \omega \tag{8}$$

with the end conditions $x^{(4)}(0) = x^{(5)}(0) = 0$, $x^{(4)}(T) = C_1$, $x^{(5)}(T) = C_2$, makes it possible, as has been shown in [7], to remove the restrictions (7). The system conjugate to the system obtained by adjoining the equations (8) to (1) differs from (4) by the adjoining of the equations

$$d\psi_4/dt = 0; \quad d\psi_5/dt = 0, \tag{9}$$

and hence $\psi_4 = \text{const} = \nu_1$; $\psi_5 = \text{const} = \nu_2$. In this isoperimetric problem the Hamiltonian

$$\mathcal{H} = \sum_{i=0}^{5} f^{(i)}\psi_i = \mathcal{H}^0 + U\nu_1 + \omega\nu_2 = (\varphi^0 + \nu_1)\,U + (\chi^0 + \nu_2)\,\omega - \lambda(\psi_2 - \psi_3) = \varphi U + \chi\omega - \lambda(\psi_2 - \psi_3) \tag{10}$$

has the same form as (5), and the switching functions $\varphi = \varphi^0 + \nu_1$ and $\chi = \chi^0 + \nu_2$ differ from (6) by constant terms. The transversality conditions on the right end for the system (2), (9) are satisfied for $\psi_1(T) = \psi_2(t) = \psi_3(T) = 0$; $\psi_4(t) = \nu_1$; $\psi_5(T) = \nu_2$ with arbitrary ν_1, ν_2.

The numerical solution of the problem is based on the method of successive approximations [8], making direct use of the maximum principle. At the k-th step the control functions $U_{k+1}(t)$, $\omega_{k+1}(t)$ are chosen from the condition

$$\mathcal{H}(x_k, \psi^k, U_{k+1}, \omega_{k+1}) = \max_{U, \omega} H(x_k, \psi^k, U, \omega). \tag{11}$$

TABLE 1. Values of Thermal Cross Sections and Resonance Integrals

i	Radionuclide	σ_t, b	I_t, b
1	^{237}Np	170	946
2	^{238}Np	2070	880
3	^{238}Pu	500	150

TABLE 2. Positions of Special Zones and Effect of Optimization

U_{max}	ω_{max}	$U(t)$		$\omega(t)$		Effect of optimization
10^{14} neutrons/cm^2·sec^{-1}		t_1, yr	t_2, yr	t_1, yr	t_2, yr	
2,00	0,20	0,22	0,29	—	—	9,60
2,00	0,40	0,21	0,27	0,25	0,25	22,90
2,00	0,60	0,02	0,34	0,25	0,43	24,38
2,00	0,80	0,01	0,38	0,25	0,50	25,61
2,00	1,00	0,01	0,41	0,28	0,50	23,41
4,00	0,20	0,08	0,19	—	—	13,10
4,00	0,40	0,00	0,27	0,13	0,39	22,88
4,00	0,60	0,00	0,33	0,15	0,50	24,37
4,00	0,80	0,00	0,35	0,19	0,50	25,62
4,00	1,00	0,00	0,34	0,22	0,50	23,47
6,00	0,20	0,02	0,15	—	—	13,94
6,00	0,40	0,00	0,26	0,09	0,47	22,38
6,00	0,60	0,00	0,28	0,13	0,50	23,70
6,00	0,80	0,00	0,32	0,16	0,50	25,00
6,00	1,00	0,00	0,34	0,16	0,50	22,95
8,00	0,20	0,01	0,15	—	—	13,95
8,00	0,40	0,00	0,25	0,07	0,49	22,28
8,00	0,60	0,00	0,28	0,12	0,50	23,77
8,00	0,80	0,00	0,31	0,14	0,50	25,03
8,00	1,00	0,00	0,34	0,14	0,50	22,88
10,00	0,20	0,00	0,15	—	—	13,82
10,00	0,40	0,00	0,24	0,06	0,49	22,12
10,00	0,60	0,00	0,28	0,11	0,50	23,94
10,00	0,80	0,00	0,31	0,13	0,50	25,03
10,00	1,00	0,00	0,34	0,14	0,50	23,04

Remark. For $\omega_{max} = 0.20$ the admissible control function is unique.

TABLE 3. Optimal Control Functions in the Special Zones for $U_{max} = 6.0$, $\omega_{max} = 0.6$

t, yr	U_{opt}	ω_{opt}	t, yr	U_{opt}	ω_{opt}
0,00	2,874	0	0,26	1,452	0,016
0,02	2,094	0	0,28	0,910	0,222
0,04	1,776	0	0,30	0	0,454
0,06	1,938	0	0,32	0	0,438
0,08	1,701	0	0,34	0	0,448
0,10	1,794	0	0,36	0	0,463
0,12	1,617	0,002	0,38	0	0,465
0,14	1,539	0,008	0,40	0	0,476
0,16	1,647	0,008	0,42	0	0,462
0,18	1,521	0,008	0,44	0	0,465
0,20	1,410	0,008	0,46	0	0,484
0,22	1,389	0,008	0,48	0	0,553
0,24	1,335	0,008	—	0	

The maximum (11), since the Hamiltonian (10) is linear, will be attained for maximum values of the control functions if the corresponding switching functions are positive, and for zero control functions if these functions are negative. On the segments where $\varphi(t)$ or $\chi(t)$ is equal to zero, the corresponding control function is considered to be constant and such that (7) is satisfied. At each step we make a search for ν_1 and ν_2 as the zeros of the functions $R_1(\nu) = \int_0^T U(t)\,dt - C_1$; $R_2(\nu) = \int_0^T \omega(t)\,dt - C_2$. The calculation process ends when the functional (3) and both control functions are stabilized with a specified accuracy. An optimization program in FORTRAN has been prepared for the solution of the problem (at Dubna).

In the calculations we used the following physical values: $\lambda = 169.1\ yr^{-1}$; $T = 0.5$ yr; $C_1 = 0.5 \cdot 3.1556926 \cdot 10^{-3}$ neutrons $\cdot b^{-1}$; $C_2 = 0.1 \cdot 3.1556926 \cdot 10^{-3}$ neutrons $\cdot b^{-1}$. The values of the thermal cross sections and resonance integrals are given in Table 1.

For optimal control the segment [0, T] is divided into three zones by means of the points t_1 and t_2: $0 \le t_1 \le t_2 \le T$. The positions and magnitudes of these zones are shown in Table 2.

In the initial zone the optimal $U = U_{opt}(t)$ is equal to U_{max}, and in the final zone $U_{opt}(t) = 0$. The optimal $\omega = \omega_{opt}(t)$, on the other hand, is equal to zero in the initial zone and ω_{max} in the final zone. The middle segments (t_1, t_2) are zones of special control both for U and for ω. The switching functions vanish in these zones, to within the accuracy of the calculations. As the maximum values of the control functions increase, the middle zone expands, mainly at the expense of the zone in which the control function is the maximum, until the latter is completely absorbed. The variation of the optimal control functions in their special zones is almost monotonic near the zero values of the control functions, after which, following a rapid drop, it takes on a jump character.

The averaging of pairwise adjacent intervals of time reveals a tendency to decrease from the highest values for $U_{opt}(t)$ and to increase to the highest value for $\omega_{opt}(t)$ (in the three-zone arrangement the highest values of the optimal control functions coincide with U_{max} or ω_{max}). The times at which the indicated drops take place for $U_{opt}(t)$ and $\omega_{opt}(t)$ coincide to within one time step Δt. In the right-hand column of Table 2 we show the effect obtained from the optimization, equal to $(F_{av} - F_{opt})/|F_{av}|$ %, where F_{opt} is the value of the functional equation (3) for optimal control functions and F_{av} is the value for constant admissible control functions, i.e., for uniform irradiation of the target by thermal and resonance neutrons. The distribution of the (pairwise averaged) values of the optimal control functions in the special zones for a typical case is shown in Table 3, where the value of t corresponds to the beginning of the intervals in which the control functions are constant.

The author wishes to express his deep gratitude to A. P. Rudik for his formulation of the problem and his guidance.

LITERATURE CITED

1. M. A. Bak et al., At. Energ., 23, No. 6, 561 (1967).
2. A. D. Galanin et al., At. Energ., 31, No. 3, 277 (1971).
3. S. A. Nemirovskaya and A. P. Rudik, At. Energ., 37, No. 5, 428 (1974).
4. A. P. Rudik, Preprint ITÉF-65, Moscow (1975).

5. T. S. Zapritskaya, A. K. Kruglov, and A. P. Rudik, At. Energ., 41, No. 5, 321 (1976).
6. L. S. Pontryagin et al., Mathematical Theory of Optimal Processes [in Russian], Nauka, Moscow (1961).
7. N. N. Moiseev, Elements of the Theory of Optimal Systems [in Russian], Nauka, Moscow (1975).
8. I. A. Krylov and F. L. Chernous'ko, Zh. Vychisl. Mat. Mat. Fiz., 12, No. 1, 14 (1972).

APPARATUS FOR REMOTE RADIATION MONITORING OF PROCESSES OF EXTRACTIVE SEPARATION OF TRANSURANIUM ELEMENTS

V. V. Pevtsov, V. I. Shipilov,
V. G. Korotkov and A. N. Filippov

UDC 621.039.59:66.012

The multichannel measuring apparatus described is used with immersible semiconductor detectors in the realm of remote radiation monitoring of processes of extractive separation of transuranium elements. Diagrams are given for continuous monitoring of the process of separation of plutonium from transplutonium elements.

Radiometric methods employing immersible semiconductors are used for continuous technological monitoring of processes of extractive separation of transuranium elements [1-3]. To obtain the fullest possible

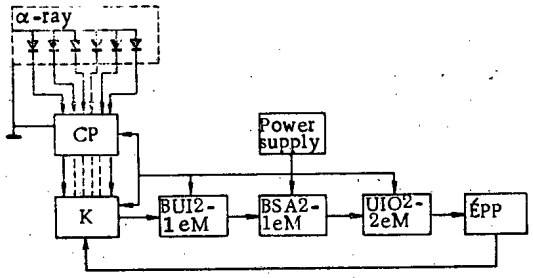

Fig. 1. Functional block diagram of six-channel measuring system.

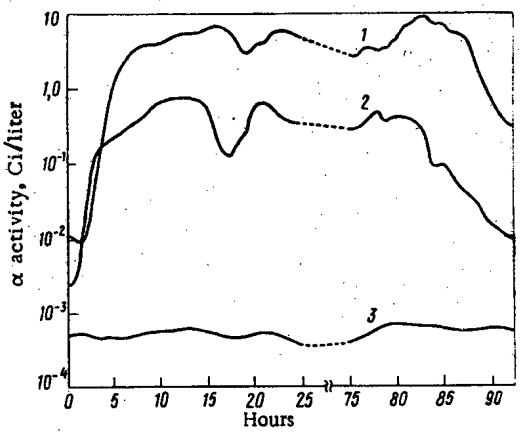

Fig. 2. Diagram of continuous remote monitoring of α activity of solutions in process of extractive separation of plutonium and transplutonium elements: 1) reextract of transplutonium elements; 2) Pu reextract; 3) effluent.

Translated from Atomnaya Énergiya, Vol. 44, No. 4, p. 369, April, 1978. Original article submitted April 12, 1977.

0038-531X/78/4404-0423$07.50

information about the operation of the extraction apparatus, radiation monitoring of solutions is usually carried out at several points of the technological line. This necessitates the construction of simple, reliable multichannel measuring apparatus. Figure 1 gives one variant of the design of a six-channel measuring system based on the functional blocks of the Shchegol-1 system.

A six-channel measuring system of this type is now in use for radiation monitoring of the extraction processes in the separation of transuranium elements under the conditions of "hot" radiochemical chambers. As an example, Fig. 2 gives diagrams for monitoring of the process of extractive separation of plutonium from transplutonium elements. The monitoring is carried out by continuous measurement of the specified α activities of solutions with immersible detectors placed in flow-type vessels of the technological lines of the respective fractions.

Continuous year-long operation with units of flow-type semiconductor detectors showed that in respect of such parameters as reliability, stability, and measuring accuracy, the measuring system considerably surpasses similar systems with separate detection channels. In combination with a standard channel for α-spectrometric measurements, it permits remote multipoint radiation monitoring of processes of separation of transuranium elements by an extraction technology.

LITERATURE CITED

1. A. I. Bychenkov, M. P. Malafeev, and A. N. Sirotinin, Prib. Tekh. Eksp., 4, 39 (1975).
2. V. V. Pevtsov, Prib. Tekh. Eksp., 4, 78 (1976).
3. V. V. Pevtsov and V. V. Krayukhina, Prib. Tekh. Eksp., 4, 80 (1976).

FLUE GAS SCRUBBING IN WIRE CLOTH FILTER IN COMBUSTION OF SOLID WASTE

N. S. Lokotanov and O. A. Nosyrev

UDC 621.928.9+621.039.75:628.4

The paper gives the results of trials with a wire cloth filter developed for scrubbing flue gas from the combustion of solid waste from atomic power plants. The possibility of reducing the volume and mass to the maximum with safer storage of the incombustible residue has extremely attractive advantages which bring attention to combustion as a method of treating solid radioactive waste [1].

Analysis of published materials shows that the principal problem in the development of installations for combustion is that of gas scrubbing. The elevated temperature and the fact that the flue gas contains unburned products (soot, tar) and corrosive and radioactive substances make the conventional means of purification inapplicable. The main reason for this is the presence of radioactive substances in the gas and, therefore, stringent requirements on the design of the scrubbing equipment as to reliability, maintenance and repair [2].

From an analysis of the practices of design and operation of installations for the combustion of radioactive waste, one can conclude that it is preferable to use cartridge filters with elements made of a heat-proof material as the main scrubbing apparatus. Such filters ensure a high degree of purification and can be relatively easily adapted to remote-controlled maintenance and regeneration [3-5].

Trials were carried out on an experimental installation (throughput 15 kg/h) with the combustion of a mixture of paper, rubber, wiping waste, absorption filters, wood, etc. imitating real waste.

The filter constituted a rectangular-shaped apparatus with a filtration area of 3.5 m^2; the lower part of the filter had a hopper with quick-detachable container for collecting and removing the trapped ash (Fig. 1). The filtering elements consist of a cylindrical shell with an SD-120 metal screen (GOST 3187-65) mounted in it. The upper part of each element ends with a diffuser for the outflow of scrubbed gas and for reverse blowing. All the elements are connected in three sections. Above each of them is a conical chamber with nozzle for feeding compressed air during regeneration of the filtering surface.

Translated from Atomnaya Énergiya, Vol. 44, No. 4, pp. 370-371, April, 1978. Original article submitted May 18, 1977.

 0038-531X/78/4404-0424$07.50

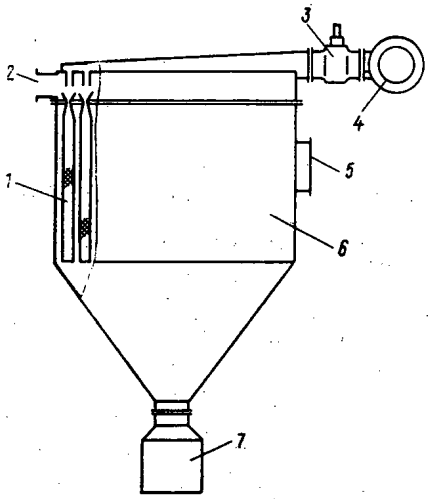

Fig. 1

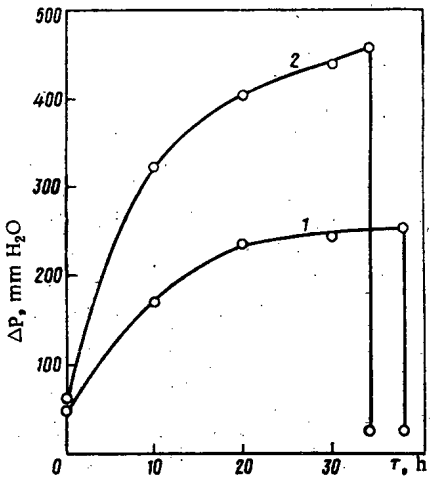

Fig. 2

Fig. 1. Wire cloth filter: 1) filtering element; 2) gas outlet; 3) electromagnetic valve; 4) receiver; 5) gas inlet; 6) housing; 7) container.

Fig. 2. Variation of resistance of filter coated with a) asbestos and b) ash, during tests.

To reduce the number of solid particles skipping through in the initial period of operation an auxiliary material was pre-deposited on the screen, the material used being finely milled asbestos or ash. The filtering elements were coated with a special arrangement (a type of "fluidized bed" apparatus) connected in place of the detachable container.

Periodically, as the deposit accumulated on the surface of the filtering elements, section by section the apparatus was blown through with bursts of compressed air.

The air was fed into the filter through an electrically operated valve from the receiver (pressure 4 kgf/cm^2).

The waste was burned with the furnace charged with portions of 2-3 kg, the average throughput being 15 kg/h. Depending on the composition of the waste burned, the weight and frequency of the individual charges, the mean mass concentration of solid particles in the flue gas after combustion varied over wide limits: from 10-15 to 100-130 mg/nm^3. For example, when wiping waste and wood was burned the concentration of solid particles in the flue gas was 10-35 mg/nm^3, and when the waste was burned with rubber, plastic, or absorption filters, the concentration was 90-140 mg/nm^3. The diameter of the particles carried from the furnace with the flue gas did not exceed 5 μ, and judging by the mass 70-80% of them had a diameter < 2 μ.

The process of the waste combustion is unsteady, this being especially pronounced with periodic charging of the furnace: partially incomplete burning is observed in the initial period of waste combustion which is characterized by the intensive emission of volatile products from the pyrolysis of the waste. As a result, the flue gas contains incompletely burned particles of soot, drops of tar, etc., in addition to ash solids.

In the experiments the flow of flue gas through the filter was 90-120 m^3 (NTP)/h at a gas temperature of 500-600°C at the inlet.

The accumulation of solid particles on the surface of the filtering elements results in the gradual growth of the aerodynamic resistance of the filter. At the same time, the efficiency of the collection of the solid phase from the flue gas increases. In the initial period of the filter operation (after the precoating) the efficiency with which the solid phase was collected from the flue gas was 80-85% for the asbestos-coated filter and 90-95% for the ash-coated filter. After 10-15 h of operation the filtration efficiency rises to 99-99.5% and the concentration of the solid phase in the scrubbed gas drops to 1.0-1.5 mg/m^3 (NTP).

Figure 2 illustrates two complete cycles (precoating–filtration–regeneration) of the change in the aerodynamic resistance of the filter during the process of flue-gas scrubbing. The process of filtration as well as combustion was carried out periodically in the form of trials lasting 5-6 h. The curves characterize the operation of filters coated with asbestos and with ash (see Fig. 2). It is seen that when the filtering elements are coated with asbestos the aerodynamic resistance increases more slowly than when they are coated with ash,

this being due to the structure of the deposited coating. The asbestos-coated filter was used without regeneration for 38 h, during which time the aerodynamic resistance rose from 50 to 250 mm H_2O. In the case of ash-coated elements the filter resistance rose from 60 to 400 mm H_2O in the course of filtration.

With regeneration about 80% of the deposit from the filtering elements was dumped into the hopper and the aerodynamic resistance was reduced to a value close to the resistance of the clean filter for the given gas flow rate. Partial cracking of the layer filtered out was observed and this facilitated regeneration.

The trials showed that a wire cloth filter with a precoating of finely milled asbestos or ash ensures effective scrubbing of flue gas from the combustion of solid waste. The deposition of an auxiliary layer makes it possible to filter aerosols containing tarry products from the pyrolysis of waste. Regeneration of the filtering surface with compressed air ensured quite long service by the filter.

LITERATURE CITED

1. M. Rodier, Nucl. Energy, 7, No. 1, 25 (1965).
2. Y. Sutra-Fourcade, B. Cair, and F. Gallisian, in: Proceedings of the Symposium "Treatment of Airborne Radioactive Wastes," New York, August (1967), p. 607.
3. Calen Bodo, U. S. Patent No. 3854902, class 55-96 (BO1d 46/30).
4. F. Billard, Nucl. Sci. Abstr., 23, No. 15 (1969).
5. F. Billard et al., Ochr. Powietrza, 5, No. 2, 10 (1971).

OBITUARY

IN MEMORIAM OF ARTEM ISAAKOVICH ALIKHAN'YAN

Artem Isaakovich Alikhan'yan, an eminent Soviet scientist in the domain of physics of the atomic nucleus, cosmic rays, and elementary particles, Corresponding Member of the Academy of Sciences of the USSR and Academician of the Academy of Sciences of the Armenian SSR, died on Feb. 25, 1978. A. I. Alikhan'yan was born on June 24, 1908, in Tbilisi in the family of a railroad worker. Upon graduation from Leningrad University in 1931, he began to work in the Leningrad Physicotechnical Institute. His first papers dealt with the physics of crystals and x rays. A. I. Alikhan'yan was one of the fathers of experimental nuclear physics in the Soviet Union. In 1942, together with A. I. Alikhanov he organized the Agarats High-Mountain Scientific Station in Armenia where the composition and spectra of cosmic rays were studied.

From 1943 to the end of his life, A. I. Alikhan'yan headed the Laboratory of the Physics Institute of the Academy of Sciences of the USSR and for 30 years he headed the Erevan Physics Institute. The largest electron accelerator (6 GeV) in the Soviet Union was built on the basis of this institute. Under the leadership of A. I. Alikhan'yan important and interesting work was done on elementary-particle physics on the accelerators of Dubna, Erevan, and Serpukhov and on the creation of new methods of particle detection.

Artem Isaakovich devoted much energy to the training of young scientists. He was the founder of the department of the atomic nucleus at Erevan University and from 1946 to 1960 he headed the department of experimental physics of the Moscow Engineering Physics Institute.

The scientific services of A. I. Alikhan'yan were appraised highly: he was awarded two Orders of the Red Banner of Labor and the Order of the Badge of Honor and was laureate of the Lenin and State Prizes.

Translated from Atomnaya Énergiya, Vol. 44, No. 4, insert between pp. 372 and 373, April, 1978.

0038-531X/78/4404-0427$07.50

The bright memory of Artem Issakovich Alikhan'yan, a restless, searching scientist, a brilliant science organizer, and a life-loving and good person, will remain in the hearts of his comrades and collaborators who worked with him and knew him well.

THIRTY-THIRD MEETING OF THE COMECON STANDING COMMITTEE ON THE PEACEFUL USES OF ATOMIC ENERGY

Yu. I. Chikul

The 33rd meeting of the COMECON Standing Committee on the Peaceful Uses of Atomic Energy was held in Moscow in Dec. 1977. It was attended by delegations of Bulgaria, Cuba, Czechoslovakia, the German Democratic Republic, Hungary, Poland, Rumania, and the Soviet Union. Representatives of the international economic associations Interatominstrument and Interatoménergo, the Joint Institute for Nuclear Research (JINR), and the UN Information Center in Moscow were also present.

The Committee heard a report by the Committee Chairman, A. M. Petros'yants, Chairman of the USSR State Committee for Atomic Energy: "Sixty Years of the Great October Socialist Revolution and the Fraternal Cooperation of the COMECON Member-Countries." He pointed out the worldwide historical importance of the Great October Revolution, the main event of the 20th century, and dwelt on the achievements of the Soviet Union in the peaceful applications of atomic energy and emphasized the importance of the cooperation of the COMECON member-countries in this area.

The delegation heads congratulated the delegation of the USSR and, through them, the entire Soviet nation on the 60th anniversary of the October Revolution, noted the international importance of the Great October Socialist Revolution, its influence on the development of the world system of socialism and the formation of a new type of economic relations between countries, based on the principles of Marxist–Leninist theory and socialist internationalism.

The meeting considered the tasks of the Standing Committee which follow from the resolutions of the 31st Session of COMECON and planned measures for further cooperation in scientific research and experimental and design work on the basis of agreements on problems agreed by the Committee for inclusion into the long-term program of cooperation on satisfying the economically justified needs of the COMECON member-countries for the main forms of energy, fuel, and raw materials up to 1990. The meeting also considered the course of work on topics from the agreed plan of multilateral integrated measures for 1976-1980 and on topics incorporated into the program of scientific and technical cooperation on the solution of fuel and energy problems over the same period and over the longer run, cooperation which is being organized by the Committee.

The Standing Committee considered topics pertaining to the elaboration of proposals on cooperation to render assistance to the Republic of Cuba in the accelerated development of science and technology in the realm of the peaceful applications of atomic energy; it discussed a report on the work and proposals for further activities of the provisional international scientfic-research group for reactor physics research on a critical assembly of the VVÉR (water-moderated–water-cooled reactor) type. The Committee discussed a report on the results of the Fourth Symposium "Research on Processing of Irradiated Fuel" and designated the main direction of scientific and technical cooperation in 1978-1980 in this field. The meeting discussed the preparations for execution of a joint expedition in 1978 to study the radioactivity of the Danube River; it approved "Technical conditions for the safe transportation of spent nuclear fuel from atomic power plants of COMECON member-countries"; and it discussed ways of increasing the efficiency of operations by Interatominstrument.

The meeting approved the 1978-1979 plan of work for the Standing Committee and the 1978 plan of work on standardization as well as the structure, contents, and order of preparation of annual Standing Committee reports on work done and on future work. Appropriate recommendations and resolutions were adopted on all topics discussed.

Translated from Atomnaya Énergiya, Vol. 44, No. 4, p. 373, April, 1978.

0038-531X/78/4404-0429$07.50

SEMINAR ON THE DEVELOPMENT OF REACTOR INSTALLATIONS FOR ATOMIC BOILER HOUSES

S. A. Skvortsov

The Seminar, which was held in Moscow in Nov. 1977, considered the overall position in relation to the application of atomic central heating plants in the COMECON member-countries, discussed the first designs of nuclear thermal electric power plants and atomic boiler houses as well as some experimental work, data from which are necessary for the construction of atomic central heating stations.

It was pointed out during the discussion that atomic sources of heat have some advantages over sources based on organic fuel, especially from the point of view of economics. Atomic boiler houses, which are less economical than nuclear thermal electric plants, at the same time have a number of other advantages: they do not require special-purpose plants to fabricate the equipment, they can be designed to operate with lower parameters, they do not have a large consumption of technical water, and they occupy a small area. The relative characteristics of atomic heat sources improve with the power of the facility. Atomic sources have ecological as well as economic advantages. Different approaches to the choice of form of heat supply (nuclear thermal electric plant or boiler house) were revealed at the seminar. Representatives of Czechoslovakia, for example, pointed out that under conditions in which electricity as well as heat was in short supply it was desirable to concentrate on the construction of nuclear thermal electric plants. The delegations from Bulgaria (a country with a warm climate) and from the German Democratic Republic (with a large number of small consumers) felt it most promising to employ boiler houses. It was, therefore, advisable to construct atomic boiler houses in addition to developing nuclear thermal electric plants.

The economic studies in COMECON member-countries are directed at determining the demand for heat over the next few decades, the choice of a rational power and optimization of the operating parameters of the central heat supply stations, and at the elucidation of the potentialities of the application of already designed reactors, especially VVÉR-440, for central heat supply purposes.

The safety studies concern the elaboration of the requirements as well as the measures for ensuring radiation safety of central heat supply stations, consideration of possible emergency situations, and provisions to prevent the spread of activity.

The design work consists in the development of reactors of various powers (100-500 MW and higher) for central heat supply stations, the choice of the principal parameters of the reactor coolant, determination of the most expeditious peak of the reactor facility, and choice of the thermal system.

Each country will determine its participation in the development of atomic stations for central heat supply.

Translated from Atomnaya Énergiya, Vol. 44, No. 4, pp. 373-374, April, 1978.

0038-531X/78/4404-0430$07.50

MEETING OF SPECIALISTS ON FORECASTING

Yu. I. Koryakin

The second meeting, which met in Moscow in Dec. 1977, was devoted to a discussion of some new tasks, goals, and needs in the establishment and coordination of methodological assumptions concerning the preparation of a joint engineering and economic report as well as a joint COMECON forecast for the development of the nuclear power industry. These tasks include the study of the economic effectiveness and scale of application of nuclear reactors in the near future for centralized heat supplies for industrial and municipal and household purposes, the interaction of the nuclear power industry with the environment, and new aspects of mathematical modeling as an instrument of optimization of the strategy for the development of nuclear power during forecasting.

The meeting heard and discussed reports and communications by Soviet specialists on the principal methodological assumptions on the determination of the comparative economic effectiveness of the use of nuclear reactors for industrial and municipal and household heat supplies, on the ecological and economic problems of the development of nuclear power, on the application of methods of solving multiple-criteria problems in the nuclear power industry, and on the principal methodological assumptions on taking account of the factor of indeterminacy in the calculated data when making forecasts for nuclear power by mathematical modeling methods. The meeting heard a report by Czechoslovak specialists "Nuclear power and the nuclear power complex of the COMECON member-countries, a systems approach."

Joint comprehensive studies on the use of nuclear reactors for large-scale centralized heat supplies are necessary for finding the prospects for the application of atomic heat supplies in COMECON member-countries with allowance for the specifics of each country, determining the overall scale of application of nuclear reactors in the near future, and coordination of efforts on the construction and introduction of atomic heat sources into the national economics of the socialist countries. Such studies according to a coordinated program will make it possible to ascertain the economic feasibility and effect of the construction of atomic sources for central heat supplies, to determine their rational profile, to formulate the requirements on the basic and ancillary equipment as well as on the atomic sources of heat proper and also on the centralized heat supply systems as a whole, etc.

The results of such studies can be useful in the development of standardized equipment for atomic sources, for central heat supplies, thus permitting the most efficient use of the productive capacities of the power engineering industries of the COMECON member-countries and to accelerate the introduction of atomic sources of heat.

With the further expansion of the scale of nuclear power construction, ecological factors associated with the interaction of nuclear power facilities with the environment take on increasing importance. The installation of power capacity is accompanied by the estrangement of large and valuable tracts of land, the intensive use of water resources (in many cases, resources which are in short supply), and the inevitable effect of waste heat on the environment. Ensuring the necessary rates of nuclear power development in the COMECON member-countries in the long term may turn into a serious ecological and economic problem; it is the purpose of joint studies within COMECON initially to establish the dimensions of the problem, its distinctive features, and the main attendant factors.

The meeting agreed upon a list of the initial data and the principal methodological assumptions for making quantitative allowance for the factors in the interaction of nuclear power with the environment during national studies. The meeting of specialists deemed it necessary to also take account of the effect that the technology employed in the various links of the fuel cycle has on the ecology (processing of spent nuclear fuel, transportation and handling of radioactive waste).

The meeting of specialists found it advisable to switch from one-criterion optimization of the development of nuclear power in the COMECON member-countries (which was used earlier) to multiple-criterion optimization and corrections for the indeterminacy of the initial data assumed in the calculations. This will

Translated from Atomnaya Énergiya, Vol. 44, No. 4, pp. 374-375, April, 1978.

0038-531X/78/4404-0431$07.50

permit the effect of a multiplicity of various factors to be taken into account more fully and concretely in the mathematical modeling.

The meeting agreed upon organizational measures concerning the development of the methodology of mathematical modeling and preparation of the necessary materials for subsequent discussion.

On the whole, the meeting of specialists proved to be extremely fruitful and useful. It not only worked out and agreed upon the necessary methodological materials, but enriched the participating specialists with information about the systems aspects of the development of nuclear power in the COMECON member-countries.

FIFTEENTH MEETING OF THE INTERATOMINSTRUMENT COUNCIL

The meeting was held on Nov. 15-19, 1977, in Warsaw, Poland. At the meeting V. F. Krasov, a Council member and President of the Soviet Foreign Trade "Izotop" gave an address on "The 60th anniversary of the Great October Socialist Revolution and its influence on the dynamics of the development of cooperation of the socialist countries in the realm of nuclear engineering."

This address and contributions by I. Kurdhalt, Deputy General Director of the KOVO trade company (Czechoslovakia), and M. Herman, First Deputy Director of the Polon trade company (Poland), emphasized that the dynamic development of the world socialist system and the many-sided strengthening of the friendship and cooperation of the nations of the socialist countries are a direct extension of the work of the Great October Socialist Revolution. One example of successful economic cooperation in the realm of peaceful applications of atomic energy is the fact of the activities of the international commercial association "Interatominstrument," uniting 15 commercial organizations of six socialist countries.

The Council considered the state of work on the specialization and subcontracting in nuclear engineering production and approved the proposals of Interatominstrument for further specialization in 1978-1980. During the meeting Appendix No. 1 was signed to the agreement on multilateral international specialization in the production of nuclear engineering instruments and apparatus. After hearing information from the Director of Interatominstrument about the analysis of the demand and production capacities of the countries, the Council decided that the manufacture of nuclear physics apparatus should be based on economic agreements.

Taking note of the forecasts of scientific-research work and experimental design work, the Council requested the Interatominstrument members concerned to conclude economic agreements with the Association in 1977-1978 for coordination, subcontracting, or joint operations.

The Council approved the plan of work and the fiscal plan of the Association for 1978 and also approved the main indices for the plans of the Interatominstrument branches on technical service in Bulgaria, Poland, and the Soviet Union. The implementation of the previous plan of work of the Association and the Council resolutions was discussed and approval was given to the report on the activities of Interatominstrument for the period Oct. 1976 to Sept. 1977 for the COMECON Standing Committee on the Peaceful Uses of Atomic Energy.

The Council made some changes in the statute on the work of the auditing commission and added three members to the commission. The auditing commission will now consist of one member from each of six countries, and not from three countries as had been the case.

Comrade I. Koshinov, General Director of the State Commercial Organization "Élektron" (Bulgaria), was elected Council President for 1978.

Translated from Atomnaya Énergiya, Vol. 44, No. 4, p. 375, April, 1978.

0038-531X/78/4404-0432$07.50

THE BAKSAN NEUTRINO OBSERVATORY OF THE NUCLEAR RESEARCH INSTITUTE OF THE ACADEMY OF SCIENCES OF THE USSR

A. A. Pomanskii

The Baksan Neutrino Observatory is a specialized complex of installations designed for the conduct of basic research on neutrino astrophysics, cosmic-ray physics, nuclear physics, gravitation, seismology, biology, and other disciplines. The complex is situated in the approaches to Mount Elbrus, in the Kabardino-Balkar ASSR; it includes some unique multipurpose underground laboratories and also some above-ground installations which serve scientific and auxiliary purposes (Fig. 1).

The Observatory is situated at an elevation of 1700 m above sea level, in the valley of the Baksan River. The underground work is done in Mount Andyrchi, which is part of the Lateral Spur of the Main Caucasus Ridge. The site of the Observatory was chosen because of the steep slopes of Mount Andyrchi and its relatively high elevation above the base (2300 m). These favorable characteristics of the mountain make it possible to set up a deep-foundation chamber which will house radiochemical detectors of solar neutrinos and electronic detectors of neutrino bursts from stellar collapses, with a relatively short (4000 m) horizontal adit. The minimal thickness of rock above the solar-neutrino detectors (in order to suppress the background from the penetrating component of the cosmic rays) will be ≈ 2000 m of rocky soil, which amounts to about 5000 m of water equivalent.

The first line of the Observatory includes the following basic scientific installations:

an underground chamber with a volume of 15,000 m^3 housing a 3200-channel scintillation telescope, together with an adjacent laboratory room which houses the systems for recording and analyzing the information transmitted from the telescope, as well as the power sources and various technical services;

an underground low-background chamber;

an above-ground experimental room housing the "Kover" ("Carpet") scintillation unit;

a chemical building, with an installation for preparing a large amount of liquid scintillator, and a computing center.

The underground scintillation telescope (Figs. 2 and 3) is shielded from the daylight surface by a rock layer equivalent to 850 m of water (the distance from the mouth of the adit is 550 m). This shielding attenuates the cosmic-ray muon flux by more than three orders of magnitude.

The structural part of the telescope consists of a reinforced-concrete parellelepiped measuring 16 × 16 × 11 m, formed by four walls 0.8 m thick and separated vertically into four levels with slabs of the same thickness. In order to reduce the radiation background, the vault, walls, and foundation of the rock excavation are lined with specially produced concrete made of ultrabasic rocks with a low natural radioactivity (Ural dunites) and Portland cement. The background is reduced even more inside the telescope, since the concrete used for its construction used as a binding component not Portland cement but special binders whose characteristic background is considerably lower than that of Portland cement.

The telescope contains 3200 individual container-detectors filled with an organic scintillator and equipped with FÉU-49 photomultipliers. Each detector contains 150 liters of liquid scintillator with a white-spirit base. The container-detectors are hung in close-packed rows on the external surfaces of the walls and are set up on the various levels of the slabs of the structural part, forming four vertical and four horizontal recording planes.

The detectors of the telescope are connected by means of a cable network with an electronic apparatus specially developed at the Nuclear Research Institute of the Academy of Sciences of the USSR and consisting

---

Translated from Atomnaya Énergiya, Vol. 44, No. 4, pp. 376-380, April, 1978.

0038-531X/78/4404-0433$07.50

Fig. 1. Overall view of the above-ground scientific and pro-

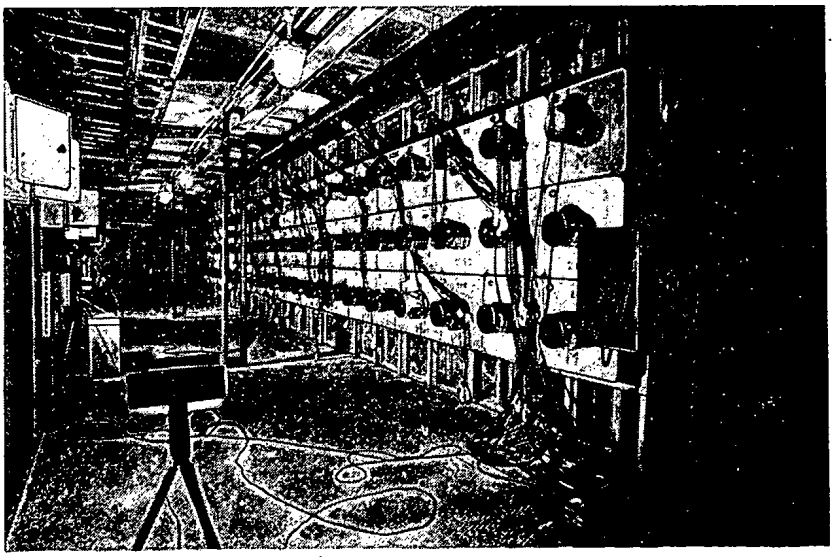

Fig. 2. One of the lateral surfaces of the underground telescope.

duction complex of the Baksan Neutrino Observatory.

Fig. 3. Top level of the underground scintillation telescope.

of two memory units of 3200 channels each and a high-speed computer for processing the information; this makes it possible to carry out exact time, amplitude, and trajectory measurements and identify the recorded particles.

The program of investigations conducted on the underground scintillation telescope includes:

recording of neutrino bursts from collapsing stellar objects;

recording of high-energy neutrinos arriving from the opposite side of the earth, as well as searches for neutrino oscillations;

investigation of the angular distribution of cosmic-ray muons;

study of the time variations of the high-energy muon flux;

investigation of groups of muons and the processes of their generation in the atmosphere;

investigation of the characteristics of muon interactions taking place in the telescope itself.

We can safely say that the parameters of the underground telescope of the Baksan Neutrino Observatory (3200 FÉUs with associated electronic equipment and 300 tons of scintillator) make it the largest nuclear-physics installation in the world.

The underground low-background chamber, lying under a layer of rock equivalent to 680 m of water (at a distance of 400 m from the mouth of the adit), is designed for testing the methods for experiments with solar neutrinos in the deep-foundation chamber of the Observatory, as well as for conducting some delicate experiments which require ultralow background. The reduction of the background in this chamber is due both to the use of low-radioactivity concrete and to the shielding of the walls, vault, and foundation of the chamber by pure dunite debris. As a result, in a space whose volume is equal to that of an ordinary room it has been possible to reduce the radiation background by a factor of 300. Inside the chamber there is some additional shielding against background γ-emitters, the basic element of which is tungsten containing a record-low amount of radioactive impurities. This has made it possible to reduce the radiation background by one more order of magnitude. Around the low-background unit (Fig. 4) there has been set up in the chamber a protective scintillation shielding (6 m^2 of methylmethacrylate plates) to suppress the cosmic-ray background.

Because of the uniquely low background of ionizing radiation in this underground laboratory, the scientists of the I. V. Kurchatov Institute of Atomic Energy were able to conduct an experiment searching for spontaneous transitions of nuclei into the superdense state and to analyze sources of the residual background of the large low-background scintillator blocks. Members of the Radium Institute have also worked here. The All-Union Institute for Scientific Research on Single Crystals is conducting work in this underground laboratory on the characteristic background of the inorganic scintillation crystals it produces and on raw material for scintillators. Scientists of the Institute of Geochemistry and Analytical Chemistry of the Academy of Sciences of the USSR are now making measurements in the low-background chamber on the radioactivity of lunar soil brought back to earth by Soviet automatic stations.

The "Kover" above-ground scintillation unit, with an area of 200 m^2, contains 400 typical detectors with a liquid scintillator which are analogous to the detectors used in the underground telescope. This unit was used for developing the methods of work used on the underground telescope (the "Kover" is identical to one of the eight planes making up the underground telescope). Today the "Kover" is being used for studying the variations in intensity of cosmic radiation and also the nuclear interactions between primary cosmic rays having superhigh energies (10^{15}-10^{16} eV) with the nuclei of atoms in air by the recording of the cores of broad atmospheric showers.

Around the above-ground experimental room, where the "Kover" unit is situated, there have been set up six outlying points, each of which includes 18 typical detectors with a liquid scintillator. They are designed for detecting broad atmospheric showers whose cores pass through the "Kover."

The scintillator production unit, situated in the chemical building, produces up to 3 tons of scintillator per day (Fig. 5). The solvent used is white spirit, the scintillating additive is PPO, and the spectrum shifter is POPOP. The technology of scintillator production and the assembly scheme for the unit were developed at the Nuclear Research Institute of the Academy of Sciences of the USSR. The unit has produced 300 tons of scintillator for the underground telescope.

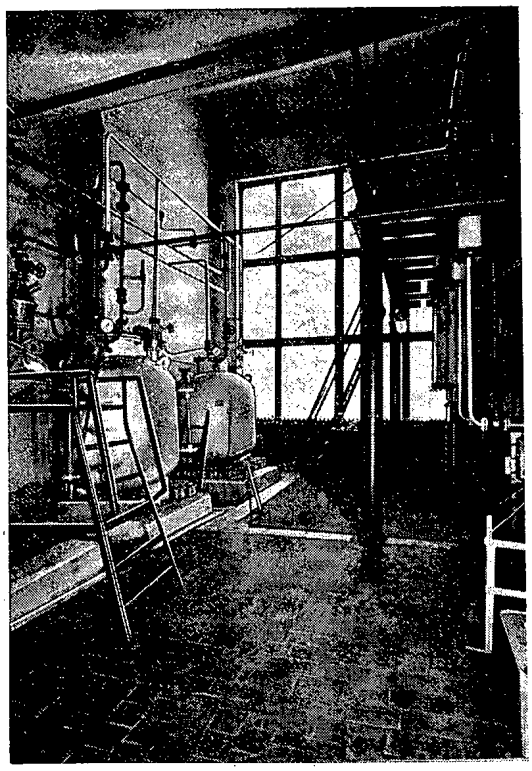

Fig. 4. Underground low-background unit.

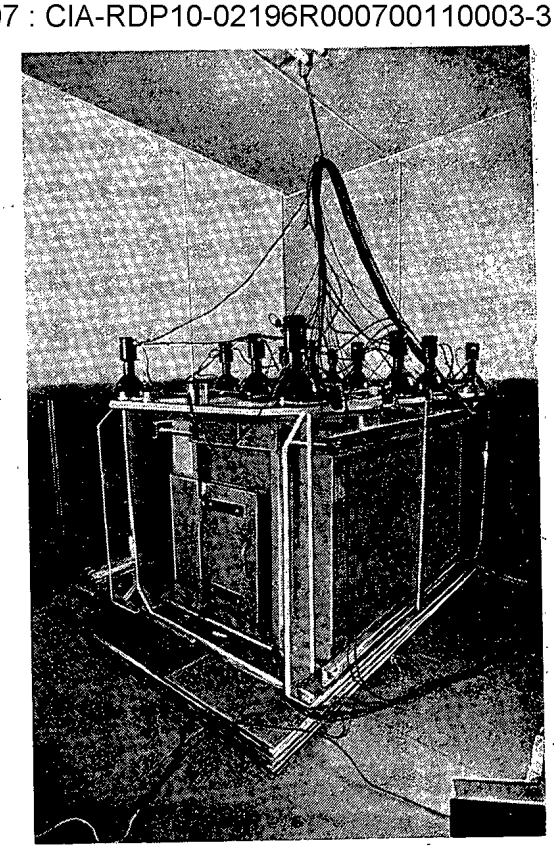

Fig. 5. Part of the liquid-scintillator production unit.

The computing center of the Observatory includes "Nairi," ES-1033, and M-222 computers and is being set up at the present time.

The construction of the deep-foundation underground laboratory – the most important part of the Observatory – is expected to be completed during the next 5 years. It will be shielded from the daylight surface by a rock layer equal to 5000 m of water equivalent. The technological schemes for the large radiochemical solar-neutrino detectors – a 3000-ton chlorine–argon and a 20-ton gallium–germanium detector – are being tested at the present time. The planned scientific program of neutrino spectroscopy of the sun is directly related to the power engineering of the future, since it will make it possible to verify our ideas about the mechanism of generation of solar energy and about the rate of the thermonuclear reactions taking place in the sun.

In the deep-foundation underground laboratory there will also be large scintillation units (1000 tons of liquid scintillator) for recording neutrino fluxes from collapsing stars and verifying the stability of baryons. Work is continuing on the search for ultralow-background materials and the development of technology for their production. This is necessary for improving the sensitivity of the radiochemical detectors and producing electronic detectors for solar neutrinos.

Various general-purpose and special-purpose low-background laboratories will be constructed on the way to the deep-foundation laboratory, along the principal adit of the Observatory.

SESSION OF SOVIET – AMERICAN COMMISSION ON COOPERATION ON POWER ENGINEERING

M. B. Agranovich

The session was held in Moscow in Dec. 1977. It was opened by the head of the Soviet delegation, P. S. Neporozhnii. In a report he acquainted the American delegation with the scientific–technical work and the development of power engineering in the USSR. The head of the U.S. delegation, J. O'Leary, spoke of the development of power engineering of his country in recent years. Then the results of cooperation in power engineering since the first session (Washington, Oct. 1974) were summed up.

The Joint Commission noted the successful implementation of programs and the desirability of extending the cooperation on the following subjects: design and operation of thermal electric power plants, including a broad exchange of experience from the use of low-grade solid fuel; the design and operation of hydroelectric plants, including construction under severe climatic conditions; the design and operation of systems for heat removal from large electric power plants and systems for protecting the atmosphere from noxious discharges from thermal electric power plants; ac and dc transmission of electrical energy at ultrahigh voltages; and the use of solar energy.

The Commission approved the state of work on the magnetohydrodynamic (MHD) conversion of energy. A significant contribution to the further growth of the program of cooperation was made by the development and construction of a Soviet MHD facility, the U-25B, in combination with the powerful American superconducting magnetic system installed in the Soviet Union on June 20, 1977. The construction of the components of the MHD facility and the fabrication of a superconducting magnet in the U.S.A. for joint research at the High-Temperature Institute, Academy of Sciences of the USSR (IVTAN SSSR), are considered as a landmark of collaboration within the framework of the 1977 agreement. Of great importance were the Soviet–American paper "MHD generation of electrical energy," presented at the World Electrotechnical Congress in Moscow in 1977, and a joint fundamental report on the technicoeconomic aspects of MHD generation of energy which will be published in both countries. The further deepening of the bilateral collaboration in the realm of MHD technology is taking on special importance as is also the construction and operation of MHD electric power plants, including types operating on solid fuel.

J. O'Leary presented to the Soviet delegation materials on the state of work on nuclear power in his country. The U.S.A. has programs on the technical improvement and increased safety of atomic power plants with conventional light-water reactors. A great deal of work is being done on the handling of radioactive waste both inside the country and within international cooperation, improvements are being made in reactors, and a search is under way for new alternative fuel cycles. An experimental fast-neutron facility which has been built is an important research improvement.

In the past year and a half successes have been achieved in confining plasma in tokamaks, in obtaining ultrahigh temperatures, and in developing heating with neutral beams.

The Joint Commission will promote the development of effective contacts between power engineering experts of both countries.

The American delegation visited IVTAN where joint experiments are being conducted on the MHD facility and also visited the Leningrad Atomic Power Plant and the Konakovo State Regional Power Plant.

Translated from Atomnaya Énergiya, Vol. 44, No. 4, p. 380, April, 1978.

0038-531X/78/4404-0438 $07.50

SOVIET – ITALIAN SYMPOSIUM "PRESENT-DAY PROBLEMS OF POWER ENGINEERING"

S. Lutsev and Yu. Klimov

The symposium, which was held in Moscow in Nov. 1977, was attended by some 250 specialists of various branches of power engineering of the USSR and Italy. About 100 papers and communications were presented at the symposium, giving evidence of the thorough discussion of the present-day problems of the organization and development of the power facilities of both countries.

The large number of papers and the multifaceted nature of the topics taken up in them made it necessary for the symposium to work in three sections, each with subsections.

The first section considered conventional electrical power engineering (production of electrical energy and heat, their distribution and demand, equipment for their production). The second was devoted to nuclear power engineering (thermal and fast reactors, components of atomic power plants, the fuel cycle, thermonuclear fusion, and nonelectrical uses of atomic energy). The third section was concerned with fuel resources (production and demand).

The plenary meeting heard papers by the head of the Italian delegation, A. Faedo, and by G. Ammassari and A. Angelini; a paper was also presented by the Soviet delegate A. A. Beschinskii. The papers illuminated the state of power facilities in Italy and the Soviet Union and their principal features and development trends.

The Italian specialists pointed out the dependence of their country on fuel imports. They noted the changes in the energy policy after the 1973-1974 crisis and the rise in the costs of useful energy. The energy difficulties resulted in a slower rate of economic growth. Domestic energy resources satisfy only 20% of the demand. Atomic power plants are therefore necessary as an alternative to hydrocarbon fuel and nuclear power is being considered as the mainstay of the electrical energy supply in the country in the long term.

Italy at the present time has four atomic power plants with a total capacity of 1400 MW and by 1990 atomic power plants will be accounting for 8% of the total electricity generated. The construction of fast breeder reactors is looked upon as the general direction in which nuclear power should develop. The orientation of the country towards fast breeder reactors and heavy-water reactors based on natural uranium calls for particular attention to the links in the external fuel cycle, viz., plutonium regeneration and processing.

Nuclear power is part of the energy concerns of the country. Economic growth can be intensified if all forms of energy sources are developed in Italy, if the output of electrical energy is doubled over the next 25 years, and if additional nontraditional energy resources are utilized, i.e., geothermal, tidal, solar, and wind sources.

In his paper, A. A. Beschinskii told of the state of and prospects for the development of a comprehensive fuel and energy complex in the USSR – the totality of the material means involved in the extraction, conversion, transportation, and distribution of all forms of energy, energy resources, and energy carriers. He gave an account of the successes of power engineering in the USSR. Nuclear power, whose total capacity is rising steadily, has become a new branch.

Various aspects of nuclear energy were discussed in greater detail at the meetings of the second session. Papers on thermal reactors, which Italy and the USSR both have, expressed the interest in channel-type reactors (the graphite-moderated high-boiling reactor and the heavy-water CIRENA) as types which have been mastered and, most important of all, display great possibilities for further engineering and economic improvement. There were many problems in common, as emerged from the papers, in vessel-type reactors which predominate in the nuclear power industry in Italy. At the same time, a specific aspect of the approach in Italy to the design of atomic power plants is the attention paid to making the structures earthquake-proof. During the discussion in this subsection, Italian specialists noted the great successes achieved in the USSR in

Translated from Atomnaya Énergiya, Vol. 44, No. 4, pp. 381-382, April, 1978.

0038-531X/78/4404-0439$07.50

the construction of commercial channel-type reactors with a high unit power. This was emphasized particularly with respect to the design of a channel-type sectional-block reactor with a power of 2400 MW(electrical).

The bulk of the papers in the subsection on atomic power plant components were presented by Italian specialists. They dealt with research on steam generators and pumps, the technology of constructing vessels and electromechanical components for reactors, and water heaters, and combined designs.

Italian specialists are devoting much attention to the organization of a machine-building base for nuclear power equipment which should meet special requirements. Firms and associations in Italy are setting up special machine-building capacities for this purpose. An important feature for Italy is the trend towards compactness in the structural designs for atomic power plants, this being explained by the high cost and shortage of land in the country. Standardized block elements for atomic power plant structures also predominate. The papers pointed out the tendency to increase the concentration of power on the sites of atomic power plants but thus far not above 2000 MW according to the conditions for connecting atomic power plants into the Italian energy system.

The papers and discussion of the subsection on fast reactors revealed a community of views as to the goals, tasks, and ways of accomplishing them in solving problems. In both countries sodium–water steam generators constitute a "sore spot," thus giving rise to greater efforts in this area. The Italian specialists stated that the complexity of the problem and the large expenditures for the development of sodium-cooled fast reactors call for cooperation with other countries, primarily France (joint construction of the 1200-MW Superphenix). Italy is specializing in the production of steam generators.

Fuel recharging occupied a special place in the discussion. It should be noted that both countries are dedicated to a gradual transition to the large-scale use of fast breeder reactors which, it appears, will determine the future of nuclear energy. It was thus acknowledged that the use of plutonium in thermal reactors may be of a partial, local, or temporary character. The general direction of its use is in fast breeder reactors.

The growth of the nuclear power industry in both countries raises the problem of processing spent fuel. The situation concerning this problem of the fuel cycle of atomic power plants and the technological regeneration and the prospects for improving it was described equally by Italian and Soviet specialists. In both countries the main attention is being devoted to the processing of fuel from thermal reactors by aqueous methods. Much progress has been made in mastering them. However, the future will evidently belong to dry (fluoride) methods since hopes for a short (up to 1 year long) external fuel cycle are linked with them. Considerable success has been achieved in both countries in the processing and disposal of radioactive waste. In their papers the Soviet and Italian specialists stressed the endeavors to concentrate and solidify radioactive waste (vitrification and bituminization). Unlike Italy, which employs the ester process, the USSR gives preference to the continuous method as the most technological method. Interest was aroused by an Italian paper on the burial of radioactive waste in deep geological formations, salt-bearing and clayey formations. The latter are saturated with water which has an almost zero velocity, this on the whole being conducive to the filtration of radioactivity. The burial of waste on an industrial scale at Trizai is expected to be mastered by the end of the 1980s.

The last group of topics in the second section concerned untraditional but promising areas of the use of atomic energy. In this connection mention should be made of a Soviet paper on the prospects for the application of the heat from nuclear reactors in high-temperature technological processes which considered various ways of obtaining and conveying a high temperature. Heat exchange by radiation as well as by convection was touched upon. Another Soviet paper dealt with energy-sociological concepts about the structure of the nuclear power industry in the more distant future. An Italian paper analyzed the consumed part of the energy balance of the country. It follows from this analysis that, first, electrification of energy consumers has its limits and, second, the main demand for energy in Italy is for low-potential heat, encompassed by the parameters of reactors. The paper concludes that it is in this direction that efforts should be made since the introduction of reactors here will save high-grade hydrocarbon fuel and will reduce the dependence of the country on imports of such fuel. Naturally, however, many problems are entailed, in the first place with the choice of sites near populated areas for atomic heating plants and with the uneven nature of the demand for heat (24-h, weekly, and seasonal).

Finally, Italian and Soviet papers gave a review of the state of the art in research on thermonuclear fusion. It was pointed out that increased interest was being taken in this subject, as exemplified by the construction of a facility of the Soviet tokamak type in Frascati.

At the closing plenary session of the symposium, Soviet and Italian specialists summed up the results of the work of the sections and emphasized the coincidence of many problems, technical solutions, and characteristic features of the approaches. The main outcome of the symposium consisted in a useful and effective exchange of views and mutual enrichment on the fundamental problems of power engineering of both countries.

THE INTERNATIONAL CONFERENCE ON VIBRATION CAUSED BY COOLANT FLOW IN FAST REACTORS

V. F. Sinyavskii

The conference held in Sept. 1977 at the Argonne National Laboratory (United States) was convened at the initiative of the International Atomic Energy Agency's International Working Group on Fast Reactors. This was the first conference devoted to a discussion of the hydrodynamics of vibrations in fast reactors. The participants heard 15 reports devoted to criteria for the construction and design of fast reactors with sodium coolant, design methods, and research programs.

The British program of research on vibrations in fast reactors with sodium coolant was described in a report by A. Collinson. The report discussed structural elements of the PFR reactor which may be subjected to extraordinarily severe vibrations and the possible mechanisms producing such vibrations. Another report (by E. Pitimada et al., Italy) described the results of research on the vibration characteristics of a model of the fuel assembly of the PEC reactor. In particular, this research yielded vibration amplitudes which varied with different structural factors and with the rate of flow.

The reports presented by V. G. Fedorov and V. F. Sinyavskii (USSR) discussed the scope and sequence of the investigations required for producing vibration-resistant tube bundles in steam generators and fuel assemblies of reactors, as well as the structural measures which will reduce the vibration. The reports described the results of vibration tests of fuel assemblies on test stands. Of particular interest were the results of research on the vibration of the tube bundles of the BN-350 steam generator and the data obtained on a model of the BN-600 evaporator. Calculated and experimental relations were proposed for computing the associated mass and damping coefficients of the tubes and tube bundles.

The program of investigation of the flow-induced vibrations in components of the CRBRP includes an estimate of the reactor components from the viewpoint of their sensitivity to vibration, design rules which can minimize the excitation of the components, investigations on models, and startup and adjustment tests (report by E. Novendstern et al., U.S.A.). An estimate was given for the vibration characteristics of the internal components of a model of the FTR reactor (scale of 0.285), as well as a survey of the results obtained at the Argonne Laboratory, which is a center for the study of fundamental problems of vibrations in the United States program on fast reactors (report by M. Bambsgans).

A report devoted to a study of the vibration characteristics of elements in the active zones of the Phenix and Superphenix (France) described methods of computational and experimental research and the variation of the vibration characteristics of fuel assemblies as a function of coolant flow velocity. It described a three-dimensional method for calculating the vibration of tubes resulting from internal flow past the tube walls. The problem was reduced to calculating the reaction of a loop to disturbances in acoustic pressure. The calculation results were found to be in satisfactory agreement with the experimental results for resonance frequencies and amplitudes.

Three types of heat exchangers developed for the SNR-300 were described in a report by A. van Beck (Netherlands). Measurements were made to determine the flow-induced disturbing forces on the tubes of flow-through steam generators. Calculations and full-scale experiments showed that no impact wear of the tubes is to be expected. The spectrum of forces produced by coolant flow for a steam generator with spiral tubes was investigated from various points of view.

Translated from Atomnaya Énergiya, Vol. 44, No. 4, pp. 382-383, April, 1978.

0038-531X/78/4404-0441 $07.50

Vibration investigations on the equipment inside the shell and on the tank of the SNR-300 (Federal Republic of Germany), conducted with water and sodium, showed that the vibration of the fuel assemblies will be insignificant. In order to collect the necessary data to demonstrate the reliability of the equipment inside the shell, a method which included both theoretical and experimental investigation and a series of measurements which will be conducted when the reactor is started up and adjusted was devised.

The participants in the conference heard the results of the investigation of hydrodynamic vibrations of structural elements of the JOYO experimental fast reactor and a prototype of the MONJU fast reactor (Japan). Particular attention was given to the fuel assemblies. The results of experimental research for a natural model of the JOYO assembly were given. The report discussed a malfunction of a sodium valve on the experimental stand. The reason for the breakdown had been fatigue failure of the sylphon bellows of the valve as a result of vibration.

It was noted at the conference that today the approach to the problem of hydrodynamic vibrations has changed considerably.

In the recent past, little attention was given to vibration in the early stages of design, and if problems arose, the project was modernized. Today the need for vibration research at the early stages of design is generally recognized. In many cases, in order to preclude the possibility of operating regimes that give rise to excessive vibration, model tests are conducted. However, in spite of calculations and model tests, there are certain difficulties in estimating the behavior of operating installations. Therefore, in order to obtain additional guarantees, full-scale vibration tests are conducted on the components of installations using sodium, and vibration measurements are made when the reactor is started up and adjusted.

The basic failure mechanisms discussed at the conference – fretting, wear, and fatigue damage – are of the greatest interest in estimating the vibration resistance of components of steam generators and fuel assemblies. Today it is not possible to establish any laws governing the variation of fretting and vibration wear while an installation is in operation.

The structural elements which require consideration from the viewpoint of hydrodynamic vibrations include those areas in which there is a sudden change in the coolant flow velocity as a result of changes in geometry. Designers endeavor to keep the characteristic frequencies of vibration of structural elements far from the frequencies caused by the separation of vortices. For cases in which it is impossible to keep the frequencies sufficiently far apart, they make experimental estimates. In order to estimate the strength of a component, the stresses arising as a result of vibrational motion are added to the stresses caused by other modes. The components which were most frequently discussed in connection with the vibrations caused by coolant flow were fuel elements and the tube bundles of steam generators; tubes and other equipment inside the shell were less often involved.

In order to predict and prevent excessive vibration, full-scale investigations were carried out for the internal components of a reactor, the heat exchangers, and the steam generators, and model investigations for large structures. Only in a few cases of simple geometry can the response to the forces excited by liquid flow be analytically calculated with acceptable accuracy if we measure the velocity distribution and the characteristics of the pressure fluctuation. When data are carried over from a model to natural conditions, there are limitations due to the difficulty of taking account of the effects of thermal expansion, radiation swelling, and boiling. Experience in the operation of fast reactors indicates that the investigative methods used are satisfactory but cumbersome and expensive.

Most of the results obtained thus far have only limited applicability, owing to the many factors that affect the vibration characteristics, and therefore they cannot be used directly by designers. Only for a few cases of simple geometry and ideal flow conditions has the information been sufficiently verified, so that it can be given in the form of handbook material for a designer.

Today, monitoring and control of vibrations is being carried out only on individual components of operating installations. However, because of inadequate experience in the interpretation of the observed results, the information cannot be used by the operators of the installations.

Using the method of expert estimates, the participants in the conference determined the basic problems in hydrodynamic vibrations which will require further study:

– flow distribution and pressure fluctuations in real hydroelastic systems; investigation of three-dimensional force functions and their space–time correlations for flows in fuel assemblies and steam generators;

– vibration wear and fatigue, which make it possible to determine the critical values of the vibration characteristics of reactor components;

– mechanisms for damping the oscillations of structural elements in a liquid;

– modeling, including the carrying over of results from water to sodium;

– observation techniques, with a view to determining the appearance of dangerous vibrations in operating reactors, as well as calculation methods.

The materials of the conference have been published as working papers of the International Working Group on Fast Reactors.

THE INTERNATIONAL CONFERENCE "BERYLLIUM-77"

G. F. Tikhinskii

The physicostructural properties of beryllium make it an interesting material for research and a promising one for practical application. The fourth conference, meeting in London in Oct. 1977, was devoted to a summary and discussion of the results of metal-physics and technological research in recent years. The conference was attended by more than 120 delegates from 13 countries who presented and discussed more than 60 papers on the materials science, technology, and practical uses of beryllium.

The conference paid the greatest attention to the cold brittleness of beryllium and discussed the results of the search for a realization of promising ways of enhancing its plasticity and toughness. New data obtained in recent years are of practical as well as scientific interest. Metal-physics research in the USSR and the U.S.A. showed that, notwithstanding the great proclivity of beryllium to brittle fracture, the plasticity of the polycrystalline metal can be increased by bringing into play additional deformation mechanisms which, according to the von Mises–Taylor criteria, it lacks. Such additional mechanisms leading to stress relaxation at crack tips and reduction of the temperature threshold of cold brittleness can, e.g., consist of a developed glide over ordinary systems (above all, over the planes of a base and prism of the first kind), weak slip along grain boundaries, and accommodated dislocation glide. However, if the last mechanism is to be realized, it is necessary that the metal be fine-grained and contain only a slight amount of impurities. This possibility of increasing the plasticity of beryllium was established by workers of the Kharkov Physicotechnical Institute, Academy of Sciences of the Ukrainian SSR (FTI AN USSR), during research on the effect of structural factors and impurities on the cold brittleness of metals. The report by the conference showed that such an approach to the cold brittleness of beryllium has at the present time become current. Thus, D. Webster (U.S.A.) reported having obtained specimens of isotropic (untextured) beryllium which has a relative elongation of up to 13% at 20°C. He also believes that the high plasticity and toughness characteristics attained in fine-grained high-purity beryllium are due to the mechanism of slip along grain boundaries. N. Pinto (U.S.A.) told of a new experimental grade of beryllium developed by Kawecki Berylco Industries (KBI); in the isotropic structural state at 20°C it has $\sigma_b = 56$ kgf/mm^2, $\sigma_s = 41$ kgf/mm^2, and $\delta = 4\%$.

High mechanical properties of pure fine-grained beryllium with an isotropic structure were also reported by F. Oldinger (German Federal Republic), G. Turner (Gt. Britain), and others.

Progress in improving the properties of beryllium with an isotropic structure has been made by the application of pure electrolytic, electrolytically refined, or distilled beryllium and new methods of powder metallurgy which permit ultrafine powders to be obtained and to be compacted without any significant contamination of the metal with impurities. Better results have been obtained with isostatic pressing of powders. The new methods of powder metallurgy are now used to obtain industrial grades of pure beryllium. For example, KBI produces two new grades of the metal: CIP/HIP-1 (the powder is first subjected to cold isostatic pressing and then to hot isostatic pressing at 1000-1100°C) and HIP-50, which are distinguished by high strength and plasticity, uniformity of structure and composition, isotropy, and enhanced resistance to microplastic deformation. Blanks and products of quite complicated shapes can be obtained by hot isostatic pressing.

Translated from Atomnaya Énergiya, Vol. 44, No. 4, pp. 384-385, April, 1978.

0038-531X/78/4404-0443 $07.50

Several papers were devoted to the study of the possibility of plasma (or thermal) spraying of beryllium in a controlled atmosphere. The method is convenient for obtaining a porous metal and some thin-walled products. Under optimal conditions of forming and heat treatment, the physicomechanical properties of the metal obtained by thermal spraying are comparable to those of hot-pressed beryllium.

An ingot-deforming technology is used abroad to obtain some half-finished and finished products. Kawecki Berylco Industries, e.g., employs this technology to produce sheet, ultrathin foil, and wire. Sheets made from ingots of pure metal have a higher plasticity and lend themselves well to welding. According to data from British researchers, products of intricate shapes can be stamped from such sheets.

Four Soviet papers read at the conference dealt with the study of the thermally activated mechanism of plastic deformation of monocrystalline and polycrystalline beryllium, realization of a subgrain (cellular) structure in the metal as a basis for obtaining a highly disoriented grain structure, and the study of plastic deformation of pure (99.95% Be) fine-grained ($\sim 5\ \mu$) metal obtained by mechanical and heat treatment of ingots. Such metal in the quasi-isotropic state can possess high plasticity at room temperature ($\delta = 22\%$) and superplasticity ($\delta \geq 300\%$) at 650-700°C. These characteristics considerably surpass those achieved by foreign researchers. The papers aroused great interest among the conference delegates.

Some of the papers were devoted to the applications of beryllium. The main consumers of the metal are, as before, the aerospace industries. The application of the metal in these areas is growing. Some papers in particular considered the use of beryllium for optical mirrors and hydraulic devices, i.e., in applications where its physical properties (rigidity, structural and dimensional stability, resistance to microplastic deformation, etc.) play a cardinal role.

An analysis of the applications of beryllium in the nuclear power industry was made by S. Pew (Harwell, Gt. Britain). At the present time this metal is used in some types of reactors as a neutron reflector and moderator. Although in the 1960s some success was achieved in improving the heat resistance, resistance to gas corrosion, and radiation resistance of beryllium as a material for fuel element cans, large-scale elements have hitherto not been conducted. Consideration is being given to the possibility of employing beryllium in the breeding blanket of breeder reactors and as a material for the walls of thermonuclear reactors.

The "Beryllium-77" conference was undoubtedly useful from the point of view of an exchange of experience and information about the state of research and prospects for the application of beryllium.

EUROPEAN CONFERENCE ON PLASMA PHYSICS AND CONTROLLED THERMONUCLEAR FUSION

V. D. Shafranov

The 8th conference, which took place in Prague in Sept. 1977, was attended by some 300 delegates from 23 countries, including the U.S.A., Japan, Canada, and Australia. Four sections discussed about 180 original papers and the plenary sessions heard 17 review papers. The largest number of papers (about 70 sectional and 7 plenary) were on tokamaks.

As is well known, plasma with a density $n \sim 10^{13}$-10^{14} cm^{-3}, temperature $T \sim 1$ keV, and lifetime of up to 50 msec is obtained at present by means of ohmic heating in the case of the large T-10 (USSR) and PLT (U.S.A.) tokamaks and with auxiliary heating by injection of a beam of neutral atoms in the case of the somewhat smaller TFP (France) and DITE (Gt. Britain). One of the cardinal problems encountered in moving towards higher temperatures is posed by impurities which affect the global stability of the plasma as well as its energy balance. In the short time since the conference at Berchtesgaden,* considerable progress has been made in explaining the mechanism by which impurities are formed and how they affect the dynamics of the plasma column. The main results were obtained on the DITE facility. Light impurities (primarily oxygen atoms) are formed as the result of desorption from the chamber walls by hydrogen atoms circulating between the plasma and the wall. Falling into the plasma, these impurities cool its periphery and lead to a redistribution of the current and subsequently cause instabilities. Heavy impurities (atoms of the wall material) are formed chiefly because of spontaneously initiated unipolar arcs. Ions of an impurity with a high atomic number penetrate deeply into the plasma, cooling its central part with their powerful radiation, and causing a "dip" in the temperature distribution. Effective ways of controlling the entry of an impurity have been devised:

gettering (sputtering titanium onto the chamber walls) to weaken the circulation of hydrogen atoms and, consequently, the desorption of light impurities;

removing the effective boundary of the plasma from the walls to prevent unipolar arcs by artificially cooling the plasma edge (admitting neutral gases, constructing a magnetic diaphragm, artificially disrupting the extreme magnetic surfaces to increase the thermal conductivity of the plasma periphery, etc.). In work on the DITE, DIVA (Japan), and T-12 (USSR) facilities under various conditions it was observed that diverter devices have a beneficial effect on the protection of the chamber walls from bombardment with particles and on the shielding of the plasma from impurities.

A great contribution towards unravelling behavior of impurities was made by experiments on the T-4 facility (USSR) during which it was discovered that ions of a high degree of ionization are ejected from the hot plasma.

Positive shifts have been made in the application of less expensive heating methods than injection, viz., rf methods of directly heating the ionic component of the plasma. The results obtained earlier on the ATC facility (U.S.A.) on heating in the region of ion-cyclotron frequencies were augmented with the first data about the effect of heating at lower hybrid resonance (Tuman facility, USSR, and Petula facility, France), as well as in helical modes (P-02, two-setting stellarator of the Sukhum Physicotechnical Institute).

In the realm of the theory of plasma confinement, the greatest interest was aroused by the theory of dimensionality developed by J. Connor and J. Taylor to obtain the dependence of the energy lifetime on the plasma parameters and by work on the calculation of the limiting pressure due to the so-called balloon instability of plasma. Numerical calculations played a great role in the latter.

*Atomnaya Energiya, Vol. 42, No. 2, 155 (1977).

Translated from Atomnaya Énergiya, Vol. 44, No. 4, pp. 385-386, April, 1978.

0038-531X/78/4404-0445$07.50 ©1978 Plenum Publishing Corporation

Good results have also been obtained with recently constructed second generation stellarators Liven'-2 (Lebedev Institute of Physics, Academy of Sciences of the USSR), Cleo (Calem, Gt. Britain), Uragan-2 (Kharkov Chemical Technological Institute, USSR), and Wandelstein VII-A (Garching, Federal Republic of Germany) as well as with tokamaks. With ohmic heating results close to those in tokamaks are obtained: $T_e = 200\text{-}900$ eV, $T_i = 100\text{-}300$ eV, $n = 5 \cdot 10^{12}\text{-}6 \cdot 10^{13}$ cm^{-3}, $\tau_E = 1\text{-}10$ msec, and $\tau_p = 5\text{-}30$ sec. The quite high efficiency of ohmic heating is due in considerable measure to the insulating effect of the specific stellarator poloidal magnetic field. However, as I. S. Shpiegel' (USSR) noted in his paper, one has the impression that ions behave somewhat worse in stellarators than they do in tokamaks. In view of the importance of elucidating the prospects of stellarators, an international working meeting was organized in the town of Zdikov, 150 km from Prague, within the program on controlled thermonuclear fusion. One of the principal tasks brought up at the meeting was that of going on to obtain high plasma parameters without ohmic heating (injection of neutral atoms, rf heating). This could throw much light on the mechanism of anomalous energy losses by plasma in toroidal systems.

Interesting research on the dynamics of stabilized pinches was reported on by British physicists. Both numerical calculations (J. Wesson and A. Sykes) and experiments at Calem showed that a stable configuration with reversed toroidal magnetic field is formed as the result of the development of a helical instability. The parameters of plasma in stabilized pinches are still considerably lower than in tokamaks and, probably, the interaction of the plasma with the chamber walls during the process of reconstruction of the configuration is responsible.

The programs for the development of research on new large facilities at Calem (HBTX-1A, RFX), Los Alamos (ZT-40), and Padua (ETA-BETA), are aimed at optimizing the conditions for the formation of a stable plasma configuration, including the choice of wall material.

As far as open traps are concerned, particular attention is now being paid to the program of large-scale experiments at Livermore (U.S.A.) which F. Coenchen described. Recent successful experiments on the confinement of plasma produced by a powerful injection of beam of neutral atoms made it one of the foremost tasks to create a reversed-field configuration (transformation of an open trap into a closed trap with high plasma pressure). This goal has nearly been reached. Another great task is that of verifying the idea advanced by D. I. Dimov (Institute of Nuclear Physics, Siberian Branch, Academy of Sciences of the USSR) about improving plasma confinement in an ambipolar trap. A trap of this kind, called a tandem, is to be constructed at Livermore within a year.

Some work, both theoretical and experimental work done on small installations, was devoted to studies on plasma in confinement and instabilities in traps by exciting oscillations or adding cold plasma.

Besides the program on controlled thermonuclear fusion, based on magnetic thermal insulation of plasma, in recent years there has been a broad development of research on the use of laser beams and beams of charged particles to heat and compress microtargets. In Livermore, experiments on the laser compression of deuterium-filled miniature glass balls produced a thousandfold compression, a temperature of 5 keV, and a neutron yield of $3 \cdot 10^8$.

Some papers presented at the conference dealt with the modeling of compression in order to explain the mechanisms of anomalous transfers, on which the development of the process depends. In a paper, N. G. Basov et al. described the 12-channel laser thermonuclear installation "Del'fin," with an energy of 10^4 J in a pulse and a duration of 10^{-9} sec, constructed in the Lebedev Institute of Physics.

Successful experiments by L. I. Rudakov et al. resulted in increased interest in the use of beams of charged particles to compress plasma. In his paper, G. Ionas (U.S.A.) presented the results of experiments on preheating and additional magnetic insulation of compressed plasma formed by passing a current of 5-10 kA through a CD_2 column of diameter 25-50 μ in a plastic envelope (diameter 3 mm). A neutron yield ($\sim 10^6$ in a pulse) was detected in the experiments.

Some papers considered the interaction of radiation with plasma, diagnostics, and reactor problems.

The Prague conference proved to be highly productive. This is evidence of the steady advance in research on controlled thermonuclear fusion and acceleration of the research through broad international collaboration. The Czechoslovak hosts displayed cordial hospitality and did everything for the successful work of both the conference and the stellarator meeting.

SEVENTH INTERNATIONAL VACUUM CONGRESS

G. L. Saksaganskii

The Congress was held in Sept. 1977 in Vienna (Austria) at the same time as the Third International Conference on Solid Surfaces. Some 1400 specialists from 40 countries participated in the work of the Congress and the conference which were organized by the International Union for Vacuum Science, Technique, and Applications (IUVSTA) and the Austrian Vacuum Society with the participation of the IAEA. A total of some 750 plenary and panel papers were presented on vacuum physics, technique, and technology, the kinetics and interphase interactions, thin films, surface analysis, etc. As part of the Congress there was an exhibition of vacuum pumping, measuring, and technological equipment, instruments, and apparatus made by major foreign firms.

The delegates visited the laboratories of the science center of the Austrian Society for Research on Atomic Energy at Zeibersdorf and the Technical University of Vienna.

The papers presented at the Congress covered the following areas: vacuum pumps, the flow of rarefied gases, electric discharge and breakdown in a vacuum; fittings and materials for high-vacuum systems; vacuum gauging and mass spectrometry equipment; vacuum metallurgy; vacuum-technical problems of apparatus for physical research (controlled thermonuclear fusion, accelerators, and space simulators).

A review paper on obtaining and measuring an ultrahigh vacuum was prepared by the ISR vacuum group (CERN). The paper generalized the experience gained in constructing and operating unique vacuum systems for proton storage rings. It was noted that the parameters attained (mean pressure $\sim 10^{-11}$ mm Hg and, in segments of contact, less than 10^{-13} mm Hg) are the result of the comprehensive solution of the threefold problem of choosing the chamber material and developing a technology for thoroughly degassing it, employing "ideal" vacuum pumps with a maximum residual pressure of less than 10^{-15} mm Hg, and designing vacuum gauges with adequate characteristics. The chambers of the storage rings are made of stainless steel and dispersion-hardened alloys of the Inconel type. After long annealing of the half-finished chambers at 950°C and repeated thermal conditioning of the chamber at 300°C (stainless steel) and 550°C (for Inconel), the specific rate of gas release is reduced to $2 \cdot 10^{-13}$ and $5 \cdot 10^{-15}$ liter · mm Hg/sec · cm^2, respectively. The storage elements are pumped down concurrently by ion-getter condensation helium pumps with cryosurfaces at a temperature of 2-4°K. To reduce the rate of evaporation of condensed hydrogen under the effect of radiation fluxes, hydrogen is condensed on a layer of nitrogen condensate deposited on a silver substrate. The condensation pumps have a pumping speed of $(4.5\text{-}27) \cdot 10^3$ liters/sec (H_2) and the operating period per filling of liquid helium at 4.2°K is up to 80 days.

The rate of evaporation of liquid helium in ordinary condensation pumps was determined to the extent of 95% by the radiative heat influx from the nitrogen shields. To reduce it, second-generation cryosorption pumps rated $4.5 \cdot 10^3$ and $11 \cdot 10^3$ liters/sec of more complicated design were constructed: the helium chamber proper was surrounded with a neon-filled hermetically sealed jacket on all sides except the one facing the entrance port. The heat influx into the helium chamber was thereby substantially decreased, and the operating life was increased to 200 days.

The design of the ionization manometers was also optimized, and this made it possible to decrease the pressure limits by ≈ 1 order of magnitude. After precision calibration jointly with the cryosorption pump, these manometers were used to measure the minimum residual pressure and the operating rate of the sublimation, sputter-ion, and nonsputtering getter pumps used with the ISR. This made it possible to optimize the evacuation regimes and the vacuum system as a whole.

A number of other papers were delivered by the same group. In particular, they discussed the results of the development tests of a model of a vacuum-chamber section for a planned proton storage ring rated 2 × 400 GeV with a superconducting magnetic system. Supplementing the vacuum technology presently used in

Translated from Atomnaya Énergiya, Vol. 44, No. 4, pp. 386-388, April, 1978.

0038-531X/78/4404-0447$07.50

the ISR, a titanium layer was deposited on the wall of the model (of 50-mm diameter and 5.1-m length), after outgassing (150°C) and attaining a residual pressure $4 \cdot 10^{-10}$ torr (a titanium wire inserted along the chamber axis was thermally evaporated in an argon medium at a pressure 0.1 torr). The chamber was then evacuated by turbomolecular and sputter-ion pumps to $2 \cdot 10^{-11}$ torr (H_2 – 91%, CO – 6%, CH_4 – 2%, CO_2 – 0.7%, H_2O < 0.5%, Ar < 0.1%). The passage of the proton beam through the chamber was imitated by exciting a discharge in the argon medium (10^{-4} torr) by applying to the titanium wire a potential + 700 V and turning on the thermionic tungsten emitter. The coefficient of ion-stimulated gas release was determined from the increase of the partial pressure of the individual components. By way of example, for CO this coefficient decreased after the sputtering of the titanium by a factor of 100. According to the authors' estimates, the use of this technology increases the limiting stored current by almost 50 times.

In connection with shakedown of the variant of the "cold" (~4°K) chamber for storage rings, with a superconducting magnetic system, the ion-stimulated desorption from the surfaces of the condensates was measured. The experiments were made with H_2, He, and N_2 condensates on a stainless steel substrate (T = 2-4°K) with the surface bombarded by H_2^+, He^+, Ar^+, and other ions at an energy of 0.5-1.0 keV. The coefficient of desorption from the surface of the layer under the influence of the bombarding ions increased rapidly with increasing surface filling coefficient, reaching a maximum or saturation at a condensate thickness of several monolayers. For example, when the condensate H_2 (3.2°K) was bombarded by its own ions (5 keV) the coefficient of ion-stimulated desorption increased from 10^3 mol/ion (surface filling 10^{19} mol/m^2) to 10^5 mol/ion (filling 10^{20}–10^{22} mol/m^2) and subsequently decreased steeply (less than 10^3 mol/ion at a filling 10^{23} mol/m^2).

The planning and technological-design optimization of vacuum systems of accelerators of various types and of storage rings was dealt with in 10 papers. Among the questions discussed were the construction and operational features of built-in sputter-ion and getter pumps (SRS, England; DESY, W Germany; CERN); the designs of vacuum chambers for electron storage rings, including the DESY-accelerator four-channel chamber, made of aluminum by an extrusion method, and the technology of vacuum-tight welding of details of aluminum and stainless steel, developed in the course of the construction of the same accelerator. The vacuum conditions and possible variants of the vacuum systems were analyzed for a synchrotron heavy-ion accelerator operating in a regime of variable charge of the accelerated particles (Efremov Research Institute of Electrophysical Apparatus), the design features of a specialized damper-type shutter for strong-current accelerators (DESY) were considered, and others.

A special group of papers were devoted to the interaction of corpuscular and radiant fluxes with solid surfaces in vacuum, and methods, based on this interaction, for the purification of surfaces of ultrahigh vacuum accelerator and thermonuclear installations. It is shown that effects of electron-stimulated and ion-stimulated desorptions are substantially selective (CERN). By way of example, the coefficient of electron-stimulated desorption of hydrogen from a stainless-steel surface is almost 10 times higher than for CH_4, CO, and CO_2 (0.08 and ~0.01, respectively, for samples subjected to preliminary 24-h heating at 300°C). When the surface is bombarded by heavy ions, the coefficient of stimulated release of H_2 and CO increases rapidly with increasing ion energy, whereas the intensity of release of CH_4 and CO_2, starting with 1 keV, is practically independent of the ion energy. The temperature of the samples influences much strongly the desorption stimulated by electron bombardment than the ion-stimulated processes.

In another paper, also presented by the CERN specialists, are summarized the experimental data on purification of storage-ring chambers by ion bombardment with the aid of a discharge in argon ($2 \cdot 10^{-2}$ torr). The known premise, that even a very prolonged high-temperature outgassing does not remove hydrocarbon and oxide films completely from the surface, is confirmed. The required degree of purification is reached by discharge in argon at a bombarding-ion dose ~10^{15} cm^{-2} (hydrocarbons) and ~10^{18} cm^{-2} (CO). A surface treated in this manner turns out to be free of contamination even after contact with atmospheric air.

Analogous results were obtained by the PETRA group (W Germany) in the course of processing, in a discharge, an aluminum electron–positron storage-ring chamber (required dose ~10^{19} cm^{-2}). Similar data as applied to tokamak conditions are reported in review articles by the TFR group (France).

A large volume of experimental data on the thermal gas release, erosion, and blister-effect of materials that are potentially suitable for thermonuclear installations were reported in the papers by the JAERI group (Japan).

Notice should be taken of the rapid progress made with cryogenic pumps of various types, including those for experimental thermonuclear reactors (11 papers). In addition to several survey papers, the Congress heard reports of experimental data on cryogenic trapping of helium and its diffusion in condensate layers of protium and deuterium (Brookhaven, USA), on the thermophysical characteristic of condensation pumps for the forevacuum region when working with various coolants (N_2, Ne, H_2, He) (Kharkov Physicotechnical Insti-

tute), on the feature of cryogetter pumps of various modifications (Institute of Theoretical and Experimental Physics; Physics and Engineering Institute; Oak Ridge, USA.). Much interest was attracted to the materials of the exhibitions and to papers describing condensation and cryogetter pumps with autonomous cryogenerators of the refrigerator type. For example, a cryopump with a pumping speed of $8 \cdot 10^3$ liters/sec (H_2) has been developed on the basis of a Philips refrigerator with a refrigerating capacity of 10 W (20°K). The cryosurface of this pump is a copper plate in good thermal contact with the second stage of the refrigerator. The maximum residual pressure is 10^{-9} mm Hg. Another refrigerator with a refrigerating capacity of 2 W has been used as the basis for developing pumps with condensation and cryogetter stages with pumping speeds of 280 liters/sec (He) and $1.6 \cdot 10^3$ liters/sec (H_2), the maximum residual helium pressure being less than 10^{-7} mm Hg.

Among papers on the vacuum-technological problems of controlled thermonuclear fusion, mention could be made of those which: describe in detail the vacuum parameters of the tokamaks TFR (France) and T-10 (I. V. Kurchatov Institute of Atomic Energy); analyze the plasma-vacuum conditions in the torsatron thermonuclear reactor with magnetic diverter in which it proves extremely effective to employ a differential pumping system based on built-in cryopumps (Kharkov Chemical Technological Institute, Academy of Sciences of the Ukrainian SSR); and give the results of the development of special-purpose modules for pumping hydrogen and other active gases based on a bulk-getter pump (84% Zr and 16% Al), with a specific pumping speed of ~ 10 liters/sec $\cdot$ cm^2 (H_2) and a high sorption capacity. It is proposed to use such modules, in particular, to construct sorption surfaces for pumping down the injectors of the JET facility (Euratom) at an overall pumping speed of $2.5 \cdot 10^5$ liters/sec (H_2) with an energy consumption of only 1.4 kW under the operating conditions (200°C) [SAES company, Italy]. An interesting analysis was made of the characteristics of various types of high-vacuum pumps, which hold out potential for use in pumping down the parameters of deuterium and tritium pumping down by turbomolecular, diffusion, evaporator, and discharge-type pumps of various modifications (NIIÉFA, VNIINM). In the realm of electric effects in a vacuum there has been a noteworthy growth of interest in field emission and field-emission devices, considerable progress in understanding the mechanism of electric discharge and breakdown, the role of the state of the surface, and cathodic processes. The electric strength of vacuum gaps has been increased substantially on this basis.

Papers read at the Congress presented detailed data on the latest designs of turbomolecular pumps (7 papers), instruments for vacuum gauging, mass spectrometry, and leak detection (29 papers), materials and fittings for high-vacuum systems (8 papers), etc.

Analysis of the Congress materials and the exhibition reveals:

a marked increase in research and development in the realm of controlled thermonuclear fusion, high-energy physics, nuclear physics, and the technique of physical experiment (more than half of the papers were entirely or partially devoted to precisely this subject);

a rapid growth of equipment for high-vacuum pumping based on cryopumps and turbomolecular pumps;

industrial mastery of condensation and cryogetter pumps with autonomous cold generators, economic ultrahigh-vacuum cryopumps of the fillable type, wholly fluid-free turbomolecular pumps with gasdynamically and magnetically suspended rotor, and turbomolecular pumps which do not require a forevacuum;

engineering studies on cryoturbopumps with an increased compression factor and turbomolecular pumps with nonmetallic rotor;

the development of work on the optimization of parameters and preparation of pumping equipment based on metallic bulk getters with an enhanced sorption capacity for use in large electrophysical installations; such equipment has advantages over cryogenic equipment in installations with a large heat release;

the growing scale of practical implementation of the principle of integrating the vacuum channel of accelerators by means of the structural and functional unification of the vacuum chambers and high-vacuum pumping equipment;

a qualitatively new approach to the choice of structural materials and technology of vacuum preparation of chambers operating under intense irradiation (ionic treatment in addition to the conventional thermal degassing);

industrial mastery of special-purpose vacuum system elements which are necessary for electrophysical installations of various types;

a significant rise in the metrological level of industrial vacuum-gauge and mass-spectrometer apparatus;

a trend towards automatic data processing with built-in computers.

The Conference proceedings will be published.

THIRD INTERNATIONAL SEMINAR-SCHOOL ON APPLIED DOSIMETRY

V. K. Mironov

The seminar of radiation safety service workers of the Academy of Sciences of the USSR and the Academies of Sciences of the union republics (SRB AN-III) was held in Odessa from Oct. 4 to 11, 1977. It was organized by the "Radiation Safety" section of the Scientific Council of the State Committee of the Council of Ministers of the USSR for Science and Technology (GKNT SM SSSR) and of the All-Union Central Council of Professional Unions (VTsSPS) on "Labor Protection", the Academy of Sciences of the Ukrainian SSR, and the Leningrad Institute of Nuclear Physics (LIYaF). The 85 participants came from 43 organizations of the Academies of Sciences of the Union Republics and other ministries and departments.

The seminar-school was organized on the principle: review papers and lecture papers (school part) and communications about practical methods of ensuring radiation safety during work with sources of ionizing radiation.

In contrast to the previous seminar, the review papers were read according to the program schedule. The following subjects were discussed: 1) the principles of the approach to the standardization of radiation factors and the main provisions of the Standards on Radiation Safety (NRB-76); 2) some current topics of environment production, including the problem of ^{85}Kr, and the economic aspects of radiation safety; 3) present-day problems of dosimetry and microdosimetry; 4) the radiation and dosimetric characteristics of tritium and methods of measuring it; 5) planning an experiment involving detection of ionizing radiation; 6) laser safety; 7) the present state of the art in research on radiation safety.

In the second part of the seminar 22 out of 35 papers were read and discussed. Attention was focused on:

method of radiation monitoring during work with tritium and its compounds (6 papers);

laser safety (dosimetry of nonionizing radiation);

ensuring the metrological and instrumental means for radiation monitoring;

the structure and organizational principles of radiation safety services.

Greatest interest was aroused by papers read by representatives of LIYaF, the Nongovernmental organization (NPO) of the Main Administration for the Atomic Energy Industry (Glavatoménergo), the Kolsk Branch of the Academy of Sciences of the USSR, the Joint Institute for Nuclear Research (JINR), the Leningrad Scientific-Research Institute for Radiation Technique (NIIRT), and the P. N. Lebedev Institute of Physics of the Academy of Sciences of the USSR (FIAN). This group of papers considered radiation safety during processing of useful minerals of the Kolsk Penisula; gave the results and methods of research on nonhermetic fuel elements from VVR-M water-moderated–water-cooled reactors; pointed to possibilities for reducing radioactive discharges into the atmosphere; reported on measurements of tritium in the water of the first loop of the VVR-M reactor using gas chromatography to identify it; reported on mechanisms of the formation of tritium in nuclear power installations, its migration over technological loops, on the processes of its diffusion into structural materials; and on methods of radiation monitoring of tritium in the form of T_2 and HTO. These papers spoke of integrated dosimetric monitoring, the achievements in the realm of laser safety, the organization and structure of radiation safety services (a draft regulation on the radiation safety service), etc. The seminar recommended the publication of the most original communications; 13 papers not included in the working program of the seminar were discussed by participants who took an interest in them.

During the discussions the participants of the seminar-school made proposals for further improvements in the system for ensuring radiation safety:

resumption of the work of the dosimetric commission of the State Atomic Energy Committee of the USSR (GKAÉ SSSR) to provide better coordination of work on dosimetric instrumentation as well as to ensure

Translated from Atomnaya Énergiya, Vol. 44, No. 4, pp. 388-389, April, 1978.

 0038-531X/78/4404-0450$07.50

supplies of equipment for the radiation safety services;

acceleration of commerical production of solid-state and emergency dosimeters based on completed developments to raise the efficiency of personal dosimetric monitoring;

development of methodological instructions on the volume and methods of dosimetric monitoring in emergency situations;

establishment of a journal "Radiatsionnaya Bezopasnost," (Radiation Safety) as an instrument for the exchange of information on topics pertaining to environmental protection and radiation safety;

systematic convening of seminar-schools (not less frequently than once every 2 years).

The next seminar-school is to be held in Sept. 1979.

TENTH MEETING OF GROUP OF SENIOR IAEA ADVISERS ON ATOMIC POWER PLANT SAFETY

O. M. Kovalevich and L. V. Konstantinov

The regular, tenth meeting in accordance with the IAEA program, on drawing up standardizing documents (codes and guides) on ensuring the safety of atomic power plants, was held in Vienna from October 10 to 14, 1977. The final code of regulations, "Design," was adopted at this meeting. Four other codes ("Operation," "Choice of Site," "Government Organizations, and "Quality Control") had been adopted at three previous meetings in December, 1976, and February and June, 1977. The tenth meeting also started the proceedings for final approval of the guides with total about 50 overall.

The program, which IAEA has dubbed NUSS (Nuclear Safety Standards), was conceived in 1974 and realization of it began in 1975. At the present time it is one of the largest programs in respect of means expended and specialists involved.* The purpose of the program is to assist IAEA member-countries which are developing their own national nuclear power industry. The codes and guides drawn up are based on national standardizing documents and experience accumulated on the safety of atomic power plants in countries pursuing the large-scale development of nuclear power. The documents are regarded by IAEA as a recommendation which member-countries can use with allowance for the characteristics and jurisdiction of these countries. Particular attention has been devoted to this aspect in drawing up the documents. In the future it will be possible to conclude agreements between IAEA and member-countries on assistance in the construction of national atomic power plants at any stage (selection of a site, construction, start up, operation, removal from operation). In this case the country is required to follow those parts of the codes and guides which are to be covered by the agreement.

The provisions of the codes and guides extend to stationary atomic power plants with thermal reactors for the production of energy. The preface to the program points out that the given set of documents will not cover numerous aspects of the subject and should be construed as a minimum of requirements and assumptions for methods for meeting those requirements and as a program to be adhered to in order to ensure the safety of atomic power plants. Other IAEA documents on safety, both those published earlier and just drawn up, should also be taken into account.

The procedure employed to draw up each document of the program is quite involved and covers a period of two to three years. The documents are elaborated in parallel by five Technical Committees in areas in accordance with the codes of the regulations. It is the task of the Technical Committees to determine the title and contents of the future document and to consider and revise draft documents at various stages. The initial version of a document is drawn up by the Working Group whose meeting is preceded by the work of the IAEA

* Each year some highly qualified experts spend some 2000 man-days in meetings while 3000 man-days go into evaluating the documents examined and making on-the-spot notes.

Translated from Atomnaya Énergiya, Vol. 4, No. 4, pp. 389-390, April, 1978.

0038-531X/78/4404-0451 $07.50

Secretariat which collects national standardizing documents and any other information on the given subject. The first draft drawn up by the Working Group goes to the Technical Committee, which discusses it and introduces appropriate changes (often extremely significant ones). The amended draft is then discussed by the Group of Senior Advisers, consisting of highly qualified experts from many countries* and international organizations, who check the program and consider all the documents at various stages. After the first consideration and introduction of appropriate changes, the document is sent to the member-countries (40-50 countries). Upon receiving their comments, the Technical Committee draws up a new version of the document (sometimes this involves recalling the Working Group) and presents it to the Group of Senior Advisers for final approval. The documents are translated from the working English text into the other original IAEA languages (Russian, French and Spanish) on three occasions: after the first consideration by the Technical Committee, before the draft document is sent to the member-countries for comments, and after final consideration by the Group of Senior Advisers.

Implementation of this procedure in practice required much more time for drawing up the documents than had been assumed. As a result, the 1977-1978 target date for the completion of the program has been changed to 1980. At the present time, all five codes of regulations and one guide have gone into the stage of final consideration. Some 25 drafts of various documents are still at various other stages in the procedure. On the basis of past experience from the passage of documents through the Technical Committees and the Group of Senior Advisers it is expected that six to eight documents a year will be given final consideration.

At its 10th meeting, the Group of Senior Advisers adopted a formulation concerning the purpose and functions of the containment system. The final version states that "in order for the escape of radioactive substances into the environment under the conditions of an accident not to exceed the allowable limits, provision should be made for a containment system, unless it can be shown that the escape of radioactive substances can be limited in other ways. This system presumes the existence of hermetic structures or enclosures, a subsystem of pressure suppression, and purification installations. A system of this kind is usually called a protective envelope system and may have various engineering designs, depending on the design requirements." This formulation is in accordance with various engineering approaches taken in various countries to the construction of systems for the containment of radioactive products in the event of an accident in an atomic power plant.

* Czechoslovakia, France, Federal Republic of Germany, India, Japan, Mexico, Sweden, Switzerland, Gt. Britain, the U.S.A., and the USSR.

WORK ON CHANNEL-TYPE REACTORS IN ITALY

V. S. Romanenko

In Oct. 1977 Soviet specialists visited Italian research centers where they became acquainted with the experience gained from work on power reactors of the channel type. Channel-type reactors are being developed in Italy on the basis of the CIRENA design. Construction of this prototype reactor with a power of 40 MW(electrical) has been started in Latina, 70 km from Rima. The physical start-up has been set for the end of 1981 and the power start-up, for 1982.

As a reactor with a heavy-water moderator, CIRENA has much in common with the well-tried and tested Canadian CANDU-PHW reactors. However, the use of boiling water as the coolant posed a number of new problems and made it necessary to carry out a large research program. This research was a topic of discussion during the visits to the centers.

The characteristic features of the reactor design, control system, and fuel recharging system were described by workers at the Cassaci Research Center (near Rima). The Soviet delegation saw the physical metallurgy laboratory, a stand for studying fretting corrosion of CIRENA, which has a high positive vapor reactivity coefficient (the derivative $\partial k/\partial \rho$ varies from -7.9 to $-6.2\%/g/cm^3$ during transition from a fresh charge to the steady state). Automatic control is effected by so-called "two-stage" rods which constitute U-shaped tubes of diameter 15 mm with a continuous circulating absorber, a mixture of borated water and hydrogen in a changing ratio. All four regulators operate synchronously from three ionization chambers installed beyond the side reflector. The total efficiency is $\pm 0.3\%$ and the rate is 0.05%/sec. In the prototype reactor there is no problem of stability of the heat release field owing to the small size of the reactor core. For the 300-MW(electrical) commercial version the problem is resolved by splitting the reactor into two zones with local regulators and automatic control operated by a computer. In the case of a larger reactor, ~ 600 MW(electrical), there should be 8-12 such zones.

An interesting feature of the reactor is the system of cold start-up which ensures a mean density of ~ 0.3 g/cm^3 of water in the core by feeding steam into the fuel channels. The steam is obtained by residual energy release and heating of water from the pumps.

Much attention is being paid to research on the behavior of the fuel assemblies of the reactor under accident conditions owing to the rupture of the piping of the loop. This work is being done at the CISE center (near Milan) on IETI-1, IETI-4, and CIRCE stands. The CIRCE stand provides full-scale simulation of the circulation loop of CIRENA, preserving marks for the location of the separator, pumps, etc. Ruptures of the piping are simulated by means of fast-acting valves with an operating time of several milliseconds. Moreover, fast-acting valves which are also used make it possible to cut off the part of the loop under study and to determine the remaining quantity of water as a function of time elapsed since the rupture of the loop. Studies on the stand showed that the allowable interruption in the water supply to the CIRENA fuel channels is 100 sec, after which the emergency cooling system must be switched on. The maximum temperature of fuel element cans reaches ~ 1200°C in the process.

The LFCEC Laboratory (near Turin) is developing and fabricating fuel elements and fuel assemblies for CIRENA as well as developing compounds of zirconium and steel in pressure tubes. Consideration is being given to both zircalloy-2 and the alloy Zr + 2.5% Nb. Fuel elements are being developed in the main on the basis of the Canadian technology, in particular, contact welding with magnetic clamping is being used to hermetically seal the cans. In-reactor tests of fuel elements are being conducted in Italy as well as in Norway, Sweden, and other countries. The testing program includes studies on the hydrogenation of the can and iodine corrosion of the can.

The LFCEC Laboratory is also developing a fuel consisting of a ThO_2-UO_2 mixture (2.2% ^{235}U). A technology for processing irradiated thorium fuel is being developed on a facility in the Rottondello Research Center.

Translated from Atomnaya Énergiya, Vol. 44, No. 4, pp. 390-391, April, 1978.

0038-531X/78/4404-0453$07.50

Specialists of the computational center at Bologna told of computational and theoretical research on the physics of CIRENA. The main experimental work is being done on the RB-1 reactor (criticality of lattices with natural and enriched uranium, measurement of the Doppler effect, etc.) and on the RB-3 reactor (heterogenous effects). In the latter case a number of fuel assemblies of the initial charge of the reactor were replaced with "new" assemblies and mixed lattice were formed or absorbers, from outside the original lattice, were introduced into the core. The value of K_{eff} and the spatial distribution of the neutron flux were determined by the three-group heterogenous method, realized in the programs HETROIS (three-dimensional, monopole) and SOS (two-dimensional, dipole). There also is the modular system NEFREM which incorporates two-dimensional monopole versions of both programs. The boundary conditions at the surface of the channels are given by the matrix of coefficients which are calculated in three different ways. Corrections are introduced into the values of the coefficients in order to improve the agreement with experiment.

A characteristic feature of nuclear power developments in Italy is the close contact with Canada, Japan, Gt. Britain, and other European countries. Italian specialists, on the one hand, make extensive use of the foremost achievements of reactor science and engineering and, on the other hand, focus their attention on solving particular problems, achieving considerable successes in the process.

NEW BOOKS FROM ATOMIZDAT (FIRST QUARTER OF 1978)*

E. R. Kartashev and A. S. Shtan', Neutron Methods of Continuous Analysis of Substances, 15 printer's sheets, 2.60 rubles.

A. M. Kol'chuzhkin and and V. V. Uchaikin, Introduction to the Theory of the Passage of Particles through Matter, 15 printer's sheets, 2.60 rubles.

I. V. Kurchatov, Nuclear Energy for the Well-Being of Mankind, 15 printer's sheets, 3 rubles.

A. A. Luk'yanov, Structure of Neutron Cross Sections, 13 printer's sheets, 2.20 rubles.

I. S. Slesarev and A. M. Sirotkin, Variational-Difference Schemes in Neutron Transport Theory, 6 printer's sheets, 90 kopecks.

A. N. Klimov and V. N. Orekhov, Telemetering Systems for Measuring and Monitoring Ionizing Radiation, 10 printer's sheets, 50 kopecks.

A. D. Frank-Kamenetskii, Modeling Neutron Trajectories in Reactor Calculations by the Monte Carlo Method, 6 printer's sheets, 90 kopecks.

G. B. Naumov, Fundamentals of the Physicochemical Model of Uranium Carbonate Ore Formations, 15 printer's sheets, 2.50 rubles.

V. I. Popov, LPE Spectrometry for Ionizing Radiation, 9 printer's sheets, 1.40 rubles.

L. A. Pertsov, Biological Aspects of Radioactive Contamination of the Oceans, 10 printer's sheets, 1.70 rubles.

V. V. Shustov, The Soviet Union and the Problem of Halting Nuclear Weapons Tests, 10 printer's sheets, 1.20 rubles.

N. B. Delone and V. P. Krainov, The Atom in a Strong Light Field, 7.5 printer's sheets, 2.60 rubles.

D. S. Zazhigaev, A. A. Kish'yan, and Yu. I. Romanikov, Methods of Planning a Physical Experiment and Processing the Results, 20 printer's sheets, 2.60 rubles.

A. A. Ivanov and T. K. Sobolev, Nonequilibrium Plasma Chemistry, 18 printer's sheets, 3.10 rubles.

Manipulators, 10 printer's sheets, 50 kopecks.

* All books are in Russian.

Translated from Atomnaya Énergiya, Vol. 44, No. 4, p. 391, April, 1978.

 0038-531X/78/4404-0454$07.50

M. F. Romantsev, Chemical Protection of Organic Systems from Ionizing Radiation, 11 printer's sheets, 1.70 rubles.

Instruments for Radiation Diagnostics in Medicine, 15 printer's sheets, 1 ruble.

Yu. V. Miloserdin and V. M. Baranov, High-Temperature Testing of Reactor Materials, 20 printer's sheets, 3.40 rubles.

Z. A. Al'bikov, V. I. Veretennikov, and O. V. Kozlov, Detectors of Pulsed Radiation, 12 printer's sheets, 1.80 rubles.

I. G. Kozlov, Contemporary Problems of Electron Spectroscopy, 18 printer's sheets, 2.70 rubles.

I. N. Klemparskaya and G. A. Shal'nov, Normal Autoantibodies as Radiation-Protection Factors, 10 printer's sheets, 1.50 rubles.

Programming and Computer Software

A cover-to-cover translation of *Programmirovanie*

Editor: N. N. Govorun

This new journal provides authoritative and up-to-date reports on current progress in programming and the use of computers. By publishing papers ranging from theoretical research to practical results, this bimonthly will be essential to a wide circle of specialists. It features results of vital research in the following directions:

- logical problems of programming; applied theory of algorithms; and control of computational processes
- program organization; programming methods connected with the idiosyncrasies of input languages, hardware, and problem classes; and parallel programming
- operating systems; programming systems; programmer aids; software systems; data-control systems; IO systems; and subroutine libraries.

Subscription: Volume 4, 1978 (6 issues) $95.00

Random Titles from this Journal

PROGRAMMING THEORY

Structure of an Information System—N. A. Krinitskii, V. N. Krinitskii, and D. A. Stepanchenko

The Active Set of Program Pages and Its Behavior—V. P. Kutepov

Estimate of the Efficiency of Replacement Algorithms—Yu. A. Stoyan

PROGRAMMING METHODS

Method and Algorithm for Checking Group Items in the Machine Processing of Economic Information—G. L. Livshin

Parallelization of the Fast Fourier Transform Algorithm in Encephalogram Spectrum Analysis—V. S. Medovyi and V. D. Trush

COMPUTER SOFTWARE AND SYSTEM PROGRAMMING

Increasing the Efficiency of Object Programs by Changing the Initial Grammar of the Programming Language—S. Ya. Vilenkin and S. M. Movshovich

A Metalanguage, a Translation Scheme, and Syntactic Analysis in a System for Constructing Highly Effective Translators—M. I. Belyakov and L. G. Natanson

Tabular Information Output System—V. D. Prachenko, V. P. Semik, N. D. Tyutvina, and K. A. Chizhov

Questions in the Creation of Software for Terminal Devices—V. A. Kitov

NEW RUSSIAN JOURNALS

IN ENGLISH TRANSLATION

BIOLOGY BULLETIN

Izvestiya Akademii Nauk SSSR, Seriya Biologicheskaya

The biological proceedings of the Academy of Sciences of the USSR, this prestigious new bimonthly presents the work of the leading academicians on every aspect of the life sciences—from micro- and molecular biology to zoology; physiology, and space medicine.

Volume 5, 1978 (6 issues) $175.00

SOVIET JOURNAL OF MARINE BIOLOGY

Biologiya Morya

Devoted solely to research on marine organisms and their activity, practical considerations for their preservation, and reproduction of the biological resources of the seas and oceans.

Volume 4, 1978 (6 issues) $95.00

WATER RESOURCES

Vodnye Resursy

Evaluates the water resources of specific geographical areas throughout the world and reviews regularities of water resources formation as well as scientific principles of their optimal use.

Volume 5, 1978 (6 issues) $190.00

HUMAN PHYSIOLOGY

Fiziologiya Cheloveka

A new, innovative journal concerned *exclusively* with theoretical and applied aspects of the expanding field of human physiology.

Volume 4, 1978 (6 issues) $175.00

SOVIET JOURNAL OF BIOORGANIC CHEMISTRY

Bioorganicheskaya Khimiya

Features articles on isolation and purification of naturally occurring, biologically active compounds; the establishment of their structure, methods of synthesis, and determination of the relation between structure and biological function.

Volume 4, 1978 (12 issues) $225.00

SOVIET JOURNAL OF COORDINATION CHEMISTRY

Koordinatsionnaya Khimiya

Describes the achievements of modern theoretical and applied coordination chemistry. Topics include the synthesis and properties of new coordination compounds; reactions involving intraspheral substitution and transformation of ligands; complexes with polyfunctional and macromolecular ligands; complexing in solutions; and kinetics and mechanisms of reactions involving the participation of coordination compounds.

Volume 4, 1978 (12 issues) $235.00

THE SOVIET JOURNAL OF GLASS PHYSICS AND CHEMISTRY

Fizika i Khimiya Stekla

Devoted to current theoretical and applied research on three interlinked problems in glass technology; the nature of the chemical bonds in a vitrifying melt and in glass; the structure-statistical principle; and the macroscopic properties of glass.

Volume 4, 1978 (6 issues) $125.00

LITHUANIAN MATHEMATICAL JOURNAL

Litovskii Matematicheskii Sbornik

An international medium for the rapid publication of the latest developments in mathematics, this quarterly keeps western scientists abreast of both practical and theoretical configurations. Among the many areas reported on in depth are the generalized Green's function, the Monte Carlo method, the "innovation theorem," and the Martingale problem.

Volume 18, 1978 (4 issues) $150.00

PROGRAMMING AND COMPUTER SOFTWARE

Programmirovanie

Reports on current progress in programming and the use of computers. Topics covered include logical problems of programming; applied theory of algorithms; control of computational processes; program organization; programming methods connected with the idiosyncracies of input languages, hardware, and problem classes; parallel programming; operating systems; programming systems; programmer aids; software systems; data-control systems; IO systems; and subroutine libraries.

Volume 4, 1978 (6 issues) $95.00

SOVIET MICROELECTRONICS

Mikroelektronika

Reports on the latest advances in solutions of fundamental problems of microelectronics. Discusses new physical principles, materials, and methods for creating components, especially in large systems.

Volume 7, 1978 (6 issues) $135.00

Send for Your Free Examination Copy

PLENUM PUBLISHING CORPORATION, 227 West 17th Street, New York, N.Y. 10011
In United Kingdom: Black Arrow House, 2 Chandos Road, London NW10 6NR, England
Prices slightly higher outside the U.S. Prices subject to change without notice.

Declassified and Approved For Release 2013/03/07 : CIA-RDP10-02196R000700110003-3